AD-A071 051 GENERAL ELECTRIC CO LYNN MA AIRCRAFT ENGINE GROUP F/G 11/6
CAST TITANIUM COMPRESSOR CASING.(U)
MAY 79 W H FICHT DAAJ02-76-C-0057

UNCLASSIFIED USARTL-TR-79-8 NL

1 OF 2
AD
A071051

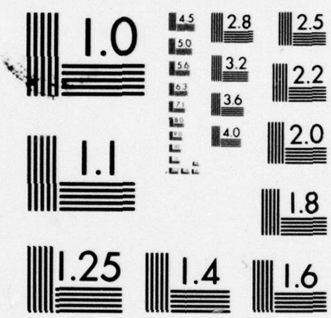

MICROCOPY RESOLUTION TEST CHART
NATIONAL BUREAU OF STANDARDS-1963-A

USARTL-TR-79-8

(12)

LEVEL

AD A071051

CAST TITANIUM COMPRESSOR CASING

W. H. Ficht
General Electric Co.
Aircraft Engine Group
1000 Western Avenue
West Lynn, Mass. 01910

May 1979

Final Report for Period July 1976 - December 1978

Approved for public release; distribution unlimited.

Prepared for

APPLIED TECHNOLOGY LABORATORY
U. S. ARMY RESEARCH AND TECHNOLOGY LABORATORIES (AVRADCOM)
Fort Eustis, Va. 23604

APPLIED TECHNOLOGY LABORATORY POSITION STATEMENT

This report is considered to provide insight to problems - the nature and causes of which will be typical of early titanium castings of any new configuration. Description of the solutions developed for problems encountered should result in substantially shortened development cycles for future applications of cast titanium. Information included on the physical properties of cast titanium is considered vital to the designer in undertaking any application of the material. Virtually no information on cast titanium properties has previously been published.

Mr. Richard F. Mulliken of the Propulsion Technical Area served as project engineer for this effort.

Unclassified

SECURITY CLASSIFICATION OF THIS PAGE (When Data Entered)

REPORT DOCUMENTATION PAGE		READ INSTRUCTIONS BEFORE COMPLETING FORM
1. REPORT NUMBER USARTL-TR-79-8	2. GOVT ACCESSION NO.	3. RECIPIENT'S CATALOG NUMBER
4. TITLE (and Subtitle) CAST TITANIUM COMPRESSOR CASING		5. TYPE OF REPORT & PERIOD COVERED Final 7/76 to 12/78
		6. PERFORMING ORG. REPORT NUMBER None
7. AUTHOR(s) W. H. Ficht		8. CONTRACT OR GRANT NUMBER(s) DAAJ02-76-C-0057
9. PERFORMING ORGANIZATION NAME AND ADDRESS General Electric Company Aircraft Engine Group 1000 Western Ave., West Lynn, Mass. 01910		10. PROGRAM ELEMENT, PROJECT, TASK AREA & WORK UNIT NUMBERS 1767046 00 001 EK
11. CONTROLLING OFFICE NAME AND ADDRESS Applied Technology Laboratory U. S. Army Research & Technology Laboratories Ft. Eustis, Virginia 23604 (AVRADCOM)		12. REPORT DATE May 1979
		13. NUMBER OF PAGES 136
14. MONITORING AGENCY NAME & ADDRESS (if different from Controlling Office) 12 137 p.		15. SECURITY CLASS. (of this report) Unclassified
		15a. DECLASSIFICATION/DOWNGRADING SCHEDULE

16. DISTRIBUTION STATEMENT (of this Report)

Approved for public release; distribution unlimited.

17. DISTRIBUTION STATEMENT (of the abstract entered in Block 20, if different from Report)

9 Final rept. Jul 76 - Dec 78,

18. SUPPLEMENTARY NOTES

19. KEY WORDS (Continue on reverse side if necessary and identify by block number)

Titanium Casting
Centrifugal Casting
Precision Casting
Net Shape
Compressor Casing

20. ABSTRACT (Continue on reverse side if necessary and identify by block number)

The development of a process for centrifugally casting the Ti 6Al-4V compressor casing for the T700 turboshaft engine is described. The cast casing results in a 35-pound saving of material input and a 30-hour saving of shop labor (at the 250th unit) compared to the forging which it replaces, due to the cast net shape outer contour which includes features formerly welded to the forged casing.

DD FORM 1 JAN 73 1473 EDITION OF 1 NOV 65 IS OBSOLETE

Unclassified

SECURITY CLASSIFICATION OF THIS PAGE (When Data Entered)

403 389

sit

Conventional expendable wax patterns and ceramic shell molds were chosen over a permanent metallic mold system. Preheated molds were mounted vertically on a centrifuge and rotated at from 350 to 500 rpm during casting.

Mechanical properties were well within design requirements although generally lower than forged properties. Ballistic testing showed the containment capability of the cast and forged material to be equal. Two cast casings were run in test engines and were judged to be equal in performance to forgings. There was no weight penalty associated with the use of a cast casing.

PREFACE

This final report summarizes the work done under U. S. Army Contract DAAJ02-76-C-0057 from July 1976 to December 1978.

W. H. Ficht was the Program Manager and Principal Investigator of the project. He provided overall supervision for this work and was responsible for meeting technical, cost and contractual commitments.

Technical direction for the program was provided by Mr. Richard Mulliken of the Applied Technology Laboratory, U. S. Army Research and Technology Laboratories, Fort Eustis, Virginia. His timely technical assistance is greatly appreciated.

The guidance and encouragement of Mr. J. I. Hsia, Manager, Technical Resources Operation, and Mr. G. V. Cash, Manager, Casting Technology, are gratefully acknowledged.

Precision Castparts Corporation served as subcontractor on the program and contributed significant technical knowledge and advice as well as pouring all castings. The enthusiasm and dedication of Mr. L. LaVoie and Mr. R. Trudo of that organization were essential to the success of the program.

The outstanding team effort of the following General Electric Co. personnel is gratefully acknowledged: R. Cimon, R. Dangelmaier, E. Dullea, G. Pariseanu, V. Protz, G. Sirois, M. Staker, D. Tapparo and R. Vertz.

TABLE OF CONTENTS

TABLE OF CONTENTS - Continued

LIST OF ILLUSTRATIONS

LIST OF ILLUSTRATIONS - Continued

LIST OF ILLUSTRATIONS - Continued

LIST OF TABLES

1.0. INTRODUCTION

The use of titanium structural components to take advantage of their high strength-to-weight ratio is well established in the aerospace industry. In many instances where titanium forgings are used, a large portion of the forging weight must be machined away to produce the desired finished configuration. The use of precision cast titanium components offers the economic advantages of a near net shape process.

Since commercial development of titanium casting began in the 1950's, significant progress has been made in the size and complexity of production castings. Titanium casting furnaces capable of pouring several hundred pounds of molten alloy are in regular use today. Despite these advances, the casting of titanium presents obstacles to be overcome that are not encountered in the casting of other engineering materials.

The extreme reactivity of molten titanium with atmospheric gases and solid oxides precludes the use of conventional vacuum induction melting and casting equipment that is used to precision cast other alloys. In order to form a pool of molten titanium without contamination, the skull melting process, originally developed by the U. S. Bureau of Mines, is used. This is a consumable electrode process, the details of which will be discussed later in this report. The main effect of the use of this equipment is that very little superheat can be employed and the molten alloy at the time of casting is just above its liquidus temperature. This results in low alloy fluidity and rapid freezing as the alloy enters the mold. The low fluidity places limits on casting of thin sections and requires an excessive amount of gating to feed the casting, thus adversely influencing the cost effectiveness of the process.

The present program is an attempt to develop a reduced-cost method of producing titanium precision castings by using a mold rotating on its own axis on a centrifuge to provide a centrifugal force assist to the alloy in filling the mold and to reduce gating and machining stock to a minimum.

The component selected to demonstrate the process is the compressor casing for the T700 engine. This part, shown in its finished machined form in Figure 1, is currently produced from a forging (see Figure 2) which has the two casing halves arranged end-to-end. The finished casing is 9 inches long with a maximum diameter of 11 inches and weighs 8.8 pounds.

The objectives of the program can be summarized as follows:

1. To produce the T700 compressor casing as a one-piece centrifugal casting.

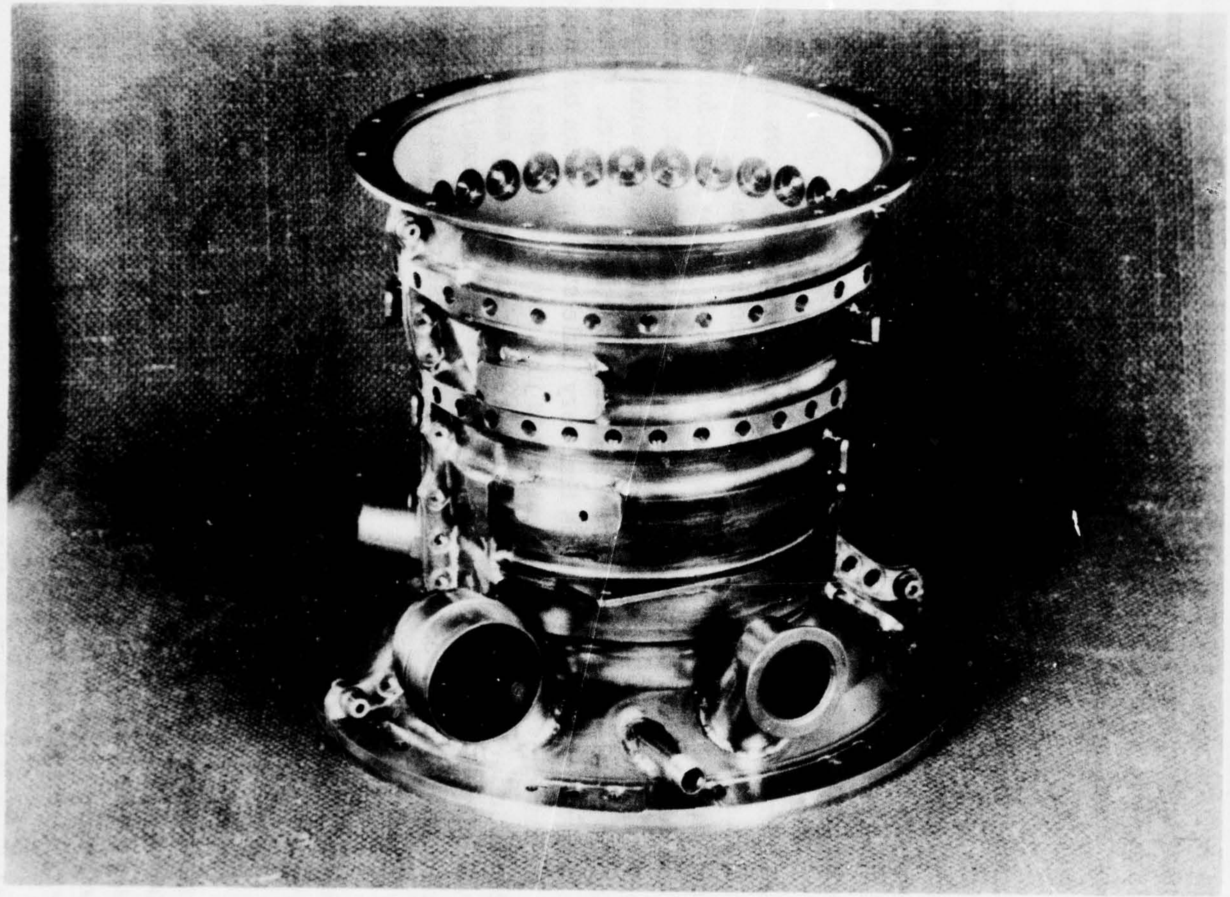

Figure 1. Finish Machined T700 Compressor Casing Made from Forging

Figure 2. Forging Used to Produce Compressor Casing
(Typical Weight 65 Pounds)

2. To cast the exterior contour as closely as possible to net shape. This includes casting integrally as many features on the outer contour that are welded to the machined forging as is economically practical.

3. To investigate the use of expendable and permanent mold systems.

4. To obtain the required material property data to demonstrate the suitability of the cast mechanical properties for the intended application.

5. To demonstrate the suitability of the cast casing by engine testing.

6. To demonstrate the cost effectiveness of the casting approach.

2.0. PROGRAM SCOPE

The program was divided into four phases, each of which contains several work elements. An outline of the scope of the program follows.

2.1 Phase I - Casting Process Development and Manufacturing Planning

2.1.1 Task I - Casting Technique Selection

This task included the selection of an economical precision casting process. Mold systems selected for evaluation included conventional ceramic shell molds and permanent molds. Optimum combinations of mold temperatures and centrifuge speeds were determined using temporary tooling designed for this purpose.

2.1.2 Task II - Casting Process Development

In this task, additional castings were produced in order to "fine tune" the casting process. Specimens for tensile, stress-rupture, high- and low-cycle fatigue and crack propagation testing were cut from castings and tested. Engineering drawings were issued for the cast and machined casing. A quality control plan covering the type and frequency of inspection for production parts was established. Permanent casting and inspection tooling was designed and built. A sample casting was poured using this tooling and was inspected.

2.1.3 Task III - Data Presentation

A review of Phase I progress was presented to the Government and an interim technical report was issued.

2.2 Phase IA - Integrally Cast Ducts

2.2.1 Task I - Casting Development

Separate pattern tooling to form three air bleed ducts was designed and built. Sample casings containing integral air bleed ducts were cast and evaluated.

2.2.2 Task II - Data Presentation

A review of the dimensional and metallurgical evaluation of the integrally cast ducts was presented to the Government.

2.2.3 Task III - Design, Fabrication and Proof of Production Tooling

Based on an analysis of sample castings produced with integrally cast air bleed ducts and the wall thickness that would be required, a decision was made to terminate the casting of integral ducts.

2.3 Phase II - Fabrication and Engine Test Evaluation

2.3.1 Task I - Fabrication of Engine Test Hardware

Tooling modifications were made and pilot production castings produced and dimensionally inspected. Two castings were finish machined and shipped for engine test.

2.3.2 Task II - Engine Test Evaluation

Two finished cast casings were assembled into test engines. A 60-hour assurance test and a 150-hour demonstration test were performed, respectively.

2.3.3 Task III - Data Presentation

Data generated in Phase II was presented to the Government in a briefing.

2.4 Phase III - Preparation of Technical Data Package

A technical data package containing all pertinent drawings and documents describing the T700 compressor casing and the process used to produce it was prepared.

3.0. DISCUSSION

3.1 Phase I

3.1.1 Task I - Casting Technique Selection

3.1.1.1 Description of Ingot and Casting Equipment

Because of the extreme reactivity of titanium, great care must be taken to prevent the contact of the molten alloy with both the atmosphere and refractory oxides. After titanium is extracted from its ore in the form of sponge it must be consolidated into an electrode using a vacuum consumable remelt furnace, shown schematically in Figure 3. A mechanically compacted bar composed of sponge, reprocessed material (gates, sprues, bar stock, turnings) and alloying elements serves as one electrode and a water-cooled copper crucible as the other in a D. C. circuit. The resulting arc causes a molten pool of titanium to form directly under the arc and solid titanium to form against the cooler crucible walls. The bar is gradually advanced and the crucible is filled with a solid ingot. It may be necessary to repeat this process to guarantee chemical homogeneity. Using this method, only a small fraction of the total mass of titanium is molten at a given time and it is in contact either with the partial vacuum or the thin shell of solid titanium formed against the crucible wall.

In order to produce a cast part from the refined electrode, one is faced with the same problems but in addition, two more:

(1) The liquid bath must be large enough to fill the desired mold cavity, and
(2) the molten titanium will come in contact with the mold material, which may be a source of contamination. The apparatus used to produce modern production titanium castings is the skull melting furnace, a development of the U. S. Bureau of Mines, shown schematically in Figure 4. Again, a water-cooled copper crucible is used within a vacuum chamber to contain the molten bath which is surrounded by a solid skull of titanium. The bottom of the crucible is covered with solid titanium, either virgin material or the residue of a previous melt. The casting chamber is evacuated; melting is initiated by striking an arc between the preweighed electrode and the titanium in the bottom of the crucible. When the desired amount of alloy is molten, the remaining electrode stub is quickly withdrawn and the crucible tilted to fill the mold.

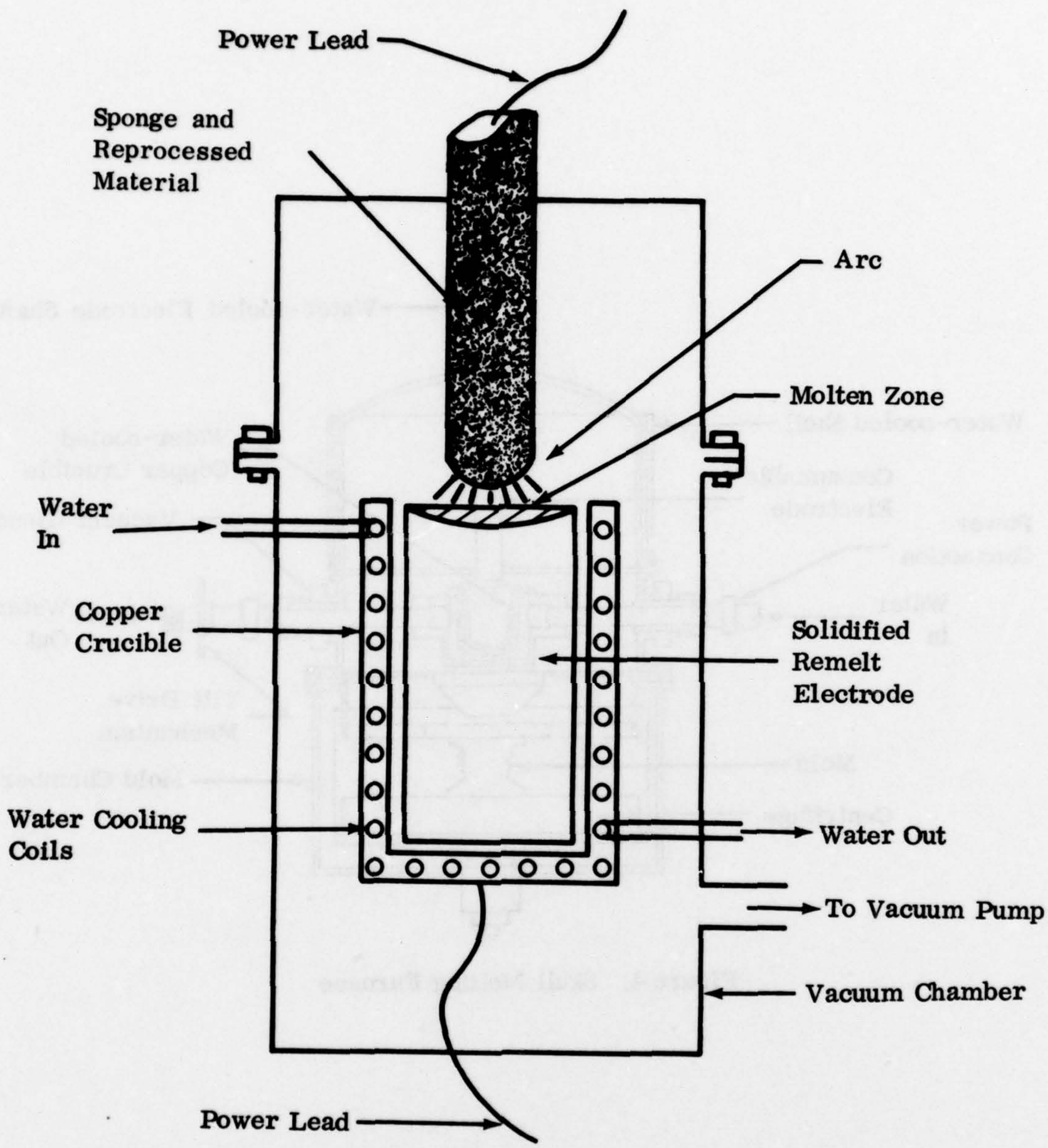

Figure 3. Vacuum Consumable Remelt Furnace

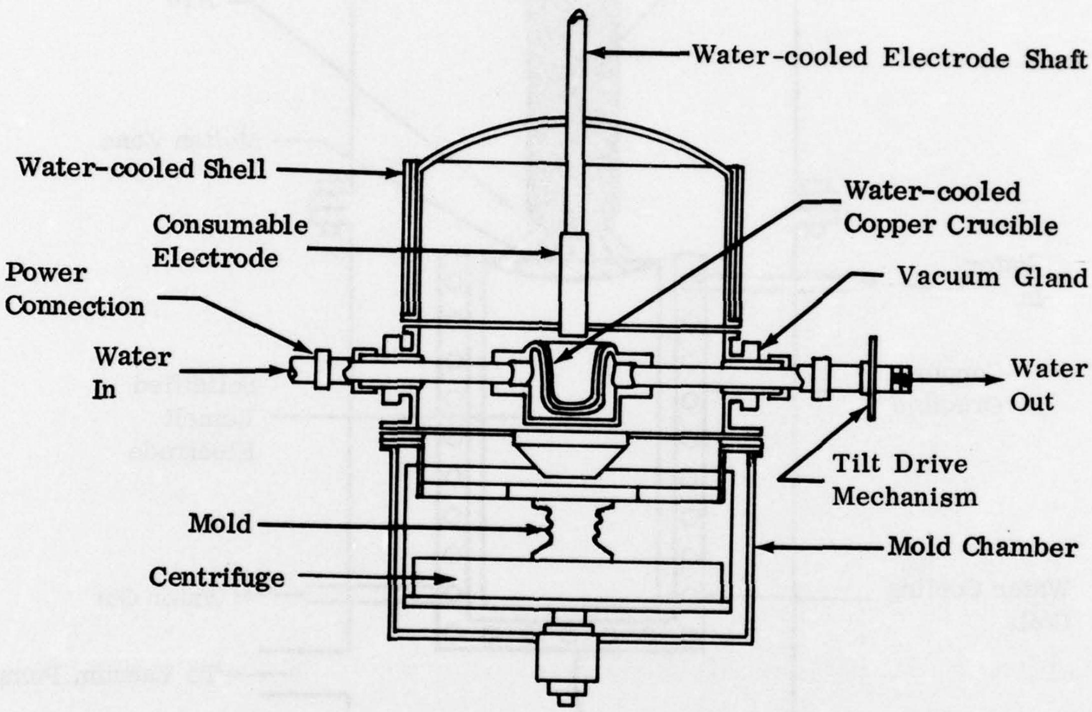

Figure 4. Skull Melting Furnace

Sinizer and Adams [1] have presented a thermal analysis of a typical skull melting system. Using their assumptions of spherically symmetrical, steady heat flow from a localized central source, through the bath and into the skull, the bath temperature T at any location is given by

$$T - Tm = \frac{3.41\ P\ (Rm - r)}{2\pi\ Kr\ Rm}$$

where	r	=	distance from heat source, ft
	K	=	thermal conductivity, Btu/ft hr F
	P	=	power transmitted through the liquid, watts
	3.41 P	=	power transmitted through the liquid, Btu/hr
	Rm	=	radius of liquid zone, ft
	Tm	=	melting point, ^{o}F

and the average temperature, Tav, is given by

$$Tav = \frac{3.41\ P}{4\pi K\ Rm} + Tm$$

Figure 5 shows the temperature vs. distance from the arc for power inputs of 2 KW and 4 KW and illustrates some general relationships involved in skull melting. The melting point shown is an approximation which is meant to be representative of a typical titanium alloy, which in this case melts at a temperature in excess of 3200^{o}F. From the equations it is clear that superheat is proportional to the power input and inversely proportional to the thermal conductivity. The thermal conductivity of titanium alloys is lower than that of most iron and nickel alloys; this is a beneficial condition for the use of skull melting, since it prevents excessive heat loss to the skull. One of the major reasons for the inability of obtaining much superheat is that as soon as the power is shut off prior to pouring, a steady-state condition no longer exists and the steep thermal gradient between bath and skull is rapidly dissipated, resulting in a rapid lowering of bath temperature.

3.1.1.2 Mold Systems

One of the first factors that had to be established in this phase of the program was the type of mold to be employed. The choice was between a conventional

1. Sinizer, D. I., and Adams, C. M., Jr., METALLURGICAL REQUIREMENTS AND PRODUCTION TECHNIQUES FOR TITANIUM CASTINGS, Trans. Am. Foundrymen's Society, V. 63, pp. 313-316, 1955.

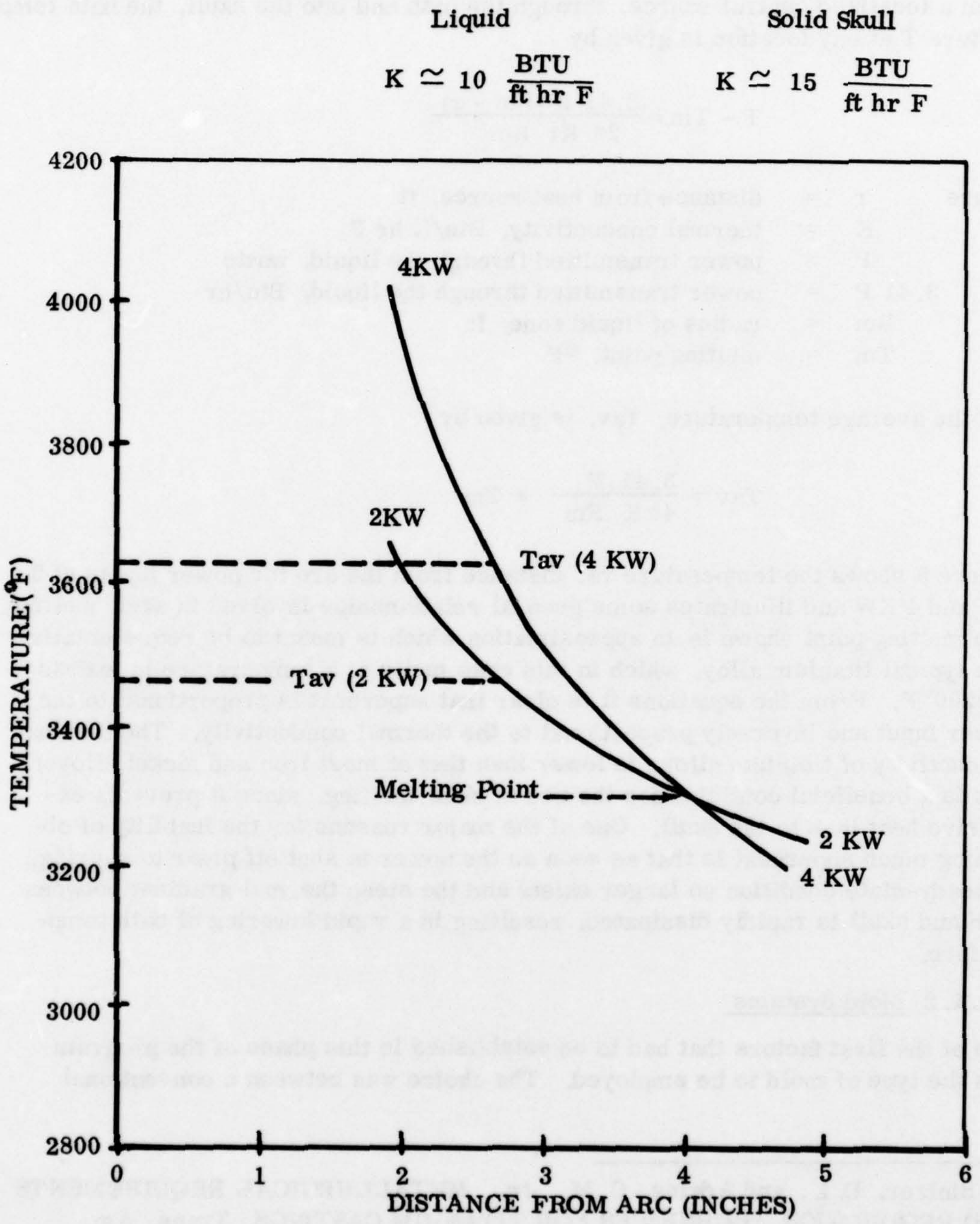

Figure 5. Temperature vs. Distance from Arc in Typical Skull Melting Furnace

ceramic shell mold formed around a wax pattern and a metallic permanent mold. A discussion of the details of each process follows.

3.1.1.2.1 Ceramic Shell Process (See Flowchart, Figure 6)

An injection die is machined from aluminum alloy. Dimensionally stable, resin-filled wax is injected or extruded into the die cavity to form a pattern. The pattern is a duplicate of the desired casting except that it is larger by the anticipated amount of metal volumetric shrinkage (about 1%). After inspection and correction of any surface imperfections the wax gating system is joined to the pattern by wax welding. The wax assembly is then dipped into a ceramic slurry, coated with fine ceramic flour and dried. The dipping, stuccoing and drying is repeated until the desired mold thickness is achieved. During drying, chemical reactions between the ceramic particles and the binder cause high strength to be developed in the shell. The wax is then removed by steam autoclaving, flash firing or by using a solvent.

Prior to casting, the mold is preheated, with typical temperatures ranging from 1800^{o} to $2000^{o}F$. The mold is transferred to the casting chamber and filled. After solidification the gating system is cut off and the gate stubs ground. After casting, the inner diameter is rough machined to remove less dense material (including gas, shrinkage). The casting is then chemically milled to remove any surface contamination. The part is inspected using visual, fluorescent penetrant and radiographic techniques. Any indications beyond drawing limits are repaired by local grinding and welding.

The casting is annealed, dimensionally inspected, given a final fluorescent penetrant and radiographic inspection, marked and shipped.

3.1.1.2.2 Permanent Mold Process (See Flowchart, Figure 7)

A mold is machined from steel, copper or other suitable alloy. A mold coating may or may not be used. The unheated mold is transferred to the casting chamber and filled. After solidification, gating material is removed and after casting the inner diameter is rough machined. Visual, fluorescent penetrant and radiographic inspection are performed.

Bench grinding and repair welding are done, as required.

The casting is annealed, dimensionally inspected, given a final nondestructive inspection, marked and shipped.

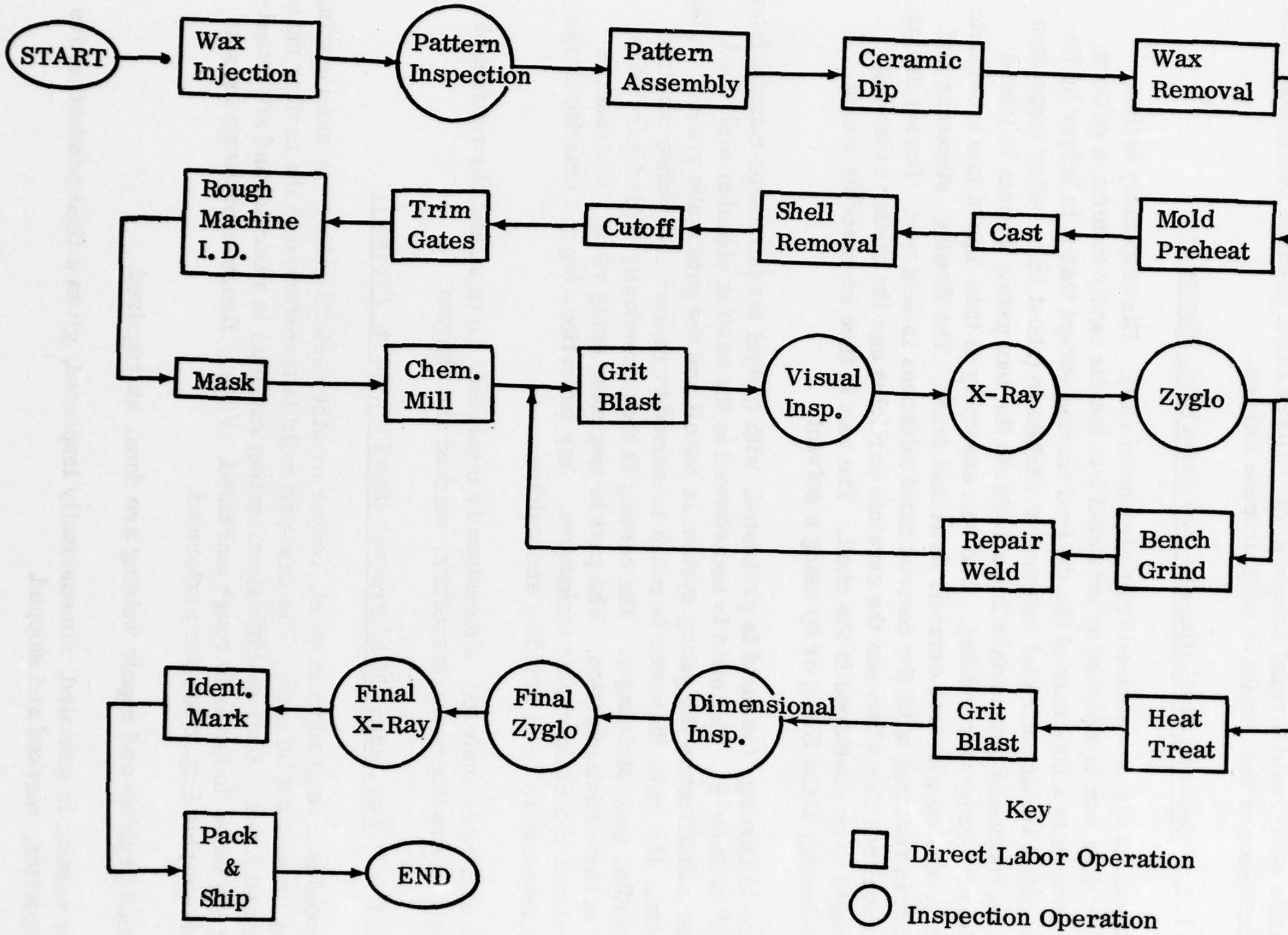

Figure 6. Flowchart - Ceramic Shell Precision Casting Process

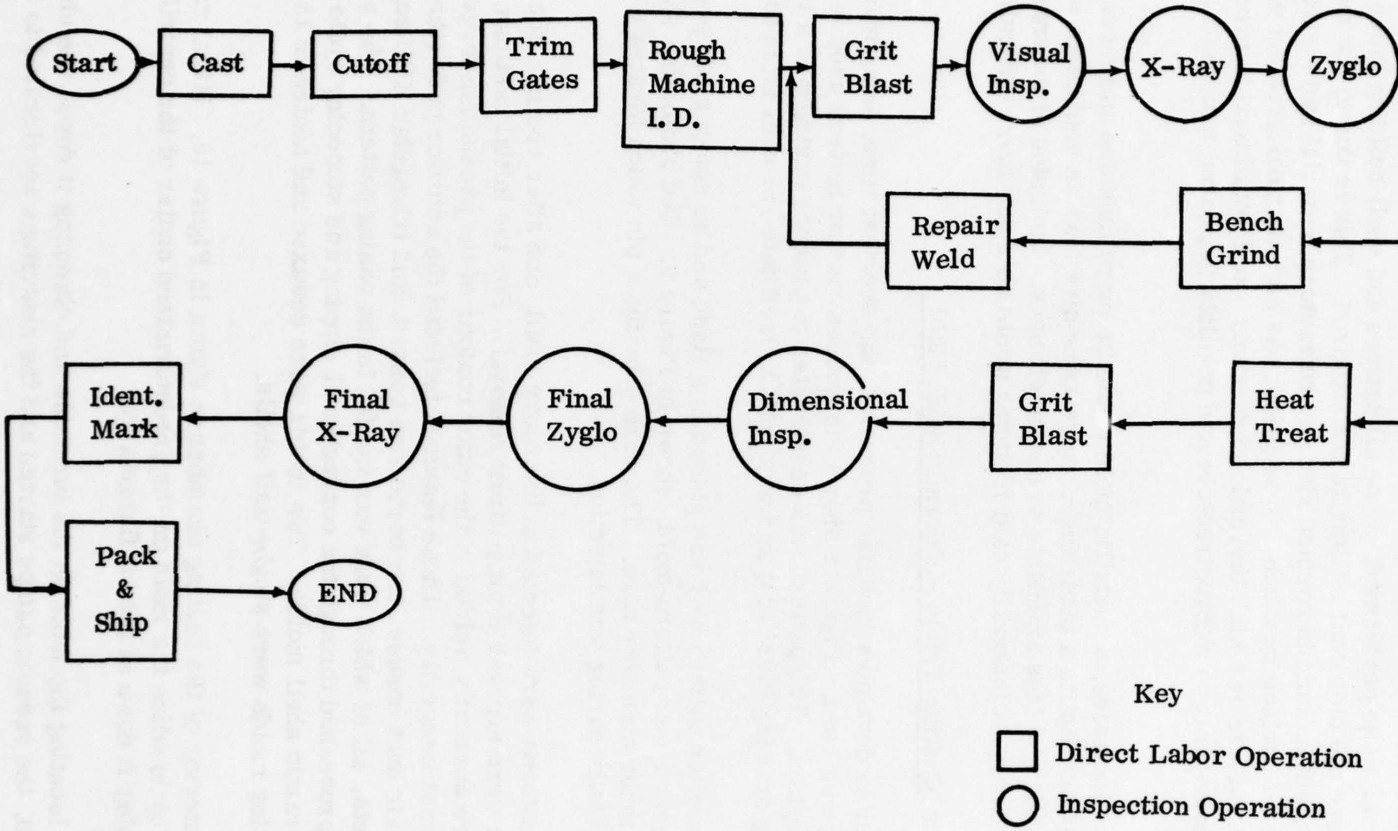

Figure 7. Flowchart - Permanent Mold Precision Casting Process

It is clear that the use of a permanent mold would result in significantly fewer operations to be performed, since all pattern and shell building tasks are eliminated and the chemical milling is not required. This is due to the molten titanium not coming in contact with any refractory material and the resulting absence of surface reaction. In addition, the high thermal gradient present through the use of a high thermal conductivity mold would tend to produce a more homogeneous microstructure and possibly improved mechanical properties.

On the minus side, a metallic mold would be more massive and therefore more difficult to adapt to a centrifuge, more expensive than an equivalent wax injection die and less amenable to design changes. Inclusion of external details of the casing as integrally cast features would be much more difficult.

3.1.1.3 Casting Trials - Ceramic Shell Mold

In order to develop a baseline process in the shortest time, temporary pattern tooling was used. Figure 8 shows the wooden master pattern used in Phase I of the program. The pattern was constructed to produce castings to a temporary casting drawing (6033T04) and was split to facilitate removal from the mold.

Each master pattern half was placed in a flask and an epoxy resin poured around it to form a wax pattern mold, shown in Figure 9. The photo also shows the epoxy inner diameter core. The core contains a pin which locates it axially and radially during wax injection.

Wax patterns were injected in the epoxy mold, and after cooling, the two mold halves were separated for pattern removal. For the initial castings, features that are currently welded to the outer contour of the production forged casing were cast integrally. These features included the actuator pads (three versions), three air duct bosses, two borescope bosses, and triangular ECU support brackets, all of which were wax welded to the casing pattern. The wax patterns were processed through the conventional dipping and stuccoing cycle to produce the ceramic shell molds. Two molds were dewaxed and heated to 1550^{o}F. The resulting molds were single-wall shells.

The interior of the casting chamber is shown in Figure 10. Initial castings were made by locating the mold on the predetermined center of the centrifuge and clamping it down at the aft flange area.

After locating the mold on the turntable and clamping it down, the chamber was closed, the vacuum pumps started and the centrifuge accelerated to 500 rpm.

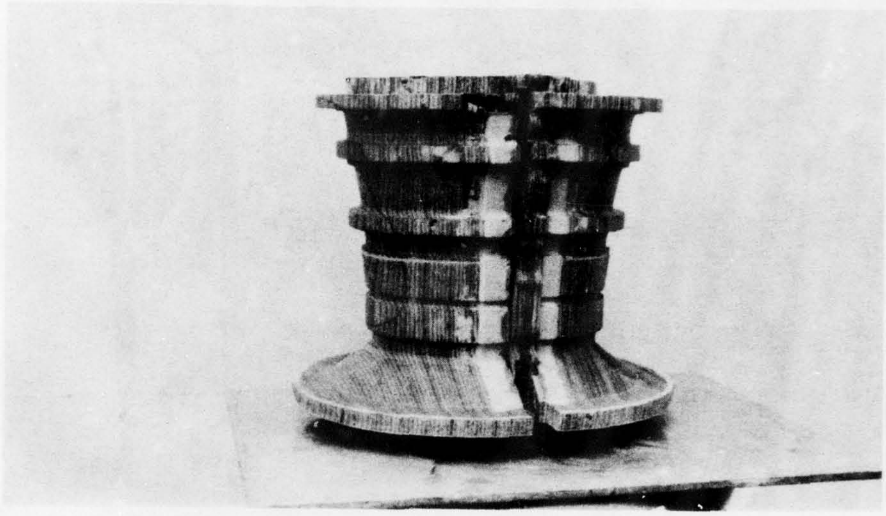

Figure 8. Wooden Master Pattern Used for Initial Trials

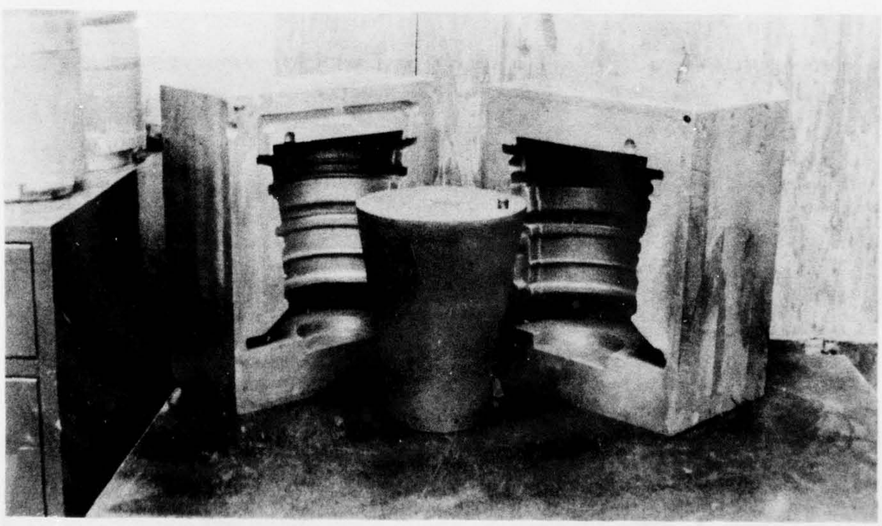

Figure 9. Epoxy Wax Pattern Mold Used for Initial Trials

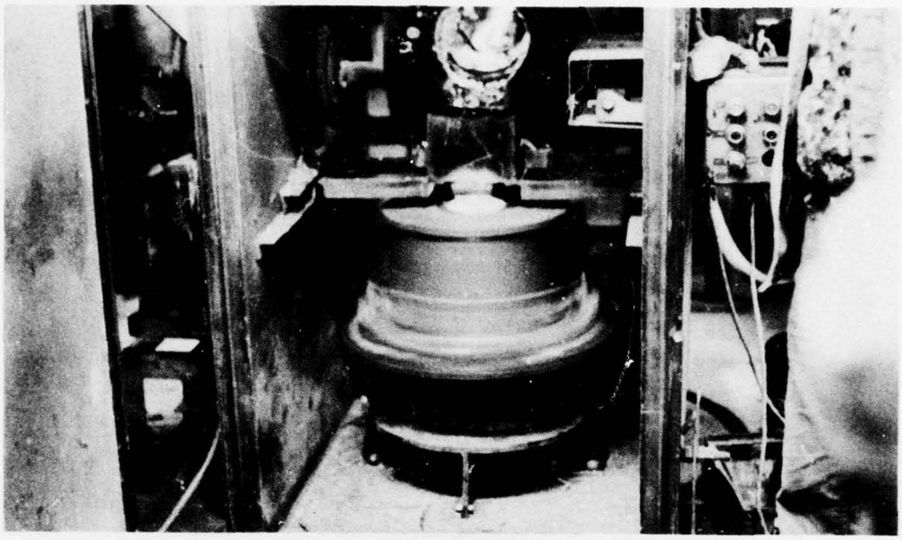

Figure 10. Casting Chamber Interior

Figure 11. Filled Shell Mold After Removal From Casting Chamber

After melting a portion of the consumable electrode slowly to form a "skull" of solid titanium along the copper crucible, the power input and electrode feed rate were increased and the balance of the portion of the electrode to be cast was melted rapidly. The electrode holder was then retracted and the molten alloy poured in approximately 3 seconds. The mold was allowed to cool for about 10 minutes before breaking the vacuum. Figure 11 shows a filled mold after removal from the casting chamber.

After mechanically removing the mold material and chemically milling approximately .020 inch from all surfaces in order to remove any products of reaction present, the castings were visually inspected. The external surface features had all completely filled and the surface finish was acceptable. The casting wall thickness, however, showed excessive variation, ranging from about .030 to over 1 inch. It was clear that the roughness of the outer contour of the ceramic shell precluded accurate location of the shell with respect to the center of the centrifuge, causing metal to be forced to the side of the mold located at the maximum distance from the center of rotation.

In order to alleviate the condition causing uneven wall thickness described above, two fixtures were designed and built in order to provide controlled pilot diameters at each end of the shell mold. Figure 12 is a photograph of the fixture to be used in dipping the wax pattern.

Upper and lower aluminum plates were machined to fit the wax pattern per Figure 13. The plates are connected by a centrally located aluminum rod. The dipping fixture is left on the wax pattern during shell building and is removed after the shell has cured. Since a gap exists between the wax pattern and fixture at the forward and aft flanges, the resulting shell mold has two smooth concentric surfaces at the forward and aft ends suitable for use as locating surfaces, as shown in Figure 14.

Figure 15 shows the steel fixture which was designed for use during casting. The pouring fixture consists of a bottom plate which is machined to accept the shell mold aft locating surface and which is attached directly to the centrifuge turntable, and an upper "can" section which accepts the shell mold forward locating surface. An outer flange on the fixture provides a surface for clamping the mold and fixture to the centrifuge. The result is a mold which is located concentrically and perpendicularly to the centrifuge.

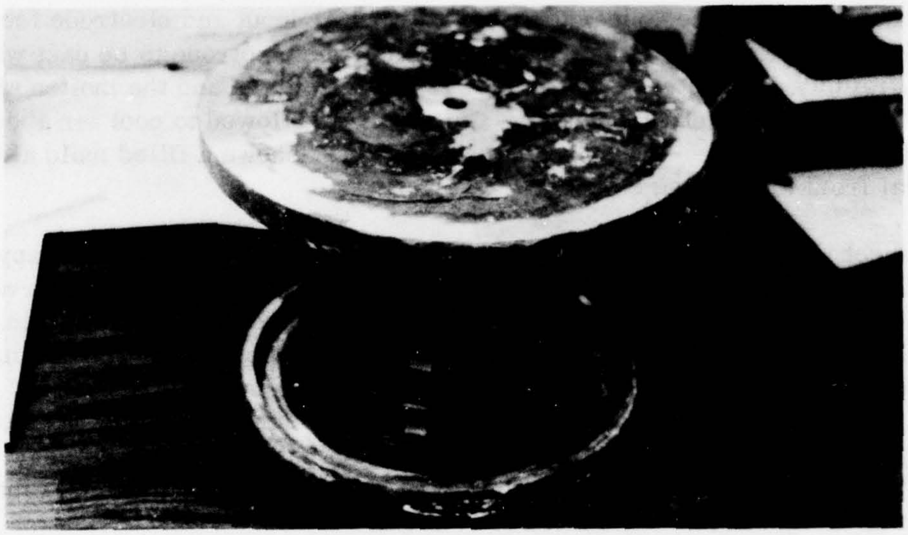

Figure 12. Wax Pattern in Dipping Fixture

A third mold was prepared using the dipping fixture for shell building. The mold was used to pour a third casting (4490-S5) using the pouring fixture, with all other parameters the same as for the first two castings.

There was no appreciable wall thickness variation on this part. The outer radial contours showed a maximum runout of .028 inch, considerably better than expected for a part made from temporary tooling.

3.1.1.4 Casting Trial - Permanent Mold

At this point, a permanent low-carbon steel mold was sand cast and machined for an evaluation of the effectiveness of a chill mold. Copper was a candidate for the mold material because of its high conductivity and heat capacity which would give high thermal gradients, a fine microstructure and possibly improved mechanical properties. Steel was chosen, however, since it was felt to be a more practical material for this application in a production environment. A steel mold would be more resistant to warpage, less susceptible to damage and more easily weld repaired than copper. In addition, previous trials of casting titanium into sections of thick-walled (.500 inch) steel pipe showed no surface reaction between the titanium and steel and relatively easy removal from the mold.

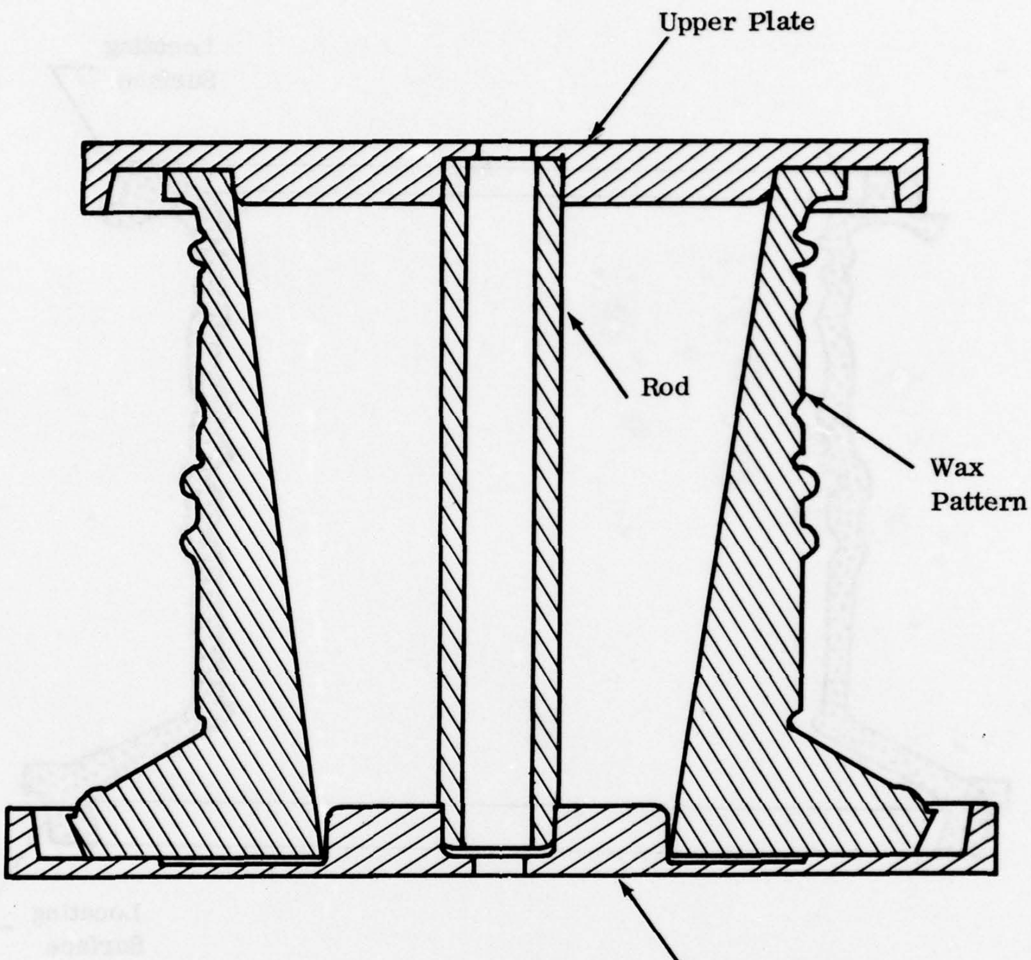

Figure 13. Dipping Fixture Details

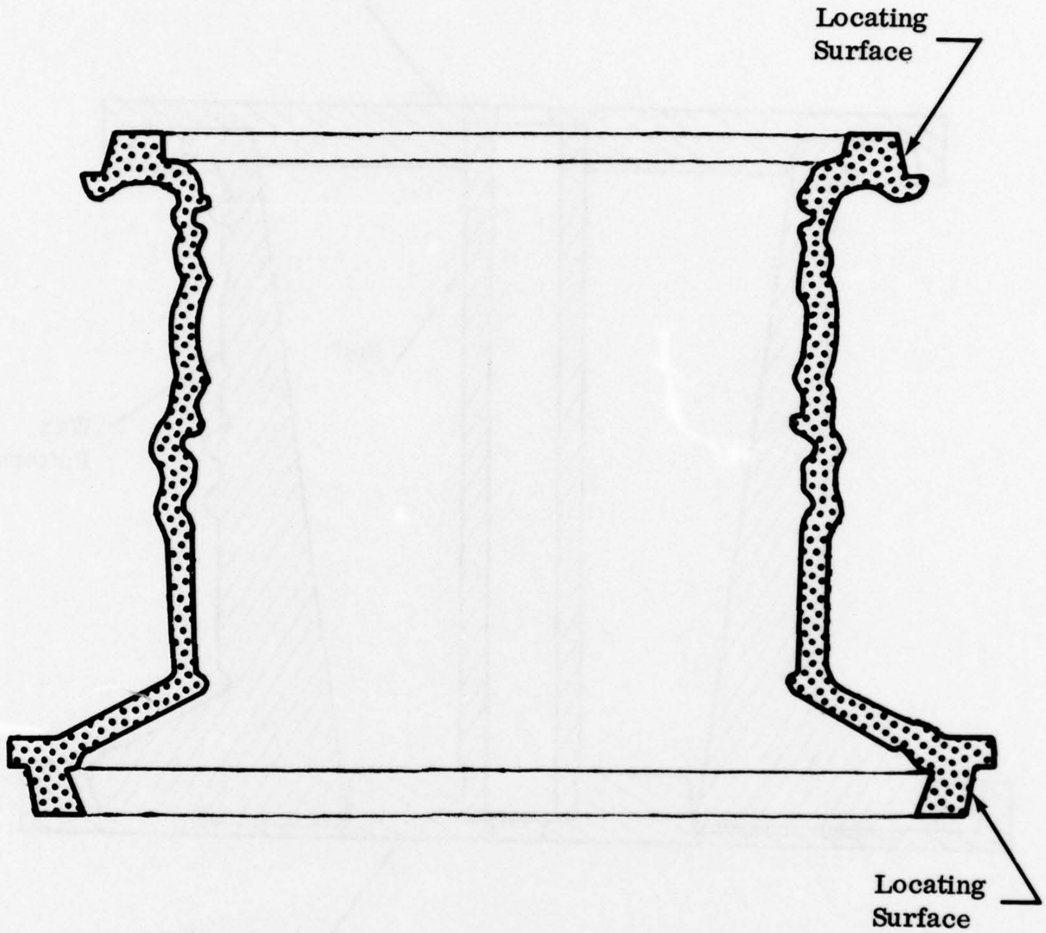

Figure 14. Ceramic Shell Mold Locating Method

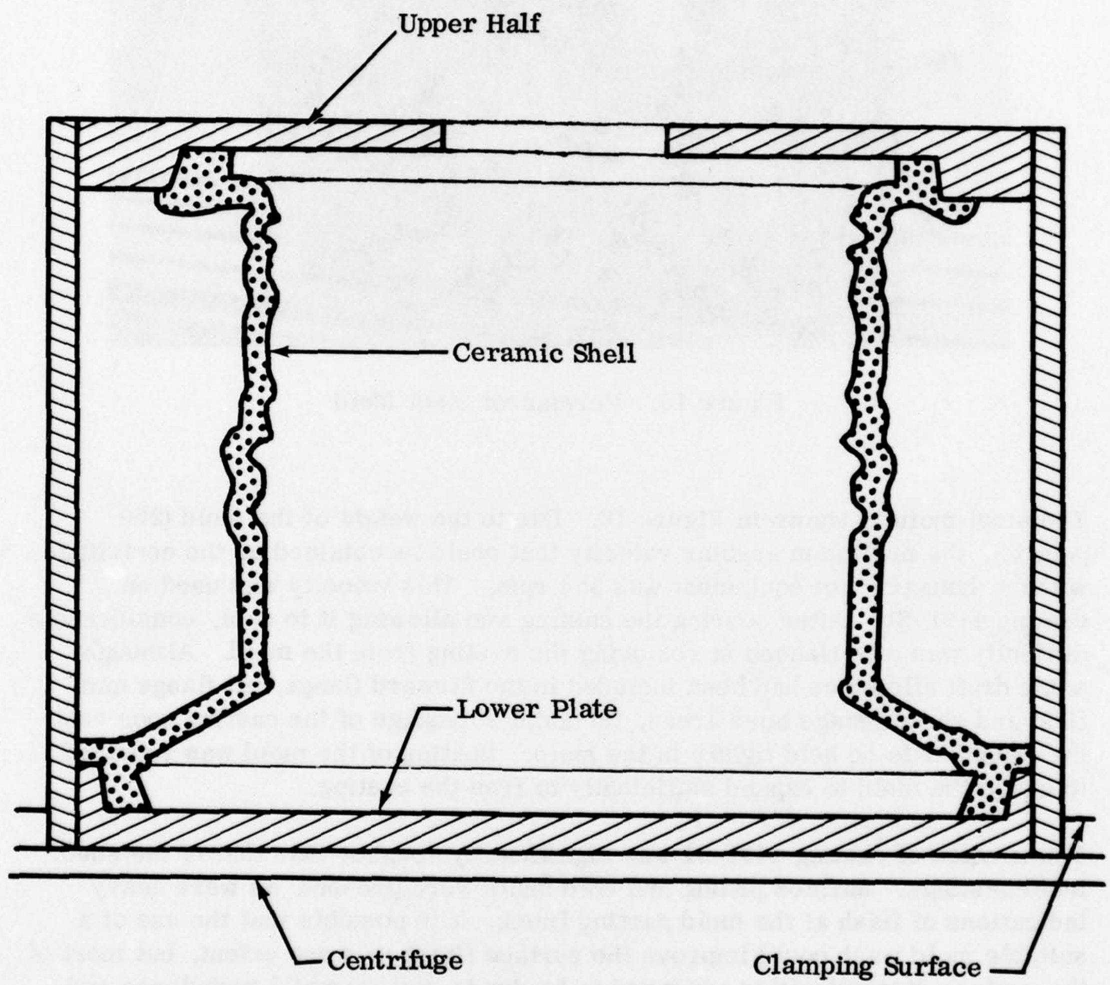

Figure 15. Pouring Fixture Details

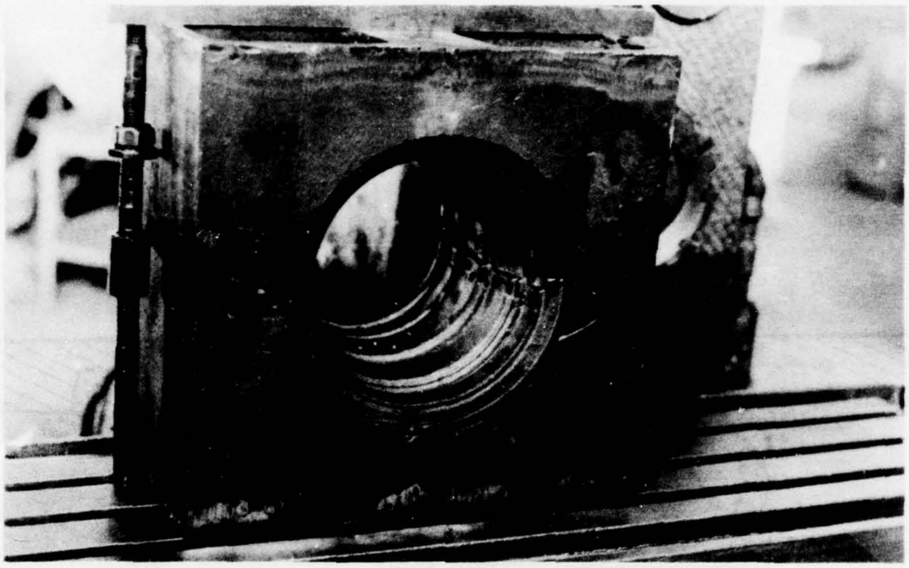

Figure 16. Permanent Steel Mold

The steel mold is shown in Figure 16. Due to the weight of the mold (200 pounds), the maximum angular velocity that could be obtained on the centrifuge without damaging the equipment was 350 rpm. This velocity was used on casting 4491-S1. After pouring the casting and allowing it to cool, considerable difficulty was experienced in removing the casting from the mold. Although some draft allowance had been included in the forward flange, aft flange and first and second stage boss areas, the axial shrinkage of the casting upon cooling caused it to be held tightly in the mold. Heating of the mold was required to cause the mold to expand sufficiently to free the casting.

The surface of casting 4491-S1 was significantly rougher than that of the shell mold castings. Surface pitting and cold shuts were present, as were heavy indications of flash at the mold parting lines. It is possible that the use of a suitable mold wash could improve the surface finish to some extent, but most of the surface discontinuities appeared to be due to molten metal turbulence and splashing which caused droplets to freeze quickly on the mold wall. These droplets were then surrounded by the balance of the molten metal which did not contain enough heat to remelt the droplets. The result was a large number of negative surface discontinuities which would not be permissible for the intended application without subsequent finishing.

3.1.1.5 Decision - Mold System

Based on the foregoing experience, the ceramic shell mold was chosen as the better mold system for use in the balance of the program. The decision was made for the following reasons:

1. The shell process allows the casting to be designed closer to net shape. Generous draft angles would have to be built into a permanent mold.

2. The shell process offers much greater flexibility for integrally casting complex features on the exterior surface of the casing, thus offering a greater cost reduction potential.

3. Tooling for the shell process is less costly, less massive and lends itself to modification far more easily than a permanent mold. Wax injection tooling for the shell process can be machined from aluminum, while the permanent mold would require at least a carbon steel and possibly a high-temperature alloy for durability.

4. The shell process is more practical for maintaining constant pouring conditions. Maintaining constant mold temperatures for successive pours with a permanent mold would present particular difficulties.

3.1.2 Task II - Casting Process Development

3.1.2.1 Process Development

Nineteen castings were poured using temporary pattern tooling in Phase I. The pouring conditions and results are given in Table 1.

Initially the aft section of the casing was cast solid as shown in Figure 17 since it was felt that a problem would exist in feeding metal through the .200-inch-thick conical section present in the finished part (Figure 18). This would require an additional turning operation to produce the final configuration. Radiographic inspection of parts cast with the aft end solid showed that shrinkage cavities formed as shown in Figure 17. Attempts at changing the centrifuge velocity were unsuccessful in solving the problem since the large mass present created a thermal center (or "hot spot") with resulting cavity shrinkage due solely to the mold geometry.

In order to produce a casing having a net shape aft end, a steel ring of suitable configuration was fabricated and installed on the bottom plate as shown in Figure 19 for castings 4490-S6 and -S7.

TABLE 1
PHASE 1 - TEMPORARY TOOLING CASTINGS

S/N	Fixture	Mold Type	Centri-fuge RPM	Mold Temp (^{o}F)	Aft End	Cast Ducts	Pour* Wt. (lb)	Remarks
4490-S3	One-piece	Shell	500	1550	Solid	No	35	Mold imbalance Uneven walls
-S4	One-piece	Shell	500	1550	Solid	No	35	Mold imbalance Uneven walls
-S5	Two-piece	Shell	500	1550	Solid	No	35	Wall thickness even/ Insufficient internal stock at aft end/shrinkage cavity at aft end
4491-S1	(None)	Permanent (Steel)	350	RT	Solid	No	35	Rough surface/difficulty in removing casting from mold
4490-S6	Two-piece	Shell	200	1800	Steel Ring	No	35	Forward end not completely filled. Shrinkage in aft flange and heavy sections
-S7	Two-piece	Shell	400	1800	Steel Ring	No	35	Slight shrinkage in aft flange and heavy sections
-S8	Two-piece	Shell	400	1800	Solid	Yes	35	Generally good quality-shrinkage in duct flanges

* Raw casting weight compares with forging weight of 65 lb

TABLE 1 - Continued
PHASE 1 - TEMPORARY TOOLING CASTINGS

S/N	Fixture	Mold Type	Centri-fuge RPM	Mold Temp (^oF)	Aft End	Cast Ducts	Pour* Wt. (lb)	Remarks
4490-S9	Two-piece	Shell	400	1800	Solid	No	35	Scattered small shrinkage indications
-S10	Two-piece	Shell	400	1800	Solid	No	31	Scattered small shrinkage indications
-S11	Two-piece	Shell	400	1800	Solid	No	35	Shrinkage indications - aft end
-S12	Two-piece	Shell	400	1800	Solid	No	39	Shrinkage indications- aft end
-S13	Two-piece	Shell	400	1800	Solid	No	38	Shrinkage indications - aft end
-S14	Two-piece	Shell	400	1800	Partial Steel Ring	No	33	Shrinkage indications - aft end
-S15	Two-piece	Shell	400	1800	Solid	No	35	Shrinkage indications - aft end
-S16	Two-piece	Shell	400	1800	Net Shape	No	34	Reduced size shrinkage
-S18	Two-piece	Shell	350	1800	Net Shape	No	34	No cavity shrinkage centerline indications in borescope bosses

* Raw casting weight compares with forging weight of 65 lb

TABLE 1 - Continued

PHASE 1 - TEMPORARY TOOLING CASTINGS

S/N	Fixture	Mold Type	Centri-fuge RPM	Mold Temp (^{o}F)	Aft End	Cast Ducts	Pour* Wt. (lb)	Remarks
4490-19	Two-piece	Shell	350	1800	Net Shape	No	35	Feeding ribs used (4) Good quality
-20	Two-piece	Shell	350	1800	Net Shape	No	34	Feeding ribs used (4) Good quality
-S21	Two-piece	Shell	350	1800	Net Shape	No	34	Added stock Feeding ribs used (6) Good quality

* Raw casting weight compares with forging weight of 65 lb

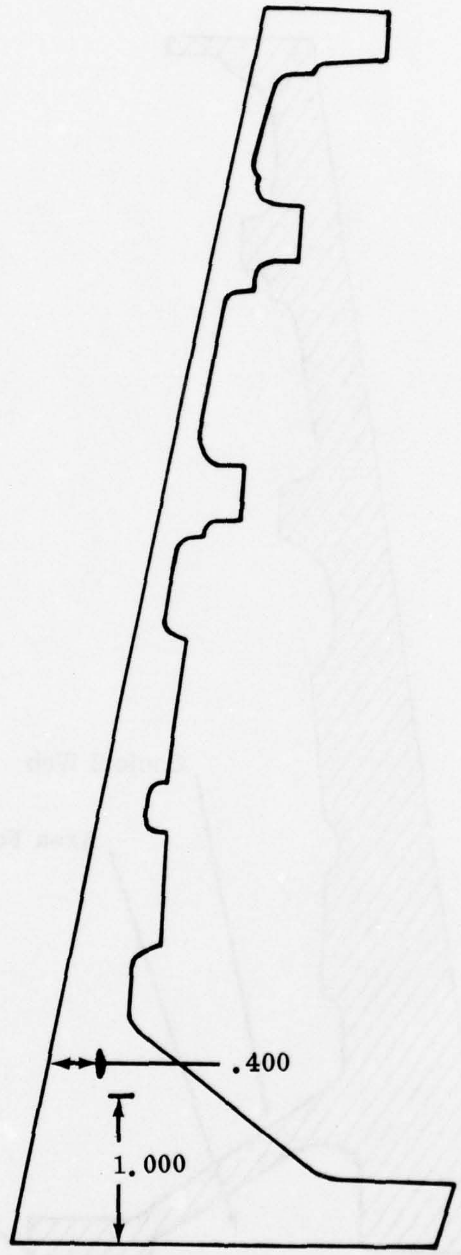

Figure 17. Shrinkage Cavity Location

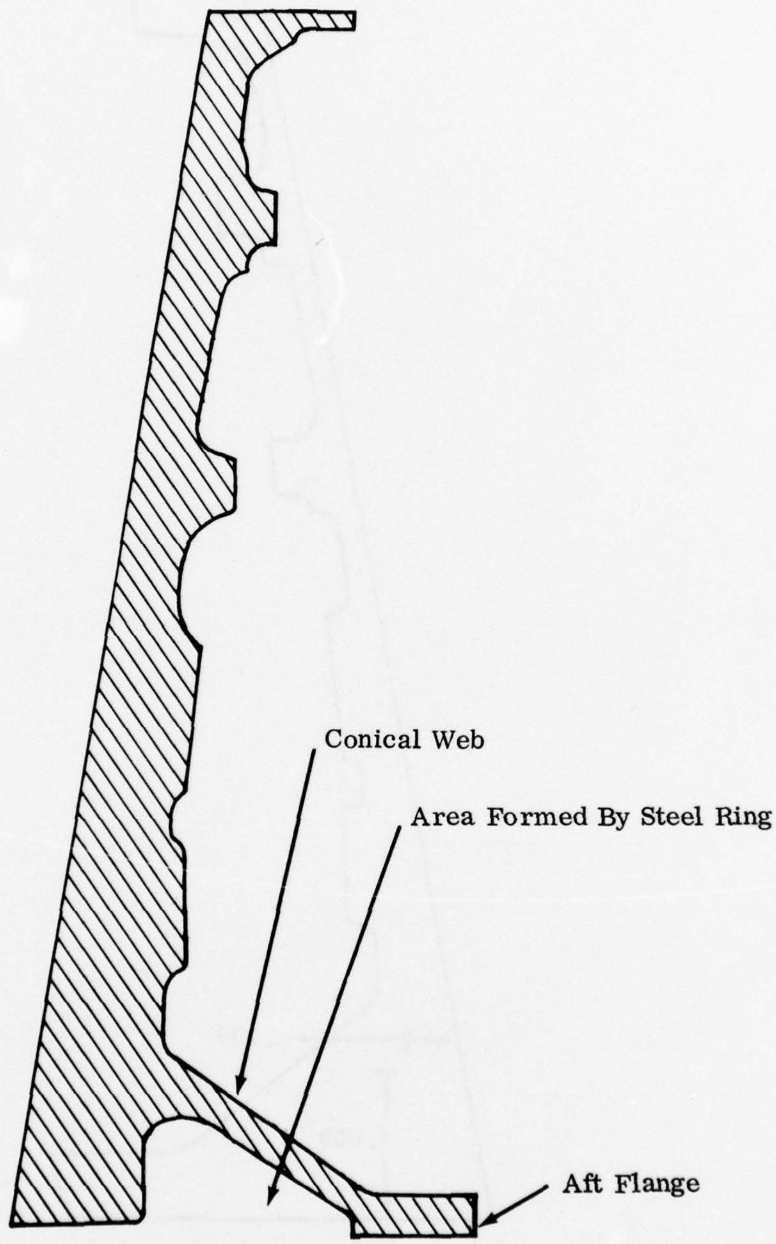

Figure 18. Cross Section of Net Shape Casting Formed by Steel Ring

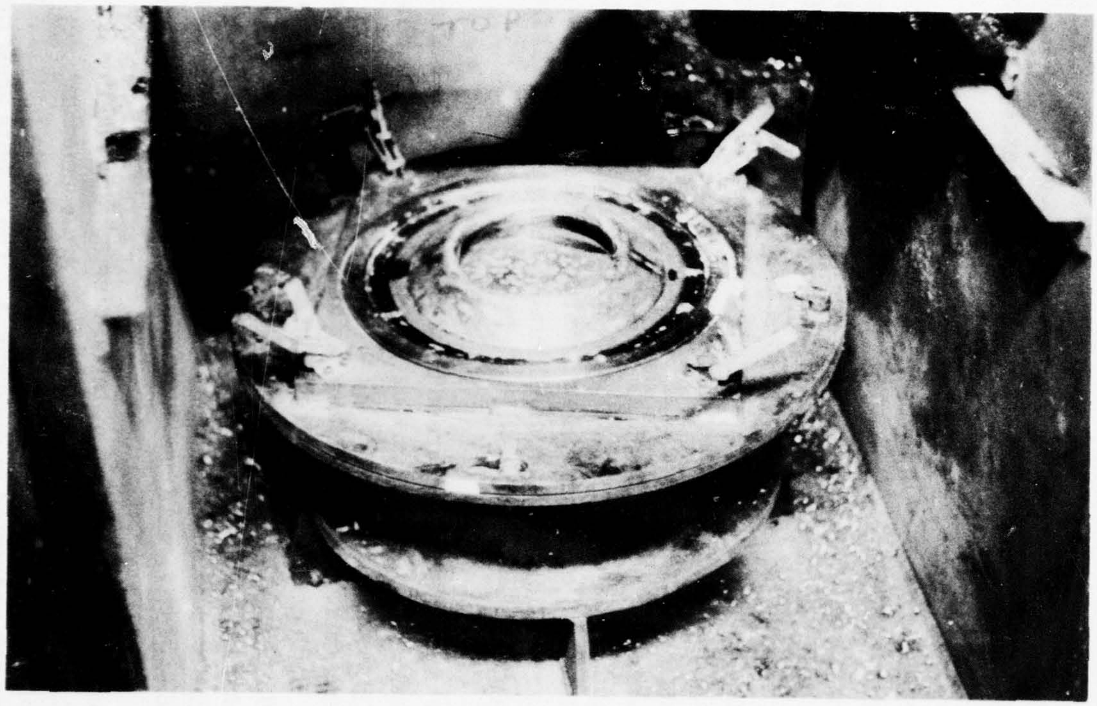

Figure 19. Steel Ring Mounted on Centrifuge

Two centrifuge angular velocities, 200 and 400 rpm, were used on these pours. The resulting castings did not contain shrinkage cavities but did have small shrinkage indications in the aft flange outer diameter and in thick sections such as the horizontal flanges. In addition, the 200 rpm speed was shown to be insufficient to fill completely the forward end of the casting. It was concluded that the steel ring was causing excessive chilling of the molten metal and that a net shape aft end would have to be made an integral part of the shell mold in order to prevent this condition. The 400 rpm gave good mold filling without excessive centrifuge vibration.

One casting (4490-S8) was made with three air bleed ducts cast integrally. Tooling was constructed to produce separate duct patterns which were wax welded onto the main body pattern. The resulting casting with integral ducts is shown in Figure 20. The wall thickness of the ducts was measured as .075 after chemical milling. This is over twice the thickness of the present sheet metal ducts and was felt to be necessary to provide adequate metal flow to fill the ducts. Visual examination of the casting showed that the ducts had filled completely, but radiographic inspection revealed shrinkage indications well in excess of drawing limits in the flanges at the duct tips. The result of casting the ducts integrally showed promise, and it was decided to conduct further trials in Phase IA (described later in this report) on a parallel and noninterference basis with the main program, since it was anticipated that considerable changes in metal feeding would have to be made.

One part (4490-S10) was cast with reduced poured metal weight (31 pounds compared to 35 pounds for previous castings) in an attempt to reduce the amount of material to be removed during the rough machining operation. This would lead to lower material and machining costs but would also represent a reduction in gating volume. Radiographic and visual inspection of the inner surface showed that the cavity shrinkage previously encountered was still present but was closer to the inner diameter surface, making machining clean-up marginal. It did not appear that the small reduction of metal weight was justified since the risk of scrapped parts and excessive weld repair would definitely be increased.

To provide a source of specimens for materials tests, four additional castings were poured using the conditions of S/N 4490-S7. After annealing, test specimens were machined from them. Complete information relative to material tests and the results obtained are presented in Appendix A. The results show that all casting properties are fully adequate for the application.

The pattern of heat flow at the aft end of the casing immediately after the molten metal filled the mold is shown in Figure 21. Since the thermal conductivity of

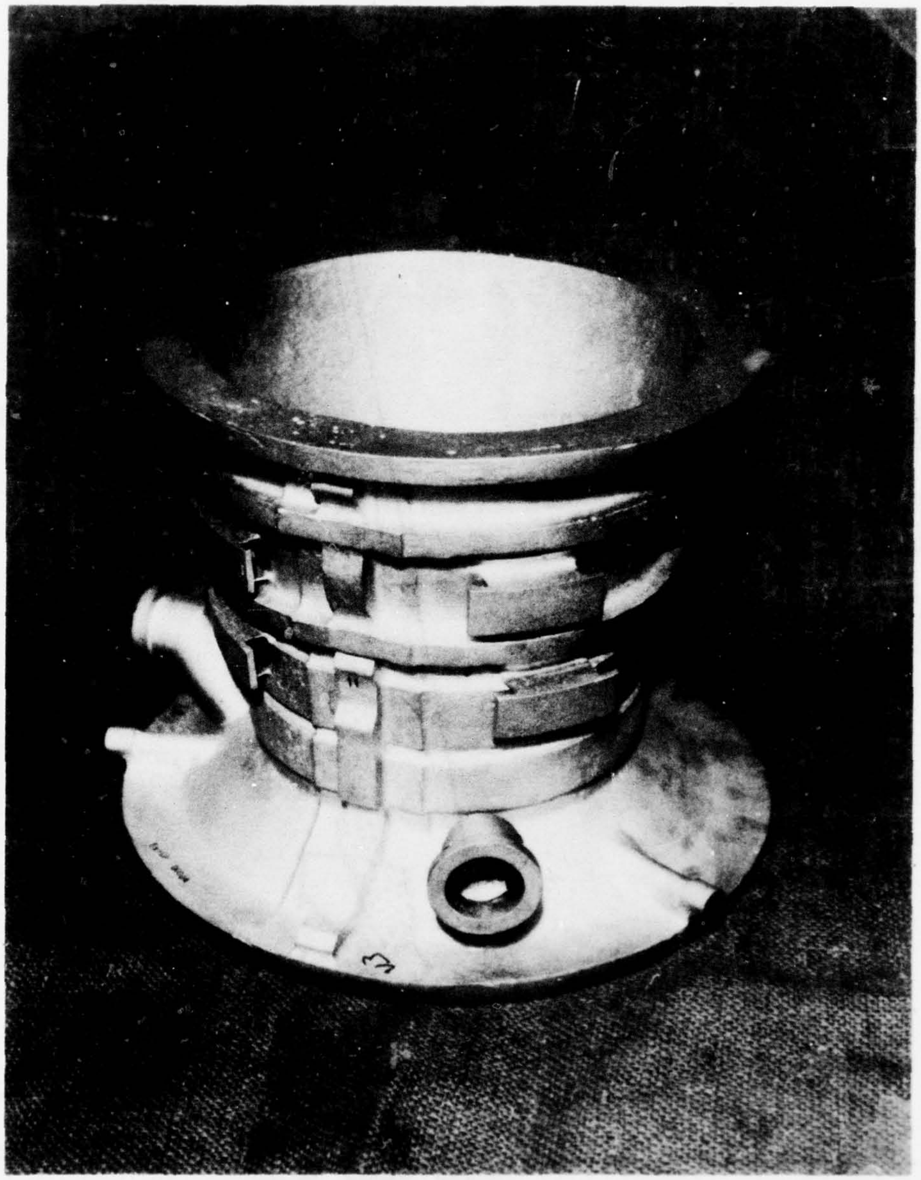

Figure 20. Compressor Casing with Integral Air Ducts Made from Temporary Tooling

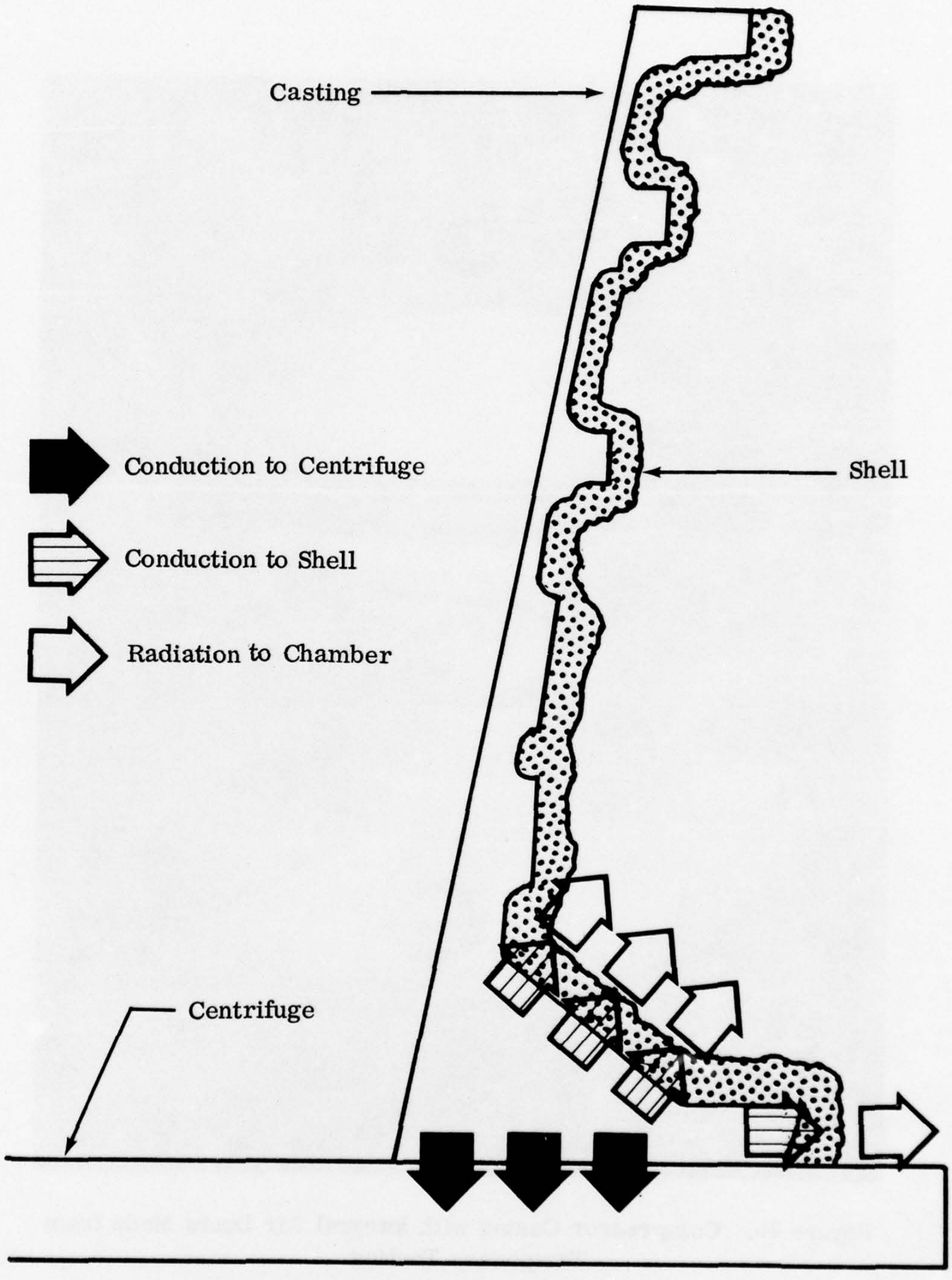

Figure 21. Heat Flow in Casing Aft End

the steel centrifuge plate was on the order of 12 times that of the ceramic shell material at the pouring temperature, and since the mass of the centrifuge was several times that of the shell, it is apparent that excessive heat was being lost in the axial direction to the centrifuge through the open bottom of the mold. The effect of this heat loss was to counteract the desired directional solidification pattern in which the outer diameter of the aft flange would solidify first with freezing progressing radially inward. Conduction to the centrifuge caused rapid axial freezing progressing in the forward direction. These competing heat flows were seen as the major reason for the presence of the shrinkage cavity problem, since the inner diameter area was forced to solidify too rapidly and molten metal was not available to act as a reservoir to compensate for the volumetric shrinkage occurring upon solidification in the balance of the casting.

An additional concern on the previous castings has been minor surface imperfections (cold shuts and flow lines) which have appeared on the outer casing contour. This condition resulted from molten metal entering the mold, striking the flat spinning centrifuge plate and spraying droplets against the cooler mold wall, causing immediate freezing of the droplets. At the completion of pouring, the last metal to enter did not remelt the frozen droplets (since it was quite close to the solidus temperature) and a surface imperfection resulted.

As a result of both the shrinkage cavity and splash conditions, a mold similar to that shown in Figure 22 was constructed and used for casting 4490-S16. Sheet wax was used to form a bottom on the wax pattern and a wax "dome" was formed on the centerline. When the shell was built these features became integral parts of the mold. When the mold was placed on the centrifuge, a layer of fibrous insulating material was placed between the mold and centrifuge. The purpose of the mold bottom and insulation was to reduce axial heat losses, and the purpose of the dome was to "split" the incoming metal steam and direct it radially outward.

Radiographic evaluation of casting 4490-S16 revealed that the shrinkage cavity was greatly reduced in size and shifted aft. When the casting was sectioned after rough machining, the cavity was found to be in excess of .125 inch below the inner surface and hence it would not be fully removed during finish machining. The surface finish of the casting was greatly improved over previous efforts and would easily meet the 125 RMS planned drawing requirement.

An additional casting (4499-S14) was made in an attempt to form the aft end web close to net shape. The steel ring that was previously used in an unsuccessful attempt to cast the .200-inch nominal thickness web was mounted farther aft in this trial to provide a .500-inch nominal web. This was a compromise between a net shape aft end and a completely solid aft end. As with earlier attempts to

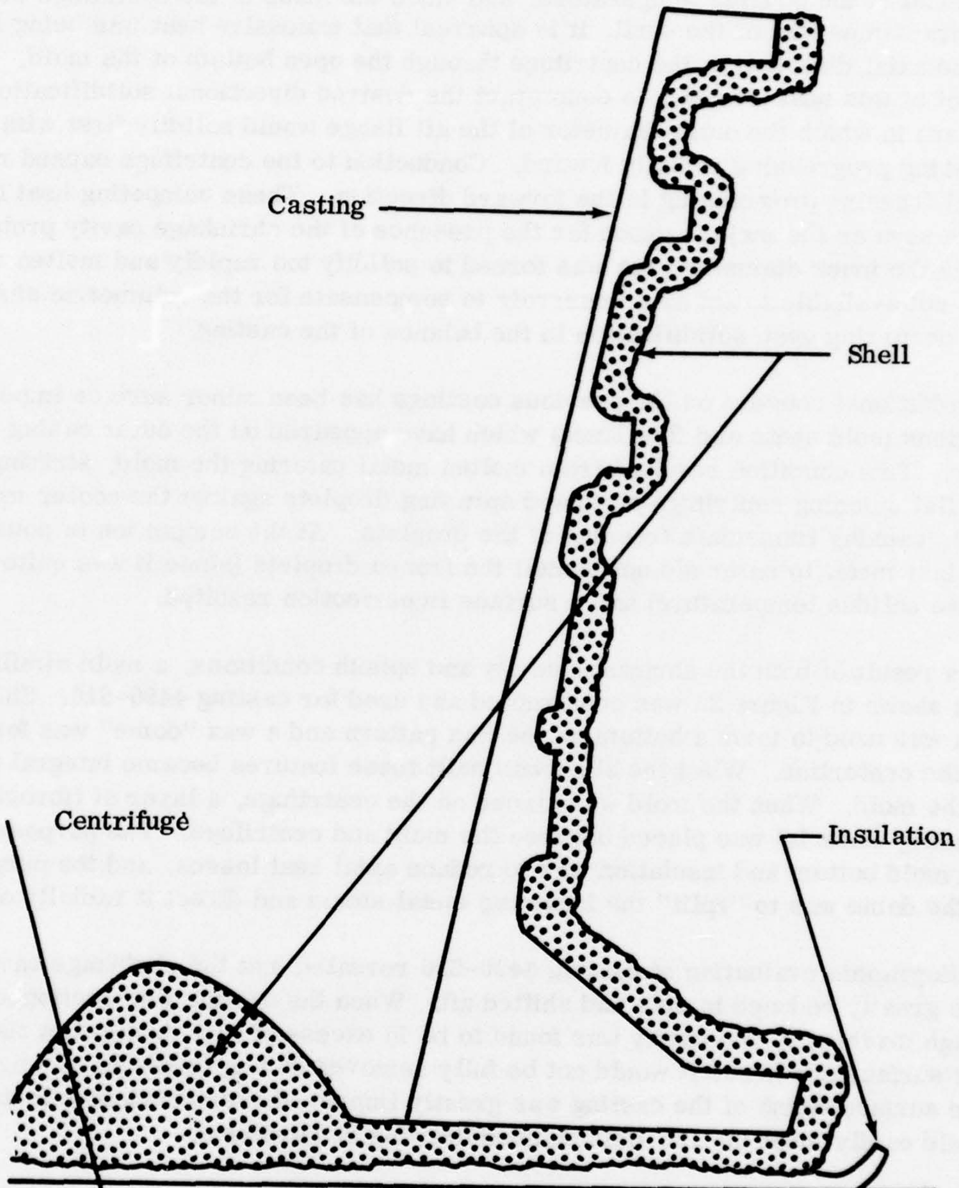

Figure 22. Ceramic Shell Mold with Dome and Insulation

use the steel ring the aft outer flange showed numerous shrinkage indications, indicating that metal was being chilled excessively while flowing over the ring. It was concluded that future attempts to form a net shape or near net shape aft end would require the aft web to be formed by the mold rather than by a steel ring.

For the next casting (4490-S18), the temporary tooling was modified as shown in Figure 23 to incorporate a ring in the pattern die and form a net shape pattern (shown in Figure 24). When casting 4490-S18 was poured, the shrinkage cavity found on previous castings was eliminated but a side effect to the change was a small amount of centerline shrinkage indications in the borescope bosses and the horizontal flanges. A similar but more severe condition existed when attempts were made on previous castings to feed through the .200-inch-thick conical section.

In order to permit more efficient feeding of the borescope bosses and split flanges, it was decided that the next castings to be poured would incorporate ribs as shown in Figure 25 to accomplish this. Castings 4490-S19 and S20 had feeding ribs attached and gave the best soundness of any method used to this point. Both the shrinkage cavity and centerline shrinkage indications were eliminated. It was decided to incorporate the supplemental feeding ribs in the pilot production castings to be made from permanent tooling.

On the last casting to be poured from temporary tooling (4490-S21) a design change was incorporated to add extra stock as shown in Figure 26. This material addition resulted from a change in the mating part and requires a rabbet to be machined into the aft flange of the compressor casing more inboard than previously. It was felt that the added material could be a source of shrinkage indications, since it must be fed by metal passing through the .200-inch-thick conical section shown in Figure 26. Radiographic inspection of 4490-S21 showed that the aft flange did have shrinkage indications which were larger than in previous castings but that in the area of the feeding ribs the flange was free of defects. To establish the properties of the cast alloy and to verify their adequacy for use in the compressor casing, test specimens were machined from castings after annealing (2 hours at 1300°F in vacuum). The tests are described in Appendix A.

3.1.2.2 Tooling and Fixtures

Pilot production wax pattern tooling was designed and built using the data gathered in Phase I - Task I. The die, shown with the top plate removed in Figure 27, was machined from aluminum and contains the basic outer casing contour, the eight actuator pads, two borescope bosses and three bosses to which the air bleed

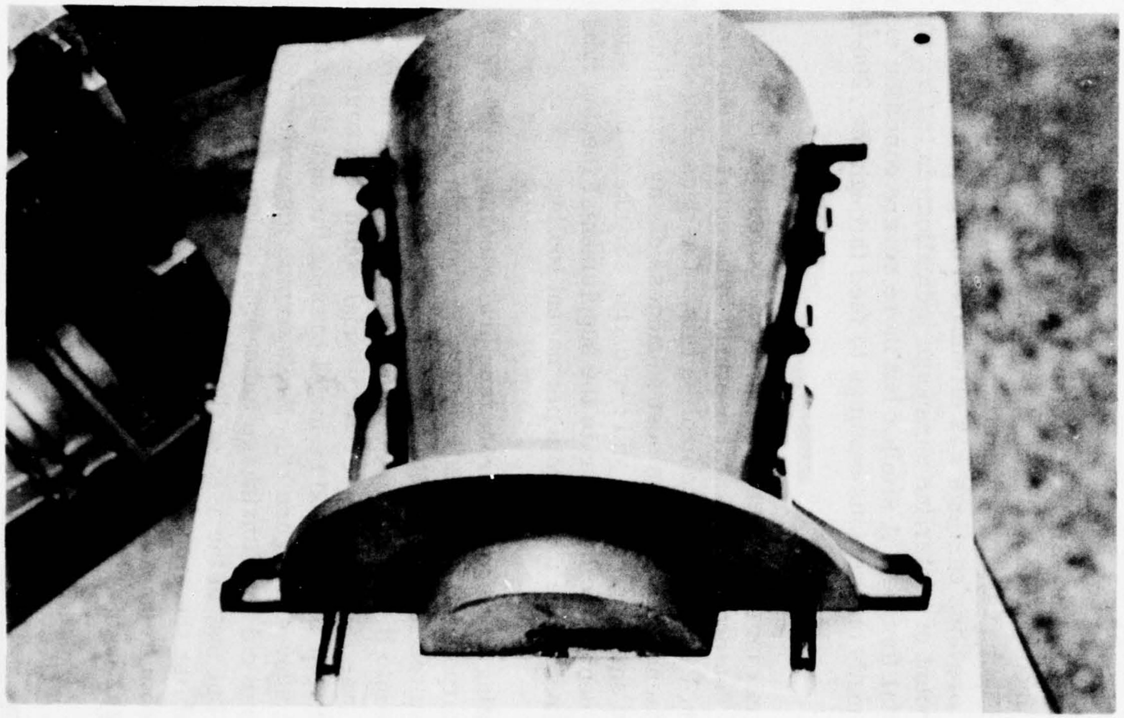

Figure 23. Temporary Tooling Modified to Produce Net Shape Aft End

Figure 24. Net Shape Wax Pattern Made from Temporary Tooling

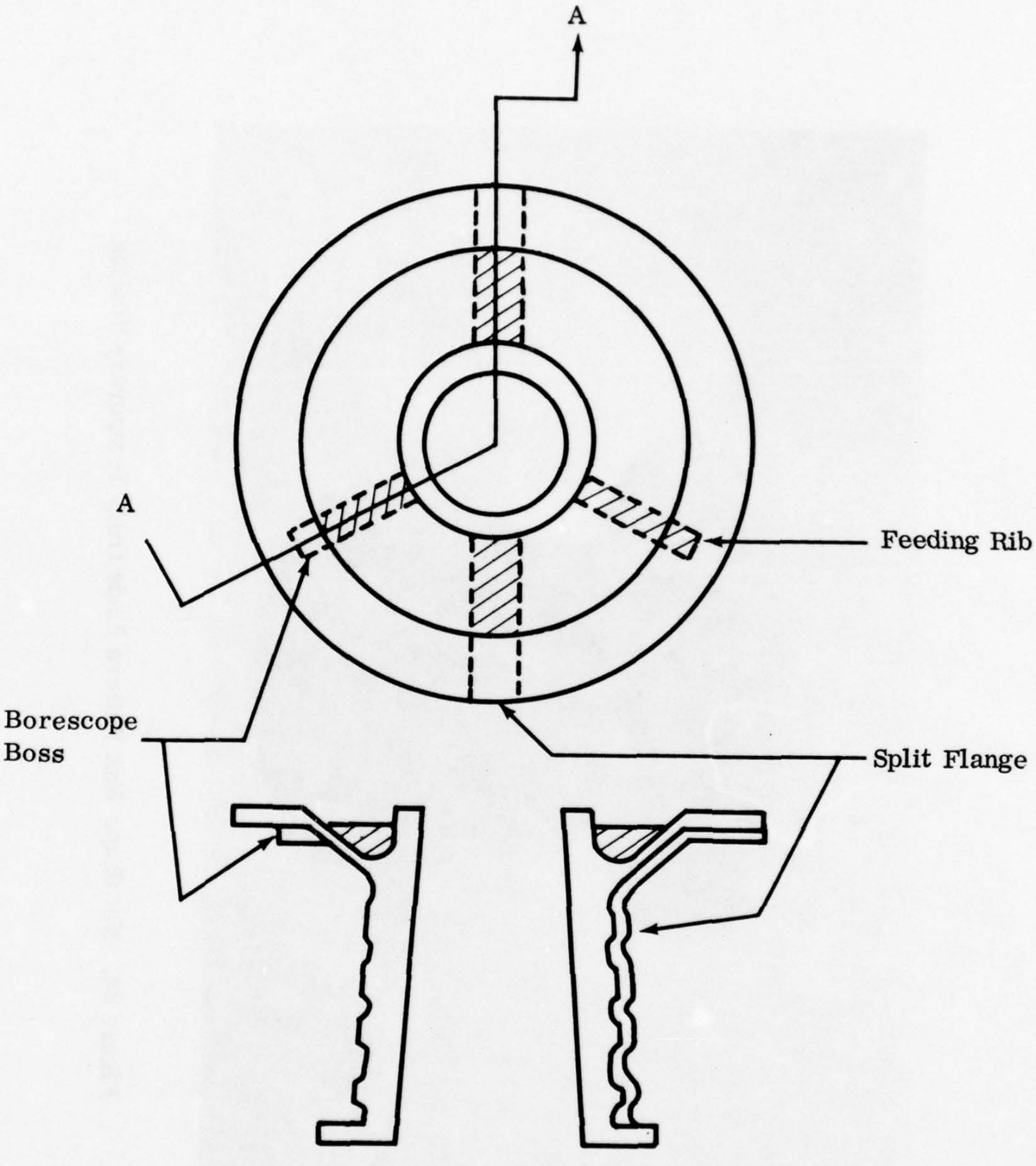

Section A - A

Figure 25. Use of Ribs to Feed Heavy Sections

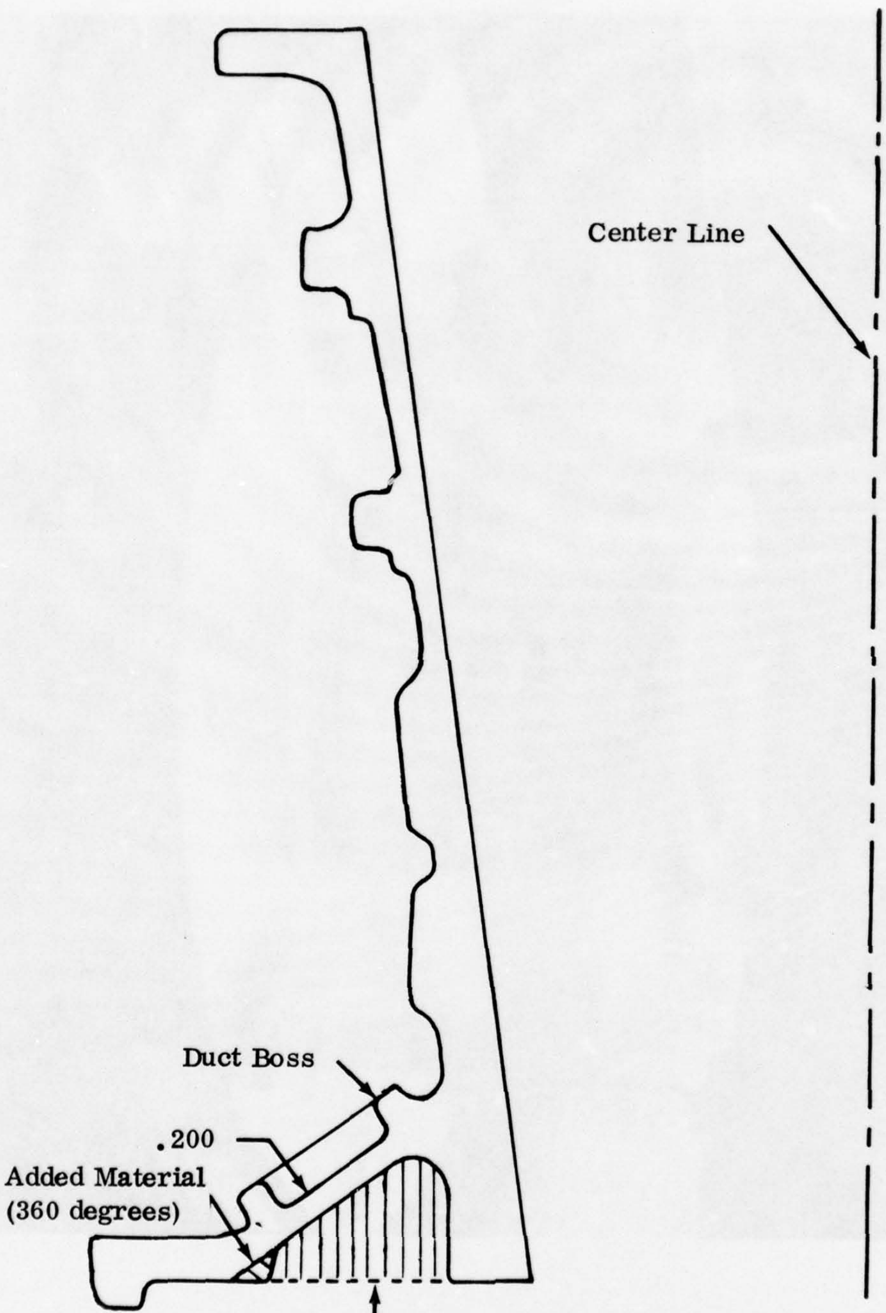

Figure 26. Modified Shape of Casing Aft End

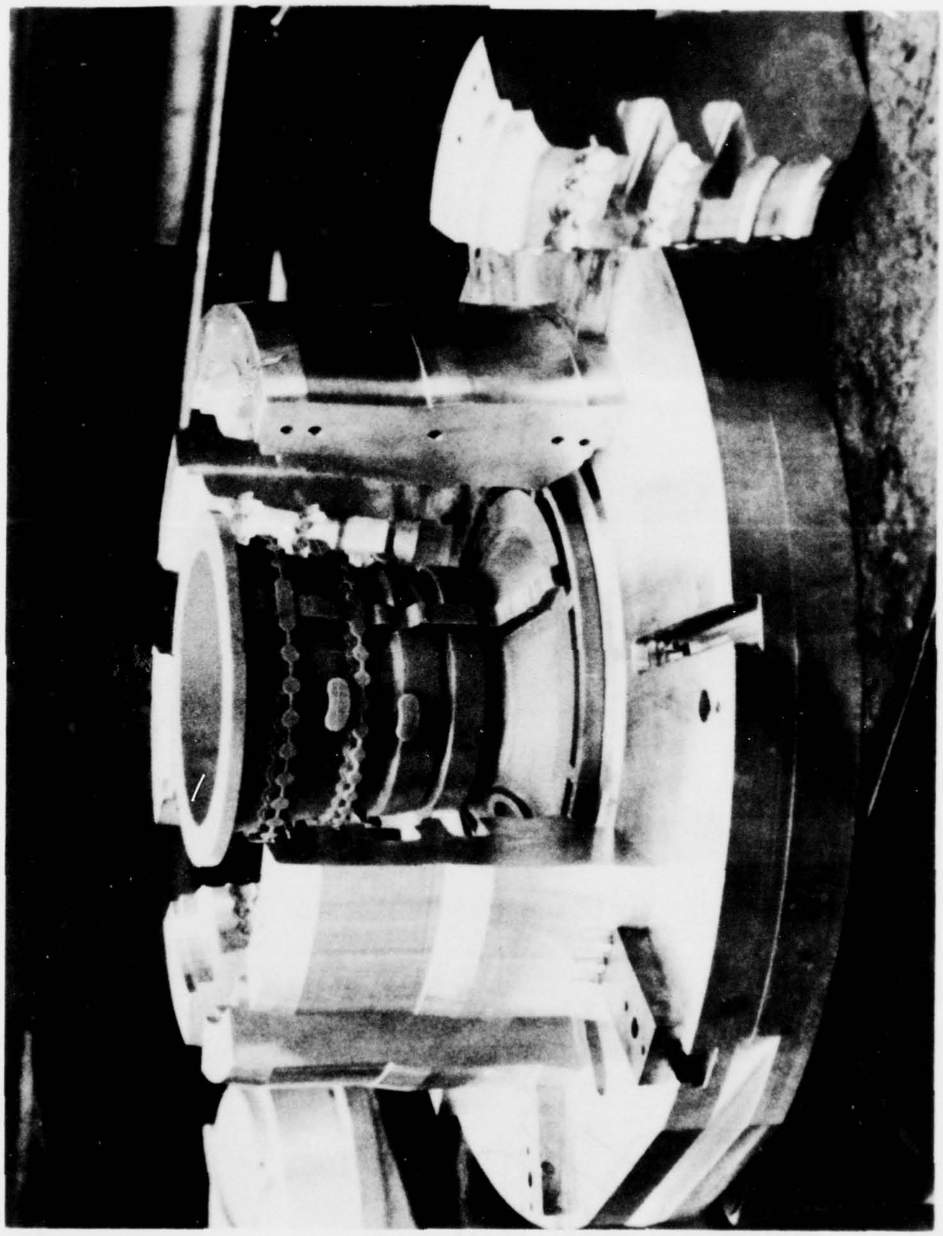

Figure 27. Pilot Production Pattern Tooling with Wax Pattern

ducts are welded. The stage 2 actuator pads are formed by removable aluminum inserts (2 per pad) and the stage 1 actuator pads are formed by solid inserts (1 per pad) and soluble wax cores (1 per pad) due to the impossibility of withdrawal of a solid insert on one side of the pad. The solid inserts and soluble wax cores are shown in Figure 28.

An inspection fixture was built and installed at the subcontractor's plant. The fixture was capable of holding the casting on the primary, secondary and tertiary datum points and sweeping the outer contour with a template made .025 larger than the nominal casting contour. The gap between template and casting could then be measured with go/no-go ball gages to determine the true outer contour. This concept is shown in Figure 29.

While sound in theory, this fixture proved to be slow in operation and not capable of measuring all areas of the casting. The design was simplified to one which simply held the casting in contact with the datum points. The outer contour of the casting nested in the fixture was then measured on a three-axis computer-controlled measuring machine. This arrangement allowed a complete inspection of the outer contour of both halves of a casting to be performed in approximately one hour, compared to at least one working day for the manual inspection.

Based upon previous work, all permanent tooling castings were poured using a mold preheat of 1800°F and a rotational speed of 350 rpm. Casting variables on pilot production castings are given in Table 2. A view of the first casting, 4580-S1, is shown in Figure 30. After the first four castings were poured, dimensional inspection was performed. Since the inspection fixture was not completed at this time, diameters were checked using conventional layout techniques in order to obtain a measure of casting size. The nominal diameters are given in Figure 31 and the actual measured diameters are shown in Table 3.

Considerable dimensional variation is evident in the diameters of the first four castings (4580-S1, -S2, -S4 and -S5) indicated in Table 3, particularly when the diameters at the casting aft area (e. g., 7.032 diameter) are compared to diameters in the forward area (e. g., 8.660 diameter). It is evident that a greater amount of contraction as a result of solidification occurred at the aft end than at the forward end. In addition, there is a total range of .065 between the largest and smallest of the four castings measured at the 7.032 diameter. The diametral variation was traced to wall thickness variations in the four castings which exist for a number of reasons. Among these reasons are:

1. Metal temperature variations causing differences in metal fluidity.

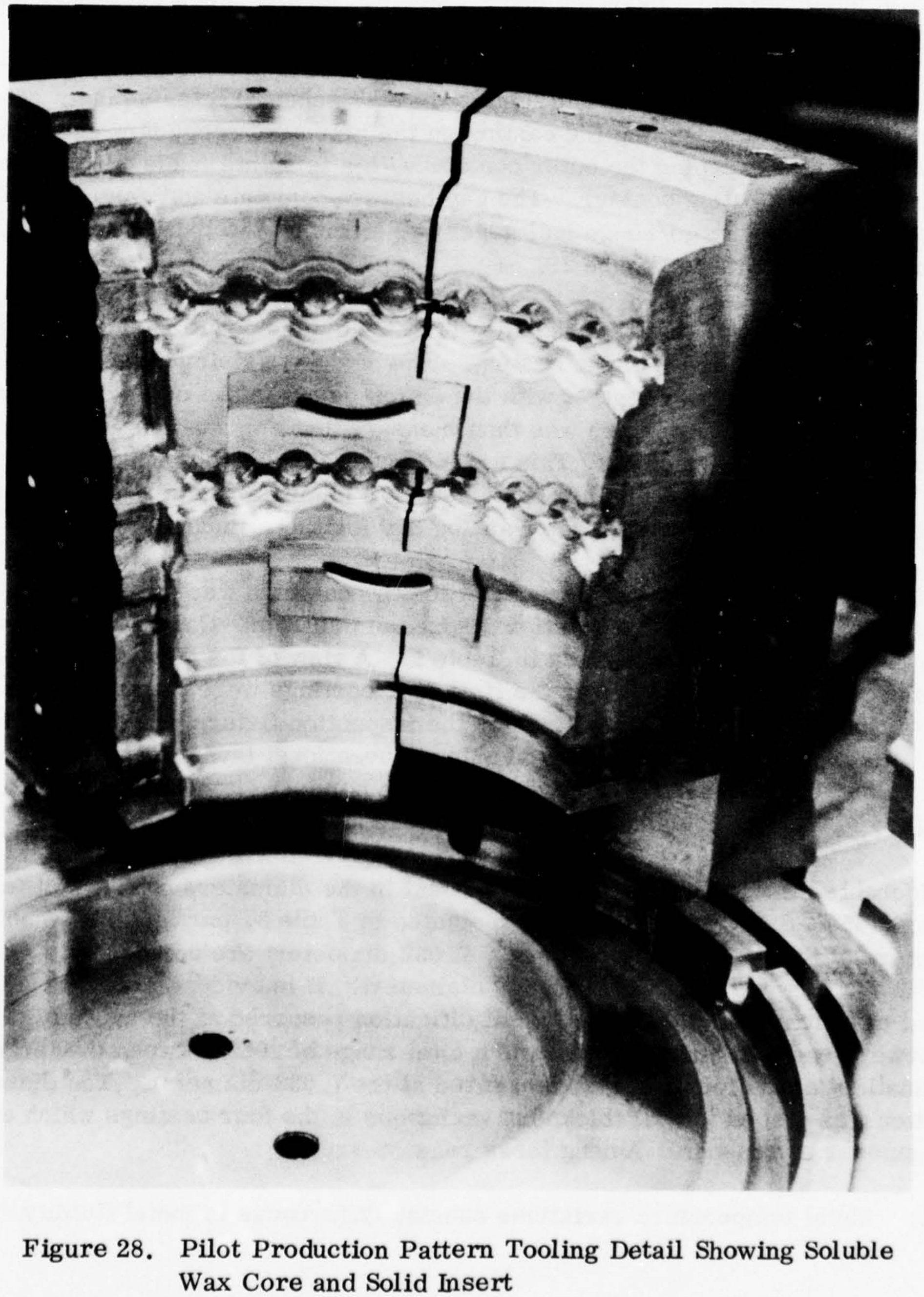

Figure 28. Pilot Production Pattern Tooling Detail Showing Soluble Wax Core and Solid Insert

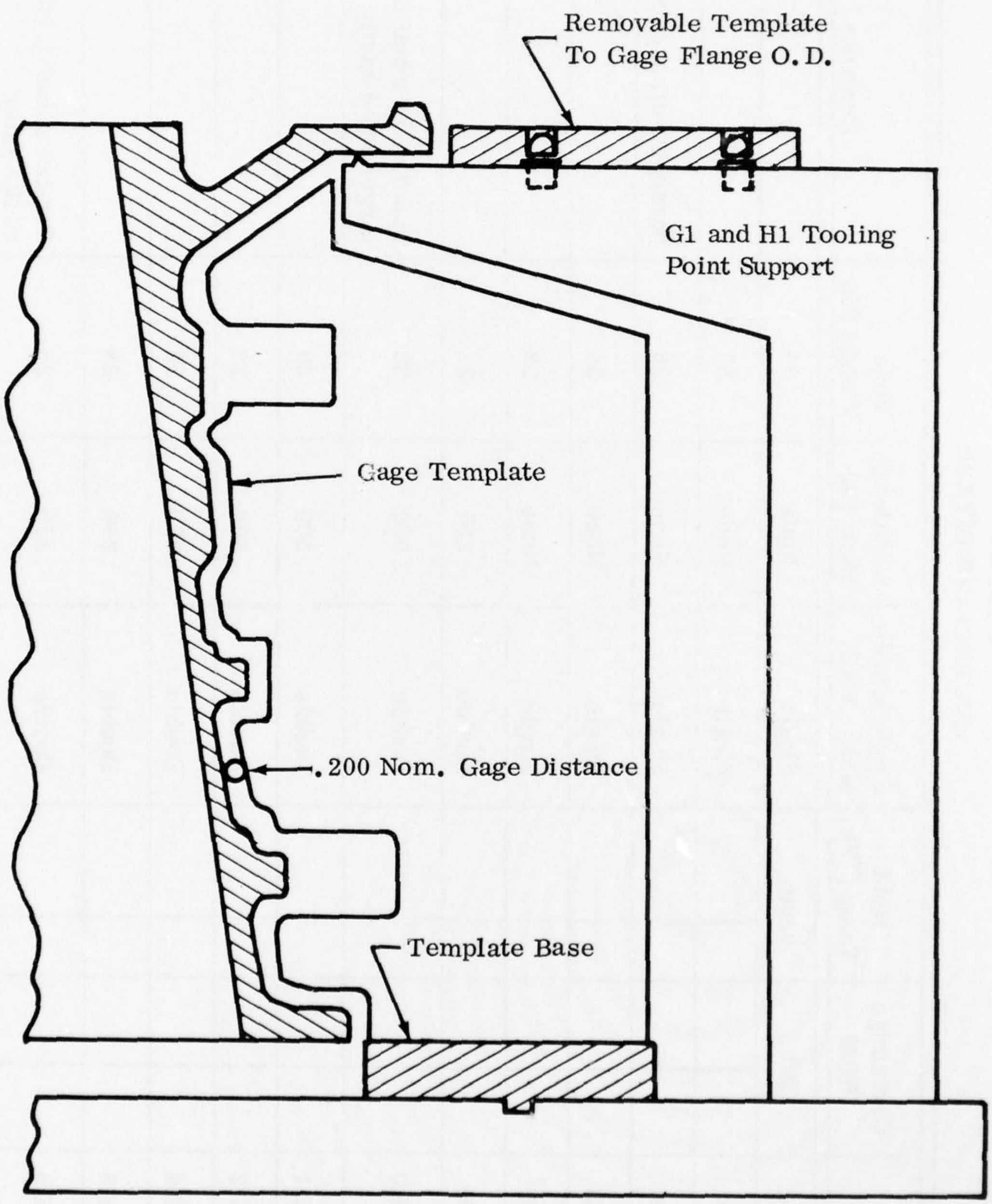

Figure 29. Inspection Gage Concept

TABLE 2
POURING CONDITIONS

S/N	Centrifuge RPM	Mold Temp (^{o}F)	Single/double Mold Wall	Additional Stock (in)	Pour Weight (lb)	Remarks
4580-S1	350	1800	Single	None	34	
-S2			Single	None	35	
-S4			Single	None	36	Scrapped-cracked mold
-S5			Single	None	34	
-S7			Single	None	33	
-S9			Double	.250	33	
-S10			Double	.500	28	Insufficient metal to fill larger mold cavity
-S11			Double	.500	28	
-S12			Double	.500	28	
-S14			Double	.250	28	
-S16			Double	.250	28	
-S19			Double	.250	28	Conical sprue/1.000 radial gates

TABLE 2 (CONTINUED)
POURING CONDITIONS

S/N	Centrifuge RPM	Mold Temp (^oF)	Single/double Mold Wall	Additional Stock (in)	Pour Weight (lb)	Remarks
4580-20	350	1800	Double	.250	28	Good radiographic soundness
-22			Double	.250	28	
-24			Double	.250	28	

Figure 30. Pilot Production Casting

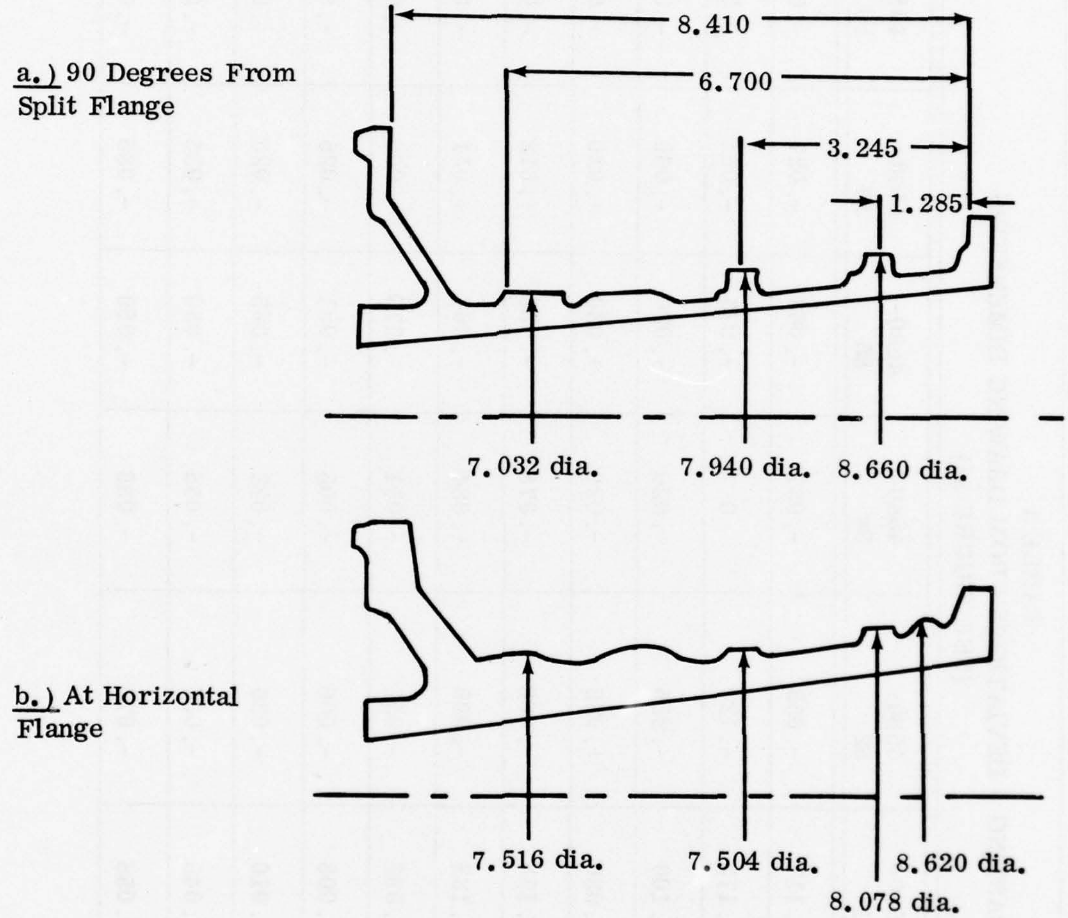

Figure 31. Casting Dimensions Measured During Preliminary Inspection

TABLE 3
CASTING - DEVIATIONS FROM DRAWING DIMENSIONS
(SEE FIGURE 31)

Drawing (in.) Dimension	4580-S1	4580-S2	4580-S4	4580-S5	4580-S7	4580-S9
7.032 Dia.	-.117	-.052	-.057	-.062	-.027	-.020
7.940 Dia.	-.175	-.120	0	-.075	-.005	-.002
8.660 Dia.	-.100	-.055	+.020	-.020	-.060	-.033
8.620 Dia.	-.030	+.025	-.025	+.030	+.030	+.010
8.078 Dia.	-.118	-.068	-.078	-.028	+.012	-.023
7.504 Dia.	-.139	-.099	-.084	-.064	+.011	-.029
7.516 Dia.	-.096	-.051	-.051	-.079	-.006	-.036
1.285 Dia.	-.008	-.006	-.005	-.001	-.025	-.029
3.245 Dia.	-.010	-.030	-.022	-.025	-.025	-.023
6.700 Dia.	-.045	-.057	-.055	-.050	-.035	-.010
8.410 Dia.	-.058	-.073	-.035	-.090	-.035	-.036

TABLE 3 (CONTINUED)

Drawing (in.) Dimension	4580-S10	4580-S11	4580-S12	4580-S14	4580-S16
7.032 Dia.	-.089	-.102	-.077	-.045	-.045
7.940 Dia.	-.095	-.090	-.080	-.058	-.025
8.660 Dia.	-.085	-.060	-.075	-.046	-.042
8.620 Dia.	+.005	-.050	+.030	+.016	-.010
8.078 Dia.	+.012	-.058	+.002	-.041	-.057
7.504 Dia.	+.026	-.021	+.011	-.032	-.051
7.516 Dia.	+.014	+.009	-.011	-.013	-.019
1.285 Dia.	-.020	0	-.020	-.001	-.013
3.245 Dia.	-.023	-.002	-.005	-.004	-.014
6.700 Dia.	-.030	-.026	-.040	-.035	-.034
8.410 Dia.	-.045	0	-.030	-.025	-.038

TABLE 3 (CONTINUED)

Drawing (in.) Dimension	4580-S19	4580-S20	4580-S21	4580-S24
7.032 Dia.	-.032	-.053	-.009	+.003
7.940 Dia.	-.040	-.077	-.046	-.020
8.660 Dia.	-.050	-.105	+.028	-.028
8.620 Dia.	+.027	+.055	-.055	+.003
8.078 Dia.	0	+.025	-.078	-.025
7.504 Dia.	-.001	+.022	-.040	-.009
7.516 Dia.	-.046	-.025	-.018	-.051
1.285 Dia.	-.005	-.025	0	-.010
3.245 Dia.	0	-.020	-.025	-.015
6.700 Dia.	0	-.035	-.013	-.025
8.410 Dia.	-.020	-.045	-.063	-.040

2. Mold temperature variations which also affect metal fluidity.

3. Rotational speed variations which can cause differing distributions of molten metal in the axial direction.

4. Differences in the amount of metal retained in the crucible and tundish.

The approach taken to control the dimensional variation on the next seven castings was to employ a central sprue as part of the mold as shown in Figure 32. The effect of this addition is to create a double-wall mold and, rather than allowing the inner surface of the casting to be formed by centrifugal force, to maintain the casting thickness constant between successive pours. When such a system was used on casting 4580-S7, it was observed that the contraction in diameter was much more regular (see Table 3). However, the observed wall thickness on this casting was insufficient to allow sufficient rough machining stock on the inner contour for removal of surface discontinuities and still provide finish machining stock. To correct this situation the patterns were modified on the next six castings to add additional inner diameter machining stock. On castings 4580-S9, -S14 and -S16 an extra .250 was added and on castings 4580-S10, -S11 and -S12 an extra .500 was added. The addition of .500 additional stock proved to be excessive, since filling the resulting mold cavity required more metal than it was possible to pour using existing equipment. The three castings with the additional .250 added had fully formed walls and were much improved dimensionally. In Table 3 the deviations from nominal blueprint dimensions for these castings are given.

Although the foregoing changes were beneficial from a dimensional standpoint, they caused a reintroduction of shrinkage indications in heavy sections, particularly the centerline of the horizontal flanges at the aft end. Although these areas were repairable by benching and welding, economic considerations dictated that the presence of these indications be eliminated in the casting process.

The approach taken to eliminate the heavy-section shrinkage is illustrated in Figure 33. The double-wall mold previously employed was modified to form a cylindrical central sprue, which had the effect of enlarging the lower end of the previously conical sprue, thus shortening the gates. The diameter of the

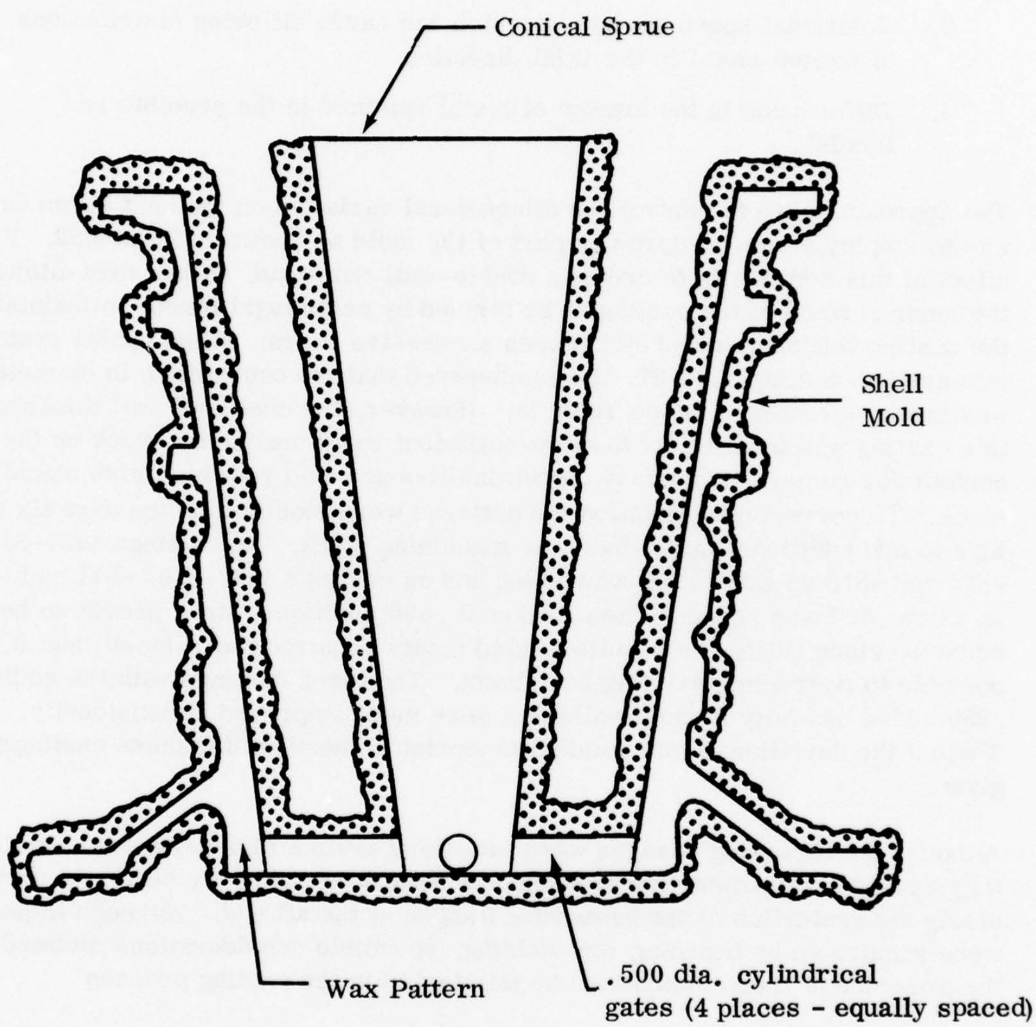

Figure 32. Double-Wall Mold (Initial Configuration)

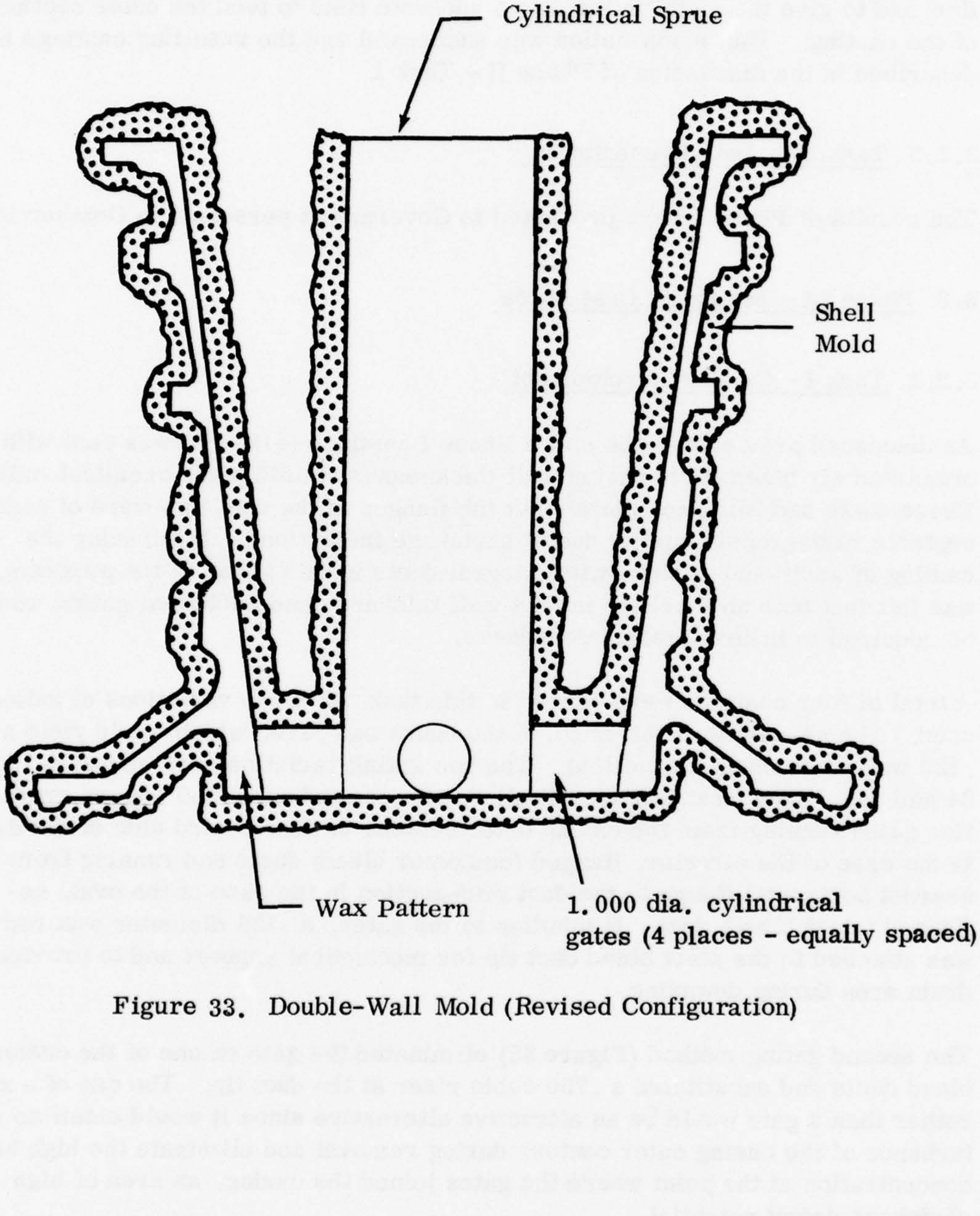

Figure 33. Double-Wall Mold (Revised Configuration)

gates was increased to 1.000 inch from .500 inch. Shortening the gates and increasing their diameter was designed to remove any restriction to molten metal flow and to give the metal in the sprue adequate time to feed the outer sections of the casting. This modification was successful and the resulting castings are described in the discussion of Phase II - Task I.

3.1.3 Task III - Data Presentation

The results of Phase I were presented to Government personnel in October 1977.

3.2 Phase IA - Integrally Cast Ducts

3.2.1 Task I - Casting Development

As discussed previously, one of the Phase I castings (4490-S8) was cast with simulated air bleed ducts having wall thicknesses of .075 after chemical milling. These ducts had filled completely but the flanges at the duct tips were of unacceptable radiographic quality due to shrinkage indications. In pursuing the casting of additional casings with integral ducts in this phase of the program, it was felt that both an increase in duct wall thickness and additional gating would be required to insure internal soundness.

A total of four castings were poured in this task, with two variations of gating used. The as-cast wall thickness of the ducts was .170, which would yield a .120 wall after chemical milling. The two gating variations are shown in Figures 34 and 35. In the first (Figure 34) all ducts were fed with .750 square cross-section gates running from the casing outer contour to the forward side of the ducts in the case of the circular, flanged (customer bleed) ducts and running from the nearest horizontal flange to the duct mid-section in the case of the oval, unflanged (start bleed) duct. In addition to the gates, a .125 diameter wax rod was attached to the start bleed duct tip for mechanical support and to provide a drain area during dewaxing.

The second gating method (Figure 35) eliminated the gate on one of the customer bleed ducts and substituted a .750 cubic riser at the duct tip. The use of a riser rather than a gate would be an attractive alternative since it would entail no disturbance of the casing outer contour during removal and eliminate the high heat concentration at the point where the gates joined the casing, an area of high shrinkage defect potential.

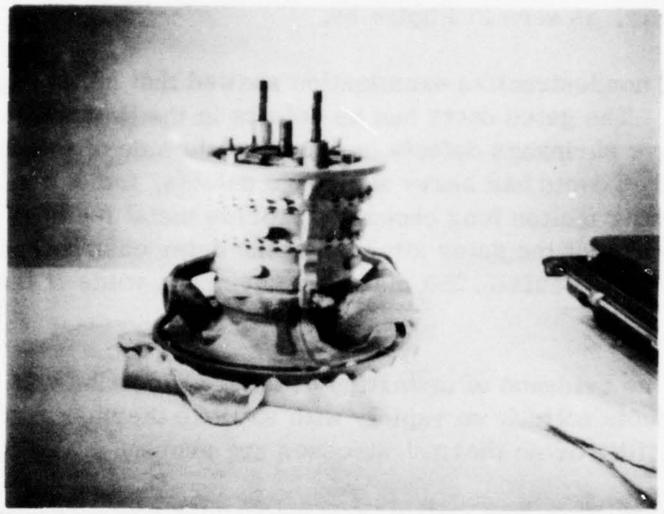

Figure 34. Pattern with Integral Ducts (Gating Method 1)

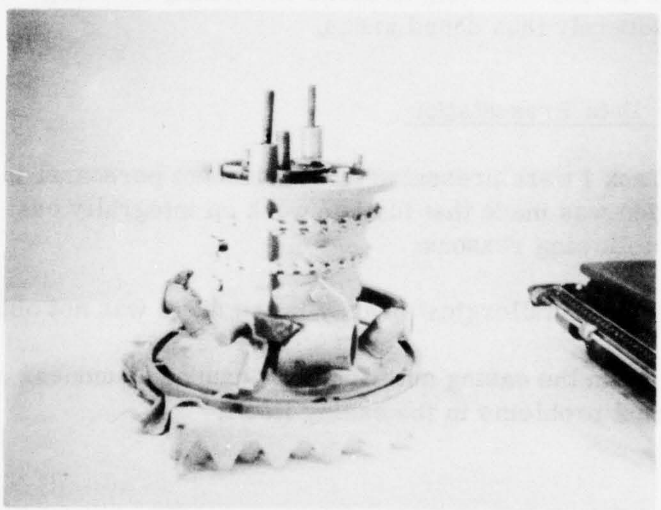

Figure 35. Pattern with Integral Ducts (Gating Method 2)

All four castings were poured using the process developed in Phase I. A mold temperature of 1800°F and a rotational speed of 350 rpm were used. All ducts filled successfully, as seen in Figure 36.

Destructive and nondestructive examination showed that neither gating system was acceptable. The gated ducts had no defects in the immediate vicinity of the gates but did have shrinkage defects on the opposite side of the duct from the gate. The risered ducts had heavy shrinkage defects, indicating that the risers were not remaining molten long enough to provide metal feeding. The most disturbing result was that the gates attached to the outer casing contour and to the horizontal flange had caused .250 diameter shrinkage voids at the point of attachment.

Dimensionally, no evidence of distortion of the duct location was found. It appears that the ducts solidify so rapidly with so little thermal gradient from casing to duct that little or no thermal stresses are present in the ducts.

In an attempt to produce duct wall thicknesses which are more acceptable from a weight standpoint, an as-cast casing with integral ducts was masked on all areas except the duct walls and .050 was chemically milled from the remaining surfaces. If successful, this would yield .070 thick ducts which would still be twice the present sheet metal duct thickness. The resulting walls were not acceptable since several areas were milled through the wall. This condition was due to thin areas in the as-cast wall and to areas containing shrinkage defects being attacked more severely than sound areas.

3.2.2 Task II - Data Presentation

The results of Task I were presented to Government personnel in February 1978. A recommendation was made that further work on integrally cast ducts be terminated for the following reasons:

1. Acceptable metallurgical quality in the ducts was not obtained.

2. Gating from the casing outer contour caused soundness and dimensional problems in the casing itself.

Figure 36. Casting with Integral Ducts

TABLE 4 - CASINGS WITH INTEGRAL DUCTS - POURING CONDITIONS

S/N	Centrifuge RPM	Mold Temp. (^{o}F)	Gating Method	Remarks
4631-S1	350	1800	.750 square gates on all ducts	Unacceptable shrinkage indications in duct walls
-S2				Shrinkage in casing outer contour at point of gate attachment
-S3 -S4			.750 square gates plus .750 cubic riser	

3. The required duct wall thickness would generate a weight penalty estimated to be in excess of .5 pound.

4. Extra labor costs involved with attaching and removing the extra gating made the inclusion of ducts of dubious economic benefit.

3.3 Phase II - Fabrication and Engine Test Evaluation

3.3.1 Task I - Fabrication of Engine Test Hardware

3.3.1.1 Permanent Tooling

Based upon the results of castings poured in Phase I, the pattern tooling was modified to provide a cylindrical central sprue, 1.000 inch radial gates, additional inner wall machining stock and feeding ribs at the aft end outer diameter as part of the wax pattern assembly. Since the additional gating capacity provided smoother metal flow, it was found that the dome in the center of the mold at the aft end which had been employed in Phase I castings to improve the surface finish was no longer required and this feature was not incorporated into the permanent tooling.

In order to provide more control on wax pattern size and shape, a simple mandrel conforming to the size and shape of the wax pattern as it is removed from the injection die was built. The mandrel is placed in the still warm pattern and the pattern is allowed to contract around the mandrel and maintain its size and shape as it cools. In addition, the aft flange of the wax pattern is clamped to a flat plate during cooling to maintain the flange flatness.

3.3.1.2 Pilot Production Castings

Four pilot production castings were poured to prove out the tooling modifications. Fluorescent penetrant and radiographic inspection showed that the parts met metallurgical requirements.

The entire casting process is outlined in the Manufacturing Methods Report, Appendix B of this report.

3.3.1.3 Dimensional Inspection

In order to obtain information on the degree of dimensional repeatability of the cast casings, the outer radial contour of the pilot production castings has been inspected on a Bendix three-axis computer-controlled measuring machine using a setup fixture to position the castings on the required datum points. The outer contour was inspected in detail since its variation has a direct effect on the final machined wall thickness variation.

The method of establishing the datum system for the cast casing is shown in Figure 37. Each casing half is dimensioned independently of the other and is joined to the other by the horizontal flanges which have a considerable amount of extra stock to allow for cutting and machining losses. As shown in Figures 37(a) and 37(b), two forward points at a fixed radial distance and orientation establish the center of a circle. Similarly, two aft points at a fixed radial distance and orientation establish the center of a second circle. The line connecting the two centers is the axis of the casing half. Note that we are establishing an axis and not a plane so that the casting can always be made to contact four locating pins at the set radii. The secondary datum is a plane passing through the axis and equidistant from the two circumferential datum points on the horizontal flange face. The distance from the circumferential points need not be a fixed value but merely equal at each horizontal flange so that the casting is oriented properly circumferentially. The tertiary datum is a plane perpendicular to the primary and secondary datums and passing through the axial point located at the Stage 1 variable vane bosses. These datums are used throughout the processing of the casing, since they are used to create pattern tooling, inspect castings and machine the finished part dimensions.

Inspection of the outer contour is performed by holding the casting in a fixture to locate the three datums and measuring radii. Figure 37(c) shows the results of checking contours that exhibit plus or minus deviations from the nominal radius. A perfectly round but small casting would show negative radial deviations from nominal at the horizontal flanges and positive deviations 90 degrees from the flanges. The situation would be reversed for a large casting. Of course, the effect of any actual out-of-roundness would be additive to the size effect.

In practice, the part is positioned in the fixture and clamped down, after which the first half contour is measured. The resulting readings give a combined measure of size and position since they are measured relative to a theoretically perfect circle whose axis is perfectly located on center.

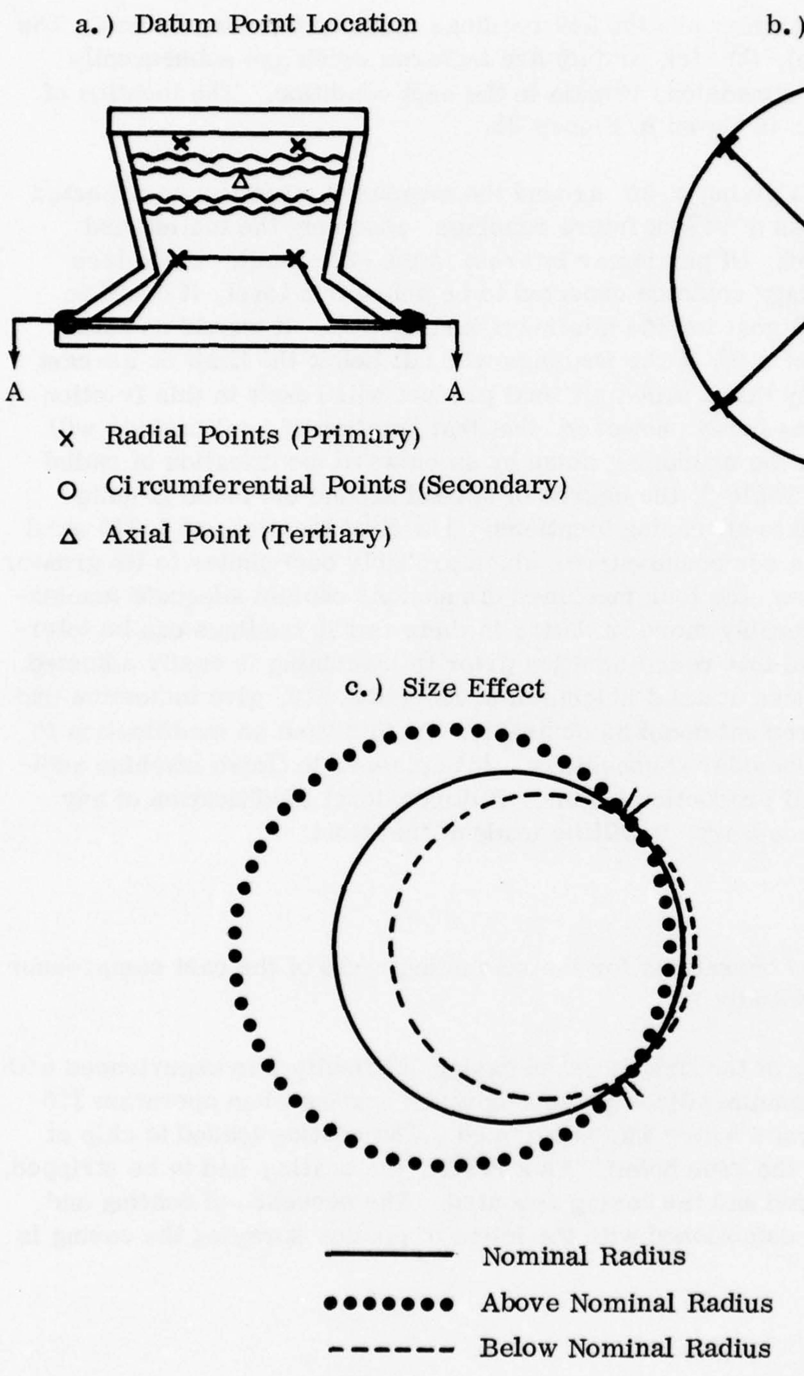

Figure 37. Casting Datum System and Effect of Size Variations on Apparent Roundness

The data in Table 5 summarizes the 540 readings made on 6 casing halves. The dimensions denoted (a), (b), (c), and (d) are features which are subsequently machined. All other dimensions remain in the cast condition. The location of the inspection stations is shown in Figure 38.

The column in Table 5 giving $\pm\ 2\sigma$ around the measured mean can be expected to encompass in excess of 95% of future readings, assuming the tooling and process are unchanged. Of particular interest is the -2σ limit. Since less than 2.5% of all readings could be expected to be below this level, it could be considered a practical goal for the minimum casting wall. It should be noted that the prediction that 2.5% of the readings will fall below the limit on as-cast casings does not imply that a thin-wall final product will result in this fraction of the casings. It does imply, however, that that fraction of total casings will need to be adjusted in the machining setup by an outward modification of radial position. As seen in Table 2, the degree of spread around the mean is quite uniform from forward to aft casing locations. The first location, at 1.315 axial height, is located on a compound curve, which probably contributes to its greater variability. In addition, the four machined dimensions contain adequate machining stock, and considerably more variation in their radial readings can be tolerated. Bearing in mind that radial position prior to machining is easily adjusted, only two locations, those at axial heights of 3.060 and 3.910, give indication that a future radial enlargement could be desirable. At this time no modification to these dimensions is considered necessary. It is planned to finish machine additional parts before full production begins. If dimensional modification of any area appears to be necessary, it will be made at that time.

3.3.1.4 <u>Machining</u>

A summary of planned operations for the machining cycle of the cast compressor casing is shown in Appendix B.

During the processing of the first finished casing, difficulty was experienced with adherence of the aluminum-silicon plasma-sprayed coating when operation 370 (drilling of variable vane holes) was performed. The coating tended to chip at the circumference of the vane holes. As a result, the coating had to be stripped, the flowpath reprepared and the casing recoated. The sequence of coating and finish machining was established with the intent of plasma spraying the casing in

TABLE 5 - SUMMARY OF MEASURED RADII ON SIX HALF CASINGS (SEE FIGURE 38)

Axial Height	Blueprint Radius	Measured Mean Radius $\bar{R}$	Measured Std Deviation σ	$\bar{R} \pm 2\sigma$	$\bar{R} \pm 3\sigma$
1.315	3.11/3.08	3.1184	.0131	3.145/3.092	3.158/3.079
2.160	3.341/3.311	3.3254	.0084	3.342/3.309	3.351/3.300
3.060	3.351/3.321	3.3321	.0092	3.350/3.314	3.360/3.304
3.910	3.432/3.402	3.4125	.0119	3.436/3.389	3.448/3.377
4.610	3.323/3.293	3.3154	.0103	3.336/3.295	3.346/3.284
5.165	3.800/3.760(a)	3.7798	.0109	3.802/3.758	3.812/3.747
5.710	3.473/3.443	3.4665	.0107	3.488/3.455	3.499/3.434
6.410	3.605/3.575	3.5946	.0092	3.613/3.576	3.622/3.567
7.125	4.160/4.120(b)	4.1272	.0082	4.144/4.111	4.152/4.103
7.810	3.874/3.844	3.8628	.0079	3.879/3.847	3.886/3.839
3.910*	3.750/3.730(c)	3.7478	.0084	3.765/3.731	3.773/3.723
5.710*	4.110/4.090(d)	4.1148	.0140	4.143/4.087	4.157/4.073

(a), (b), (c), (d) - Machined Dimensions

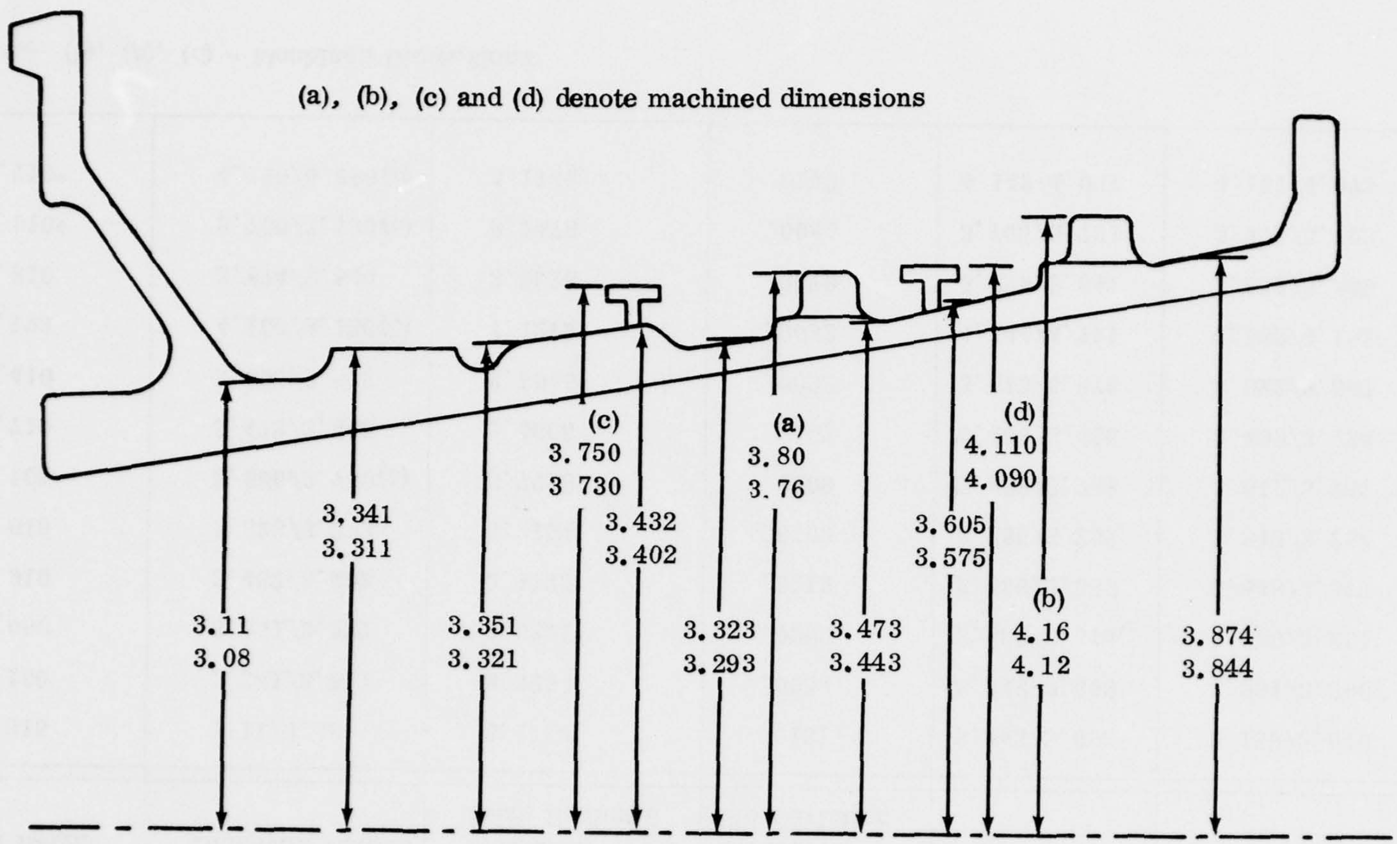

Figure 38. Casting Drawing Radial Tolerances

its most stable condition (as early as possible in the machining cycle) in order to minimize distortion. On the second finished casing, the sequence of operations was revised to call for preparation of the flowpath and application of the coating after all finish machining operations were complete. This resulted in perfect coating adherence and no flowpath distortion. Two views of the finished machined casing are shown in Figures 40 and 41.

The weight of the first and second finished machined and coated casings was 8.591 pounds and 9.042 pounds, respectively. This compares to an average weight of finished forged casings of 8.8 pounds, indicating that no significant weight penalty is associated with the use of a cast compressor casing. Figure 39 shows the improvement in material utilization.

3.3.2 Task II - Engine Test Evaluation

The two finished casings were assembled into test engines. The first casing was run for 60 hours in an endurance test. Views of the inner and outer contours of this casing are shown in Figures 42 and 43. At the time of assembly, rotor tip clearances were at nominal and typical of clearances that had been present on previous tests using forged casings. A very light local rub was in evidence, as is normal after engine disassembly, indicating that the dimensional stability of the cast casing is comparable with forged casings.

The second finished casing was assembled into a second maturity engine and was subjected to an official 150-hour endurance qualification test. The results of this test were equally as successful as the 60-hour test.

The 150-hour test was conducted in accordance with DARCOM-CP-2222-02000B, paragraph 4.5.1.6. The total operating time was 210 hours, 55 minutes and there were 164 starts involved in the test cycle. There were no unexpected incidents associated with the casing during test. Testing was conducted from 5 September 1978 to 19 September 1978.

The result of teardown inspection and any corrective action required are shown on pages 77 to 80.

3.3.3 Task III - Data Presentation

Dimensional, material property and cost data contained in this report were presented to Government personnel in a briefing.

	FORGING	CASTING
MATERIAL WEIGHT	65 LBS	35 LBS (AS-CAST)
FINISH WEIGHT	8.8	8.86 (AVERAGE-FIRST TWO PIECES)

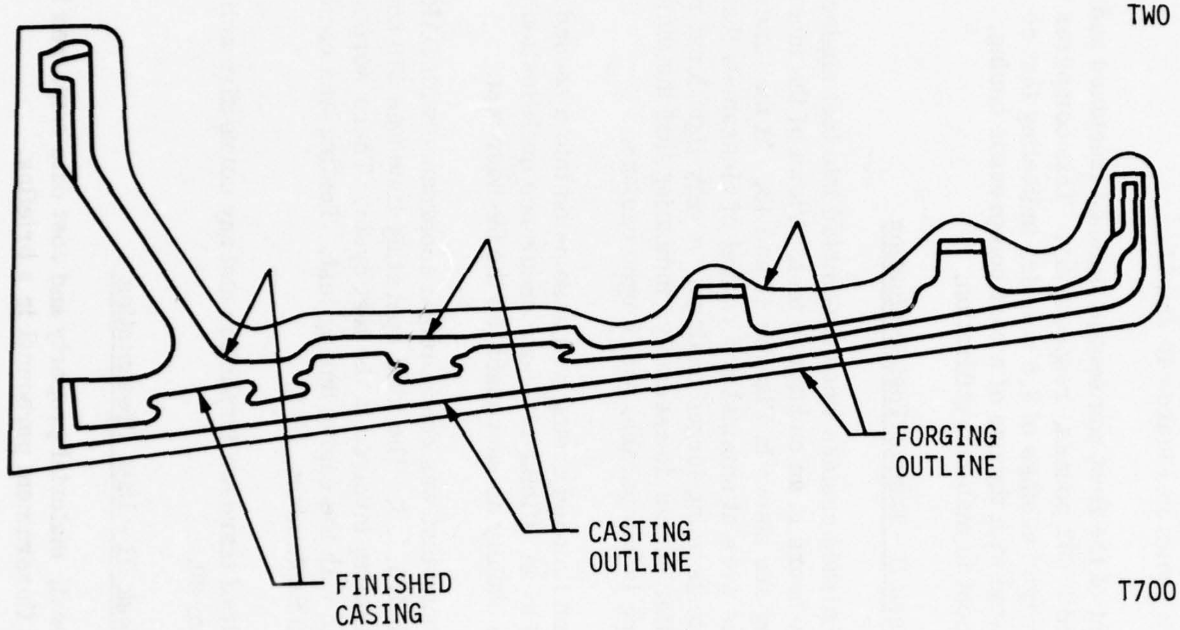

Figure 39. T700 Compressor Casing Casting vs. Forging

TEARDOWN INSPECTION

☐ PRELIMINARY FLIGHT RATING TEST ☒ QUALIFICATION TEST DATE 4 October 1978

1. ENGINE MODEL & SERIAL NO.: T700-207011-14A	2. ENGINE SECTION: Cold Module	3. VENDOR:	4. PART SERIAL NO.
5. PART NUMBER: 6039T04G01	6. PART NAME: Compressor Casing	7. HOURS ON PART: 150 Hr. (Qual)	

8. DISCREPANCY: (CODE: A-CRITICAL; B-MAJOR; C-MINOR)

☐ CORROSION	☐ FAILURE	☐ MISALIGNMENT	☐ WEAR
☐ CRACKS	☐ FASTENERS	☐ NICKS OR SCRATCHES	☐ MAGNETIC INSPECTION
☒ DEPOSITS	☐ F.O.D.	☐ OPERATION	☐ PENETRANT INSPECTION
☐ DISCOLORATION	☐ FRETTING	☐ PIECES MISSING	☐ X-RAY
☐ DISTORTION	☐ LOSS OF TORQUE	☐ PITTING - SPALLING	☐ OTHER

9. DETAILS OF DISCREPANCY:

Possible over spray of graphite coating on inside (surface) rabbit of casing flange.

SUBMITTED BY: A. Mello/C. Simmons

10. DISCUSSED WITH CONTRACTOR'S REPRESENTATIVE: NAME: J. Fallon	11. SAFETY OF FLIGHT INVOLVED: NO ☒ YES ☐

12. CONTRACTOR'S COMMENTS:

Al-Si over spray observed in the fillet radius. This over spray results from incomplete masking of the fillet area. New masking has been purchased to correct this condition.

SIGNATURE: [signature]

13. INSPECTION TEAM'S RECOMMENDATION:

NAVPRO Engineering recommends acceptance. A. Mello 10/30/78

NAVPRO-QA concurs with NAVPRO Engineering recommendation. D. F. O'Neill 10/30/78

SC 726 (6-61)

SIGNATURE

TEARDOWN INSPECTION

☐ PRELIMINARY FLIGHT RATING TEST [X] QUALIFICATION TEST DATE 4 October 1978

1. ENGINE MODEL & SERIAL NO.	2. ENGINE SECTION:	3. VENDOR:	4. PART SERIAL NO.
T700-207011-14A	Cold Module		
5. PART NUMBER:	6. PART NAME:	7. HOURS ON PART:	
6039T04G01	Compressor Casing	150 Hr. Qual.	

8. DISCREPANCY: (CODE: A-CRITICAL; B-MAJOR; C-MINOR)

☐ CORROSION	☐ FAILURE	☐ MISALIGNMENT	☐ WEAR
☐ CRACKS	☐ FASTENERS	☐ NICKS OR SCRATCHES	☐ MAGNETIC INSPECTION
☐ DEPOSITS	☐ F.O.D.	☐ OPERATION	☐ PENETRANT INSPECTION
☐ DISCOLORATION	☐ FRETTING	☐ PIECES MISSING	☐ X-RAY
☐ DISTORTION	☐ LOSS OF TORQUE	☐ PITTING - SPALLING	[X] OTHER

9. DETAILS OF DISCREPANCY:

Elliptical Holes on the fwd & aft flange at the 8:00/9:00 O'clock position of the left half (aft looking forward) compressor casing.

SUBMITTED BY: A. Mello/C. Simmons

10. DISCUSSED WITH CONTRACTOR'S REPRESENTATIVE:

NAME: J. Fallon

11. SAFETY OF FLIGHT INVOLVED: NO [XX] YES ☐

12. CONTRACTOR'S COMMENTS:

These elliptical holes are per the drawing, and are required for tolerance stack up for a bushing in the forward and aft VG mounting brackets.

SIGNATURE:

13. INSPECTION TEAM'S RECOMMENDATION:

NAVPRO Engineering recommends acceptance. A. Kelly 10/6/78

NAVPRO-QA concurs with NAVPRO Engineering recommendation. D. P O'Keele 10/2/78

SF 726 (1-61)

SIGNATURE

TEARDOWN INSPECTION

☐ PRELIMINARY FLIGHT RATING TEST ☒ QUALIFICATION TEST DATE 4 October 1978

1. ENGINE MODEL & SERIAL NO.	2. ENGINE SECTION:	3. VENDOR:	4. PART SERIAL NO.
T-00-207011-14A	Cold Module		

5. PART NUMBER	6. PART NAME:	7. HOURS ON PART:
6039T04G01	Compressor Casing	150 Hr. Qual.

8. DISCREPANCY: (CODE: A-CRITICAL; B-MAJOR; C-MINOR)

☐ CORROSION	☐ FAILURE	☐ MISALIGNMENT	☐ WEAR
☐ CRACKS	☐ FASTENERS	☐ NICKS OR SCRATCHES	☐ MAGNETIC INSPECTION
☐ DEPOSITS	☐ F.O.D.	☐ OPERATION	☐ PENETRANT INSPECTION
☒ DISCOLORATION	☐ FRETTING	☐ PIECES MISSING	☐ X-RAY
☐ DISTORTION	☐ LOSS OF TORQUE	☐ PITTING - SPALLING	☐ OTHER

9. DETAILS OF DISCREPANCY:

80% to 90% of the outside surface of the casing was discolored (ranging from light to dark blue). Discoloration was noted on the machine surface of the aft flange (connects to diffuser casing). In addition, split line bolt holes machine surface had similar discoloration.

SUBMITTED BY: A. Mello/C. Simmons

10. DISCUSSED WITH CONTRACTOR'S REPRESENTATIVE:	11. SAFETY OF FLIGHT INVOLVED:
NAME: J. Fallon	NO ☒ YES ☐

12. CONTRACTOR'S COMMENTS:

Discoloration is a result of temperature changes in the material. Some of color results from the heat treating in air per note 18 of the drawing. Some color results from the operating temperature of the part during engine running. This coloration has been observed on forged casing prior to introduction and is not detrimental to material properties. A CID has been processed to anneal the cast casing in vacuum, the same as the forged casing is now done.

SIGNATURE: [signature]

13. INSPECTION TEAM'S RECOMMENDATION:

NAVPRO Engineering recommends acceptance. 10/31/78 H. Mell Jr

NAVPRO-QA concurs with NAVPRO Engineering recommendation. D. P. O'Keefe 10/30

SE726 (6-61)

SIGNATURE:

TEARDOWN INSPECTION

☐ PRELIMINARY FLIGHT RATING TEST ☒ QUALIFICATION TEST DATE 4 October 1978

1. ENGINE MODEL & SERIAL NO.	2. ENGINE SECTION:	3. VENDOR:	4. PART SERIAL NO.
T700-207011-14A	Cold Module		
5. PART NUMBER: 6039T04G01	6. PART NAME: Compressor Casing	7. HOURS ON PART: 150 Hr. Qual.	

8. DISCREPANCY: (CODE: A-CRITICAL; B-MAJOR; C-MINOR)

☐ CORROSION	☐ FAILURE	☐ MISALIGNMENT	☐ WEAR
☐ CRACKS	☐ FASTENERS	☐ NICKS OR SCRATCHES	☐ MAGNETIC INSPECTION
☐ DEPOSITS	☐ F.O.D.	☐ OPERATION	☐ PENETRANT INSPECTION
☐ DISCOLORATION	☐ FRETTING	☐ PIECES MISSING	☐ X-RAY
☐ DISTORTION	☐ LOSS OF TORQUE	☐ PITTING - SPALLING	☒ OTHER

9. DETAILS OF DISCREPANCY:

Heavy bench marks in the area below the flange which attaches to the diffuser casing.

NOTE. For a production item, excessive hand benching was performed on casing, which in turn, could affect our controllability for wall thickness.

SUBMITTED BY: A. Mello/C. Simmons

10. DISCUSSED WITH CONTRACTOR'S REPRESENTATIVE:

NAME: J. Fallon

11. SAFETY OF FLIGHT INVOLVED:

NO ☒ YES ☐

12. CONTRACTOR'S COMMENTS:

Benching is done to remove gates in the casting which are used to control the filling of the aft flange and cone section. Wall thickness is controlled on the drawing. Will investigate relocating the gates away from the wall of the cone or EDM process for better control of material removal in this area.

SIGNATURE: [signature]

13. INSPECTION TEAM'S RECOMMENDATION:

NAVPRO Engineering recommends acceptance. A. Mello 10/20/78

NAVPRO-QA concurs with NAVPRO Engineering recommendation. [signature]

SI726 (6-61)

SIGNATURE:

Figure 40. Finished Machined and Fabricated Casting - View 1

Figure 41. Finished Machined and Fabricated Casting - View 2

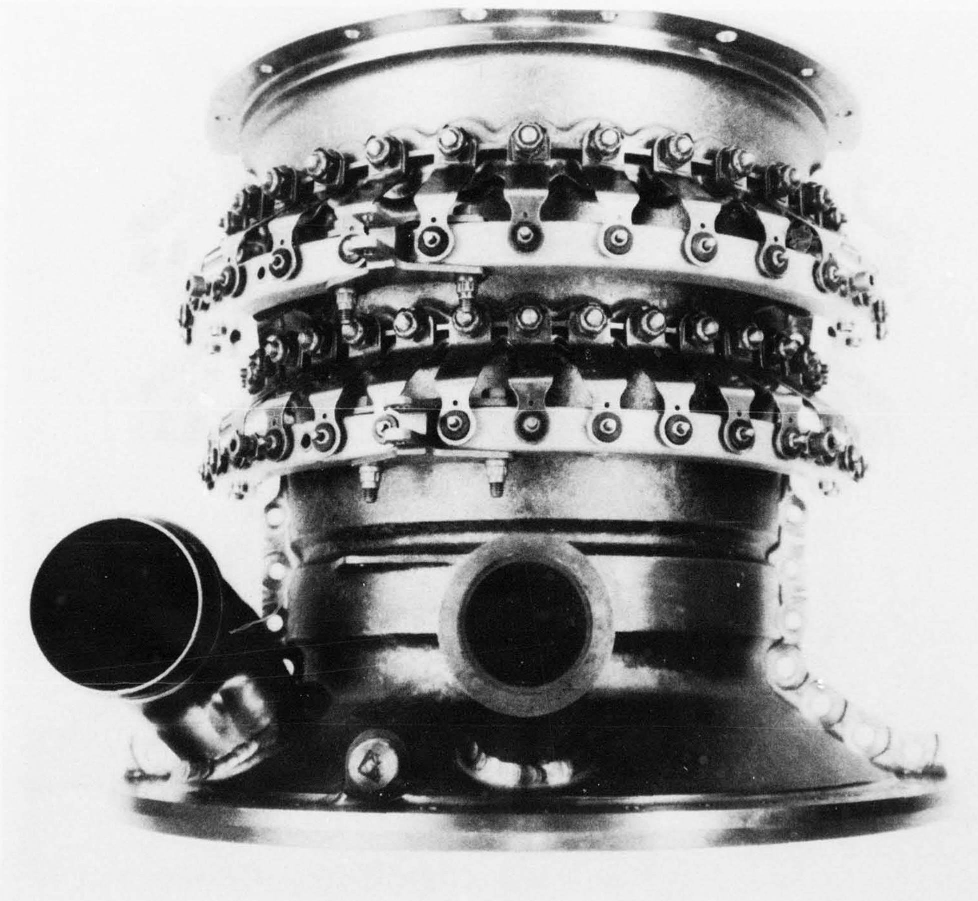

Figure 42. Assembled Casing After Engine Testing - Outer Contour

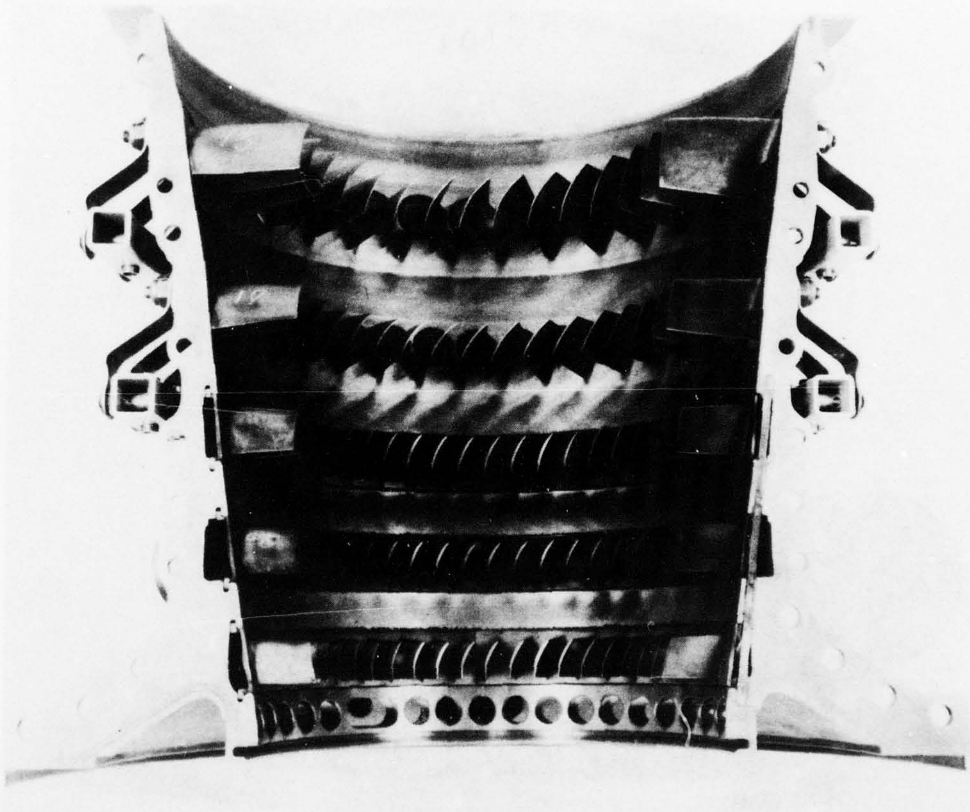

Figure 43. Assembled Casing After Engine Testing - Inner Contour

A value engineering cost analysis showed a total production quantity (250th unit-shop cost) saving of $658 per engine in 1976 dollars, as a result of replacing the forged compressor casing with a casting. The saving was due to the significant reduction in labor input required, resulting from the elimination of milling operations on the outer contour and the casting integrally of the actuator pads, borescope bosses and associated hardware that had to be separately machined and fabricated on the forged casing. The total material costs for the cast and forged versions of the compressor casing are approximately equal.

3.4 Phase III - Preparation of Technical Data Package

A technical data package consisting of the following drawings developed during the course of this program was assembled and presented to Government personnel:

Drawing No.	Title
6038T86 (1 Sheet)	Case, Compressor (Casting)
6039T04 (2 Sheets)	Case, Compressor (Matched Parts)
4096481-133 (7 Sheets)	Set-Up Fixture
1001	Set-Up Fixture Photograph
1002	Set-Up Fixture Photograph
1003	Set-Up Fixture Photograph

No additional documents were generated in the Program.

4.0. CONCLUSIONS

1. The one-piece cast compressor casing for the T700 engine was successfully produced and completed engine endurance testing. Cast casings will be introduced on T700 production engines in 1979.

2. Compressor casings can be successfully cast to near-net shape, including several features that were previously required to be welded to the forging.

3. Final casting procedure was selected to utilize an expendable (lost wax/ceramic) mold system for optimum flexibility in definition of external contour and added features.

4. All mechanical property design requirements were met.

5. Two cast casings were fully machined, fabricated and assembled into test engines. A 60-hour and a 150-hour endurance test were successfully completed.

6. A value engineering cost analysis showed a 250th unit (shop cost) saving of 30.6 manufacturing labor hours as compared to the forged casing due primarily to reduced machining and welding on the cast casing.

7. Raw material utilization is markedly improved. As poured, the casting weighs approximately 30 pounds compared to a 65-pound forging weight.

8. The predicted manufacturing cost savings of $658 (250th unit) per engine in 1976 dollars has been verified.

APPENDIX A - MECHANICAL PROPERTIES

A. Scope

This appendix details physical property tests performed on the cast material, Ti 6Al-4V, used in the compressor casing. Chemical analyses of the master heats used are included in Table A-1. The locations in the casting from which specimens were machined are shown in Figure A-1.

Tensile, stress rupture, high- and low-cycle fatigue, crack growth rate and fracture toughness tests at room and elevated temperature were run. Microstructure was examined.

Comparative ballistic data on cast and forged Ti 6Al-4V developed prior to the present program is presented to cover blade containment capability.

TABLE A-1 - CHEMICAL ANALYSES OF Ti 6Al-4V MASTER HEATS USED FOR TEST SPECIMENS

Heat No.	Al	V	O_2	N_2	H_2	Y	Fe	C	Ti
12765	5.90	3.70	.180	.0067	.0046	12 PPM	.17	.03	Balance
12766	6.00	3.80	.187	.0071	.0036	16 PPM	.17	.03	Balance

Raw Material Vendor: Reactive Metals, Inc.

All material met General Electric Specification B50TF102-S2.

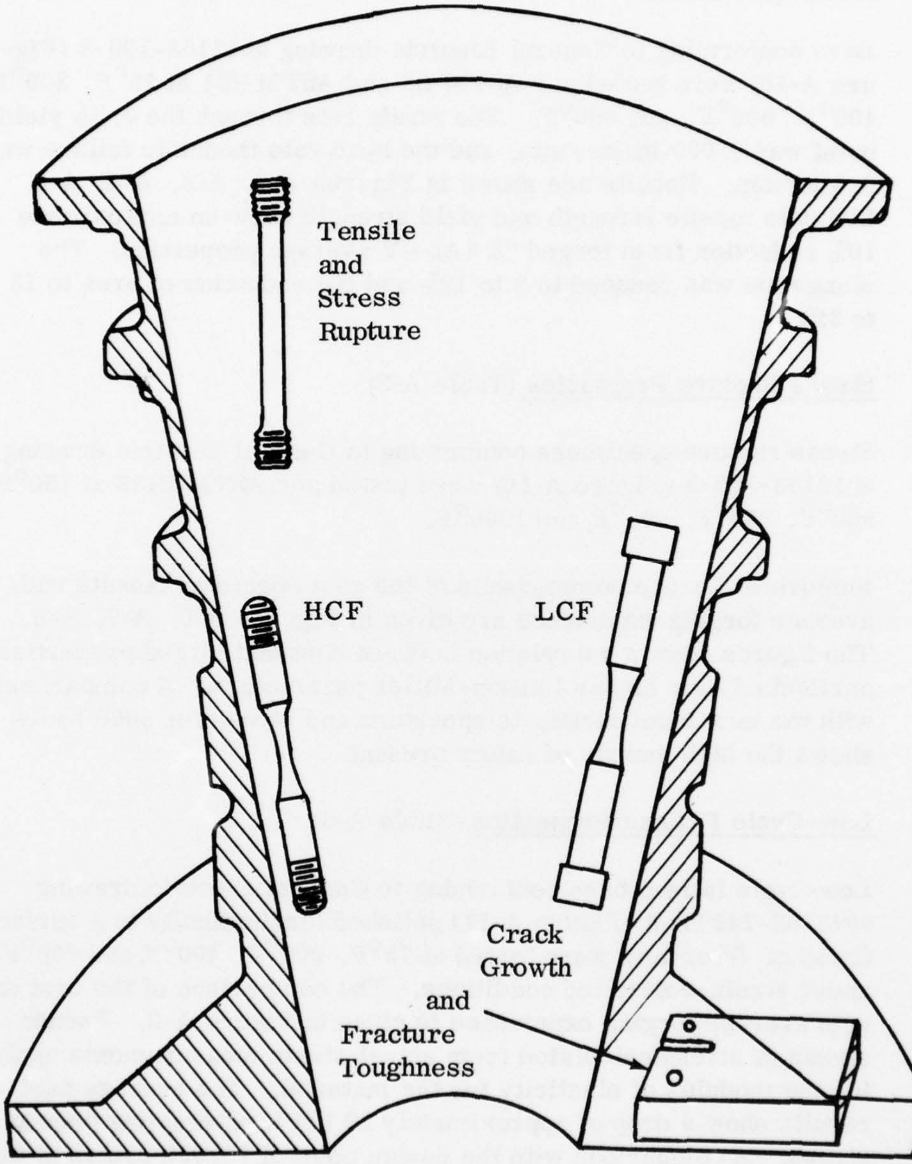

Figure A-1. Test Specimen Location

B. Discussion

1. Tensile Properties (Table A-2)

Bars conforming to General Electric drawing 4013163-100-3 (Figure A-16) were tested per ASTM E8 and ASTM E21 at 75°F, 200°F, 400°F, 600°F, and 800°F. The strain rate through the 0.2% yield point was 0.005 in/in./min. and the head rate thence to failure was 0.5 in/min. Results are shown in Figures A-2, A-3, A-4, A-5. Ultimate tensile strength and yield strength show an approximate 10% reduction from forged Ti 6Al-4V average properties. The elongation was reduced to 8 to 12% and the reduction of area to 13 to 32%.

2. Stress Rupture Properties (Table A-3)

Stress rupture specimens conforming to General Electric drawing 4013163-100-3 (Figure A-16) were tested per ASTM E139 at 750°F, 800°F, 850°F, 900°F, and 1000°F.

Rupture and creep comparisons of the cast specimen results with average forging experience are given in Figures A-6, A-7, A-8. The figures show a correlation between cast and forged properties, particularly for higher Larson-Miller parameters. A comparison with the maximum casting temperature and stress for 5000 hours shows the high margin of safety present.

3. Low-Cycle Fatigue Properties (Table A-5)

Low-cycle fatigue bars conforming to General Electric drawing 4013163-140TL-3 (Figure A-17) polished longitudinally to a surface finish of 8√ or less were tested at 75°F, 200°F, 400°F, and 600°F under strain-controlled conditions. The comparison of the cast data with average forging experience is given in Figure A-9. Pseudo stress is stress calculated from actual strain measurements applying the modulus of elasticity for the material. The average cast results show a drop of approximately 20 ksi in alternating pseudo stress. A comparison with the design point of 15,000 cycles at the maximum casing stress shows the high safety margin.

4. <u>High-Cycle Fatigue Properties</u> (Table A-4)

Bars conforming to General Electric drawing 4013163-127-1 (Figure A-18) polished longitudinally to a surface finish of 8√ or less were tested at 75°F and 600°F.

High-cycle fatigue results are presented as S-N curves (Figures A-10 and A-11) and as modified Goodman diagrams (Figures A-12 and A-13) in which the alternating stress for 10^7 cycles (100 hrs.) is plotted versus the means stress. The high-cycle fatigue strength shows approximately a 40% reduction from average forged properties. Fortunately the compressor casing is not subject to any appreciable high-cycle fatigue loading.

5. <u>Crack Growth Rate</u> (Tables A-6 and A-7)

Figures A-14 and A-15 give plots of crack growth rate versus stress intensity range performed at room temperature and 600°F on specimens conforming to General Electric drawing 4013163-176 (Figure A-19).

The curves show that little difference exists between the crack growth rate at room temperature and 600°F and that at room temperature, where a comparison with forging data is available, the crack growth rate in cast material is the same or slightly slower than in wrought metal.

6. <u>Fracture Toughness</u> (Table A-8)

While it was planned to include fracture toughness testing as part of the program, because of the dimensions of the casing a valid fracture toughness specimen in accordance with ASTM Specification E399 could not be obtained. Data obtained is given in Table A-8. Specimens conformed to General Electric drawing 4013163-176 (Figure A-19).

C. <u>Microstructure</u>

Figures A-20 through A-22 show the microstructures of specimens. The figures show a typical annealed alpha-beta titanium structure with a matrix of transformed beta phase containing acicular alpha and alpha at the prior beta grain boundaries.

Since .025 was chemically milled from all surfaces of the cast castings, no evidence of oxygen-rich alpha case (typically found on titanium castings in the as-cast condition) was observed.

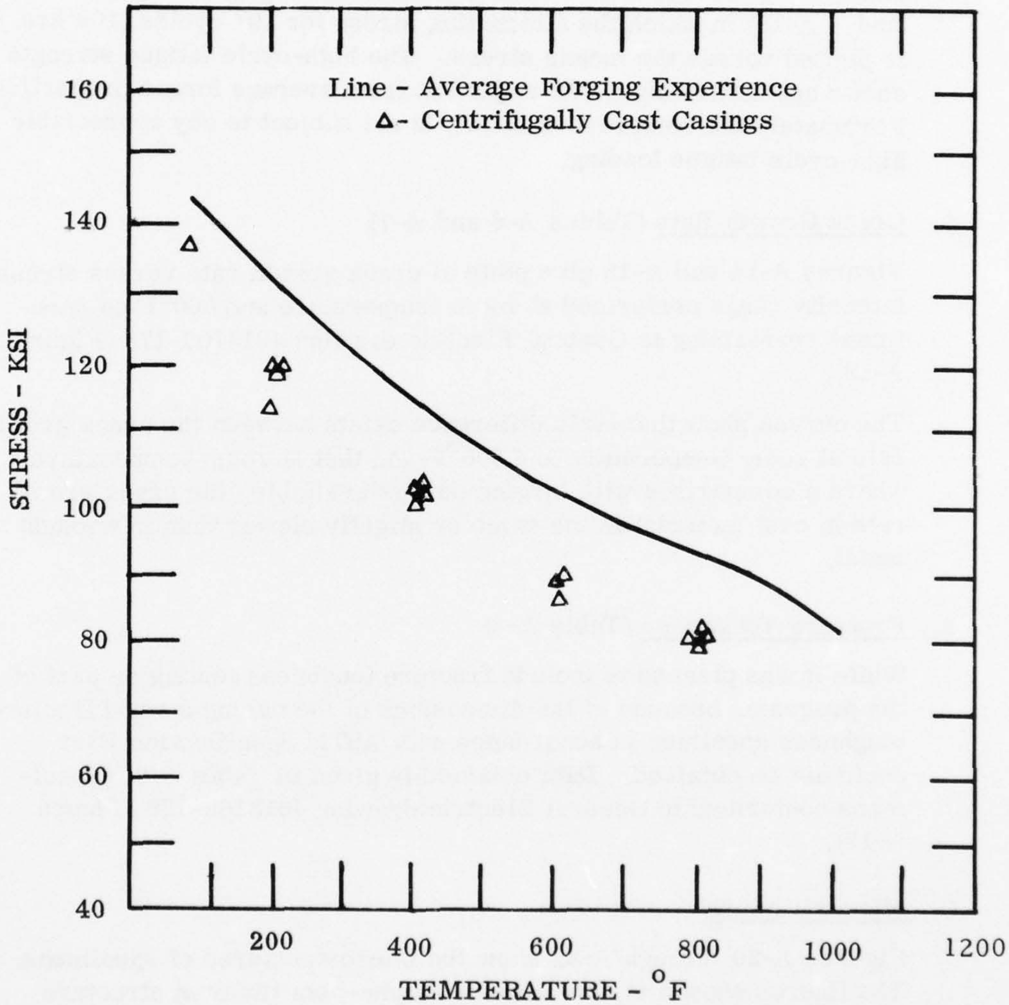

Figure A-2. Ultimate Tensile Strength vs. Temperature

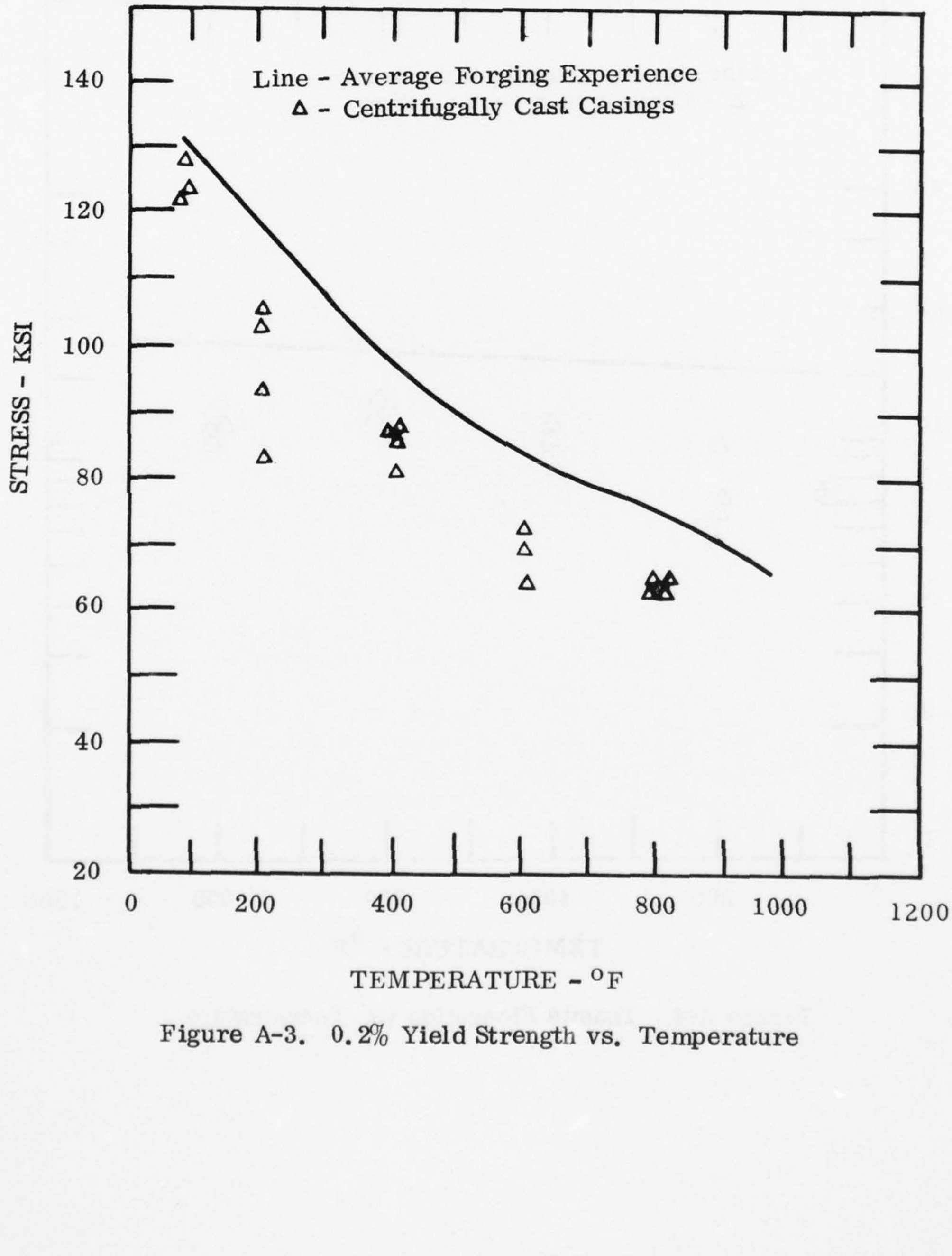

Figure A-3. 0.2% Yield Strength vs. Temperature

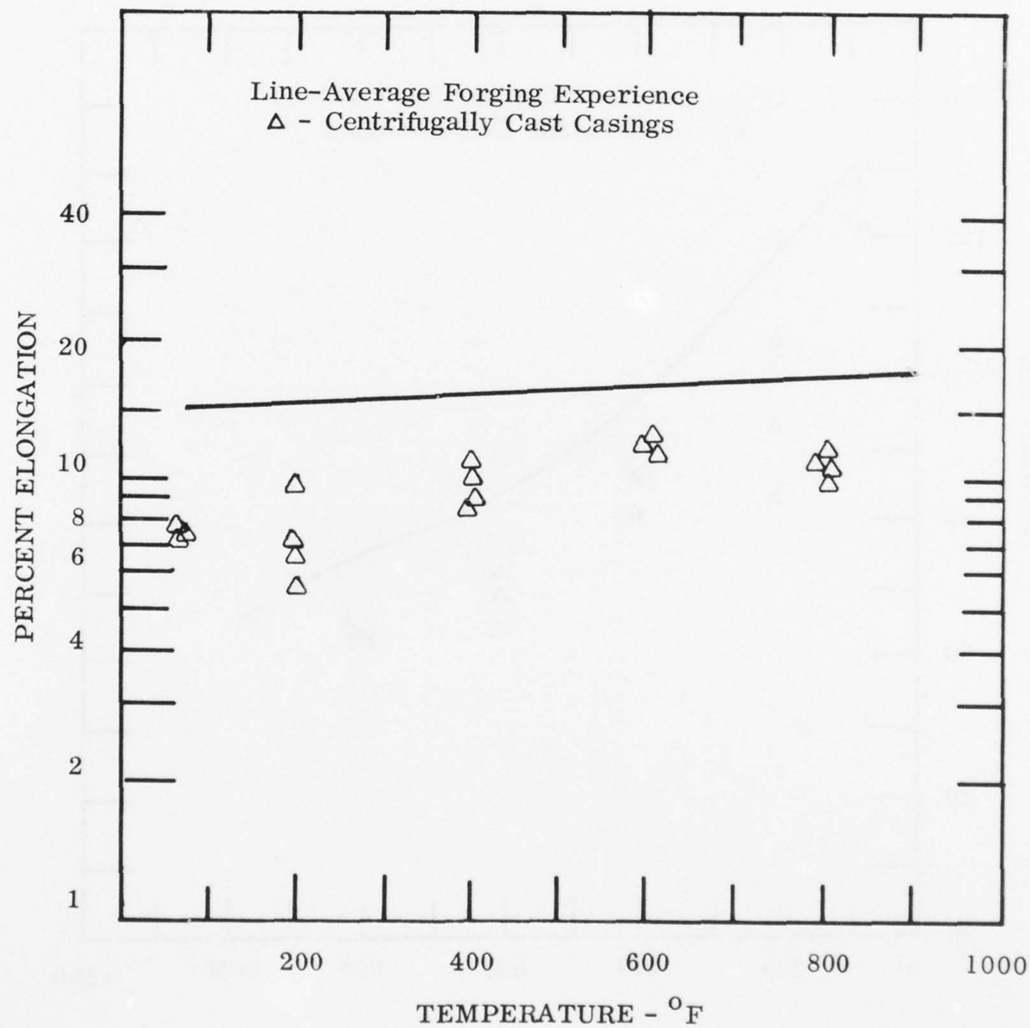

Figure A-4. Tensile Elongation vs. Temperature

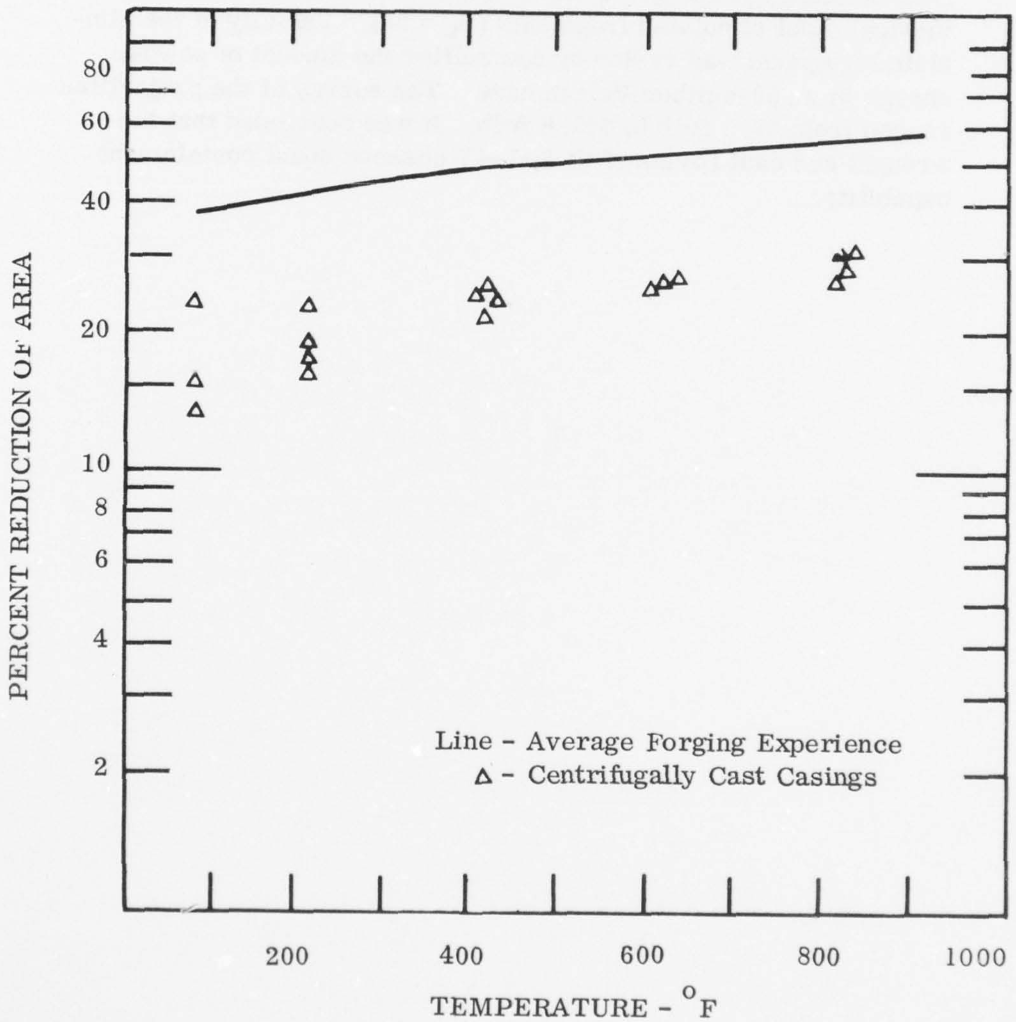

Figure A-5. Tensile Reduction of Area vs. Temperature

AD-A071 051 GENERAL ELECTRIC CO LYNN MA AIRCRAFT ENGINE GROUP F/G 11/6
CAST TITANIUM COMPRESSOR CASING.(U)
MAY 79 W H FICHT DAAJ02-76-C-0057

UNCLASSIFIED USARTL-TR-79-8 NL

2 OF 2
AD
A071051

END
DATE
FILMED
8 -79
DDC

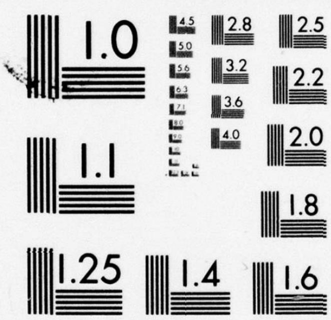
1.0
4.5
5.0
5.6
6.3
2.8
3.2
3.6
4.0
2.5
2.2
2.0
1.1
1.8
1.25
1.4
1.6

D. **Ballistic Impact** (Table A-9)

Work done prior to the start of the present program compared wrought and cast Ti 6Al-4V material in ballistic impact testing. Plates of each material were annealed at $1300^{o}F$ for 2 hours and ground to .088 nominal thickness. Tests were conducted using 240 grain cylindrical steel simulated fragments ($R_c = 35$). Velocity of the simulated fragment was varied by controlling the amount of powder charge in a .50-caliber Vulcan case. The energy of the projectiles ranged from 67.5 ft-lb to 307.8 ft-lb. It was concluded that the wrought and cast forms of Ti 6Al-4V possess equal containment capability.

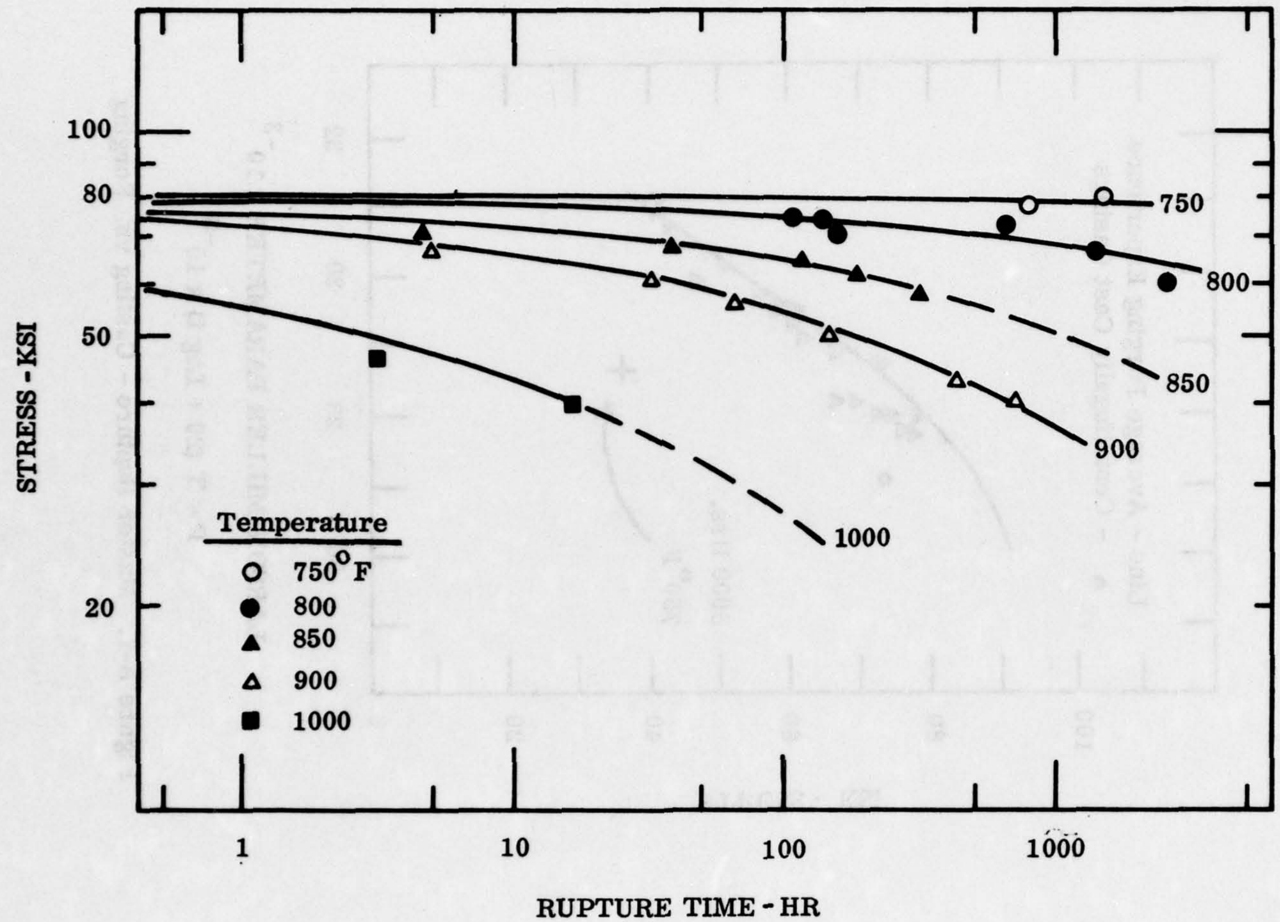

Figure A-6. Cast Stress - Rupture Properties vs. Temperature

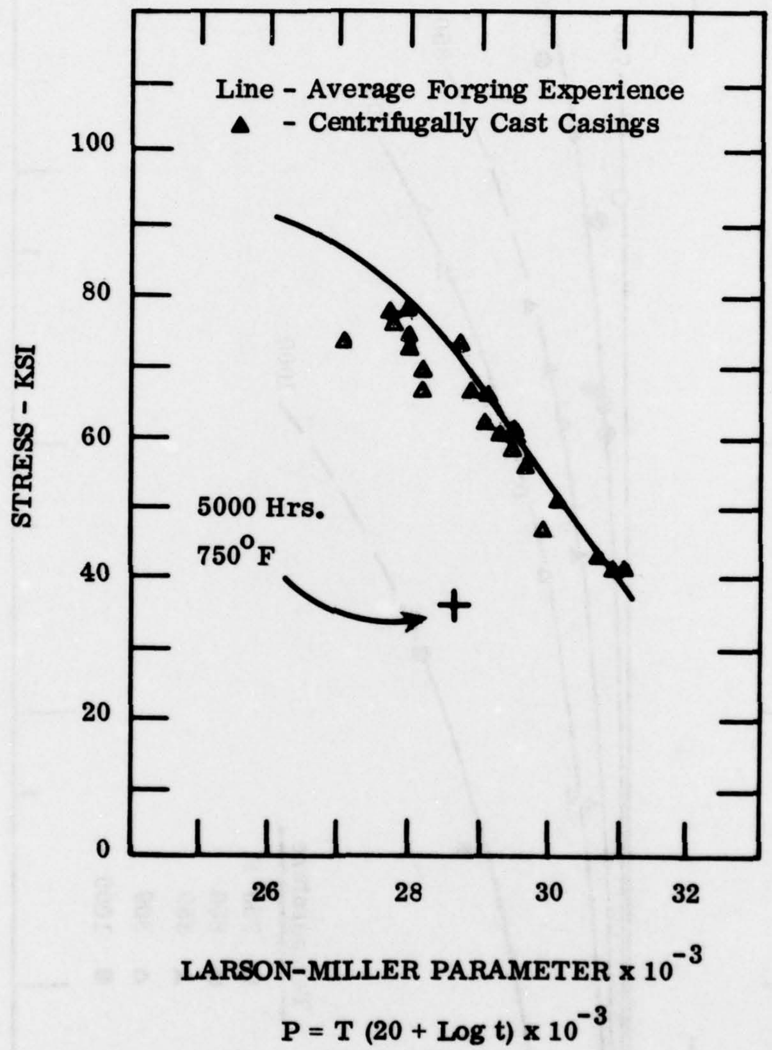

Figure A-7. Master Rupture - Casting vs. Forging

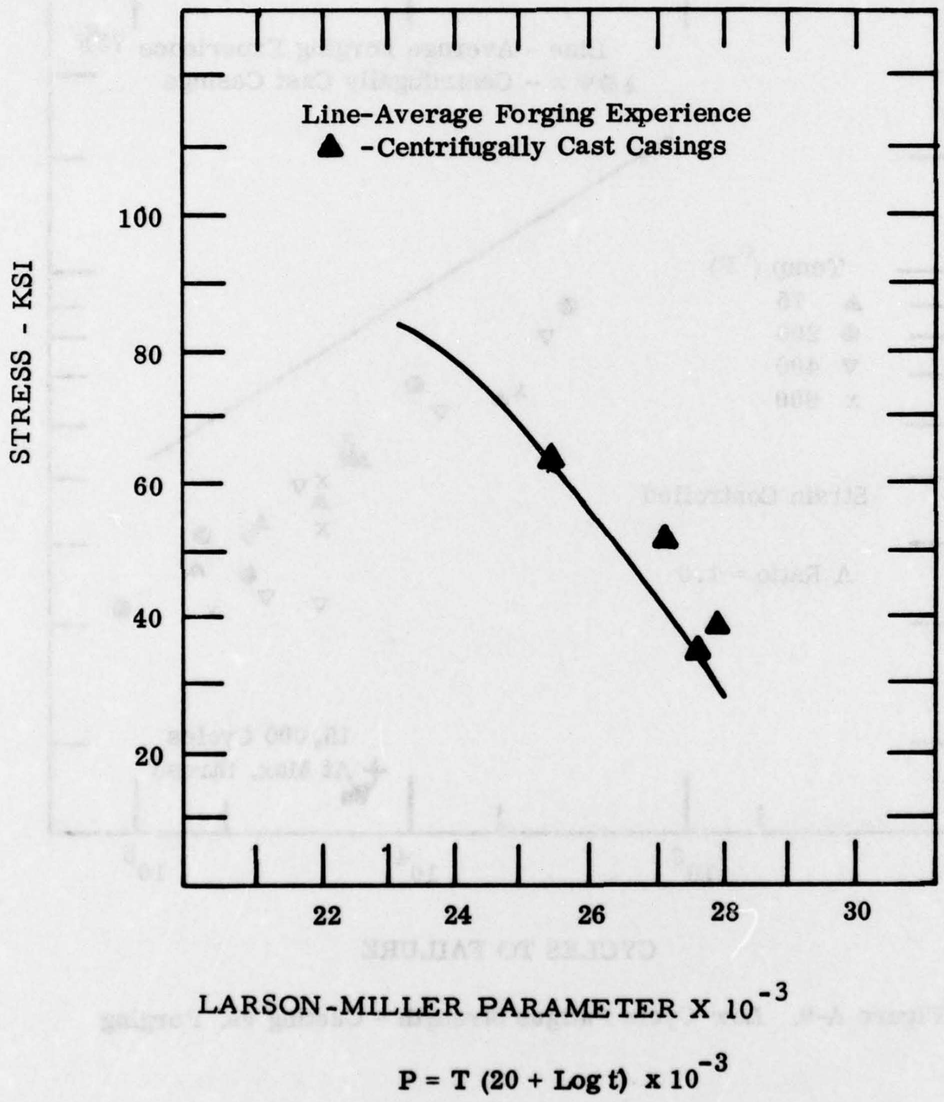

Figure A-8. Master Creep - Casting vs. Forging (.2% Plastic Creep)

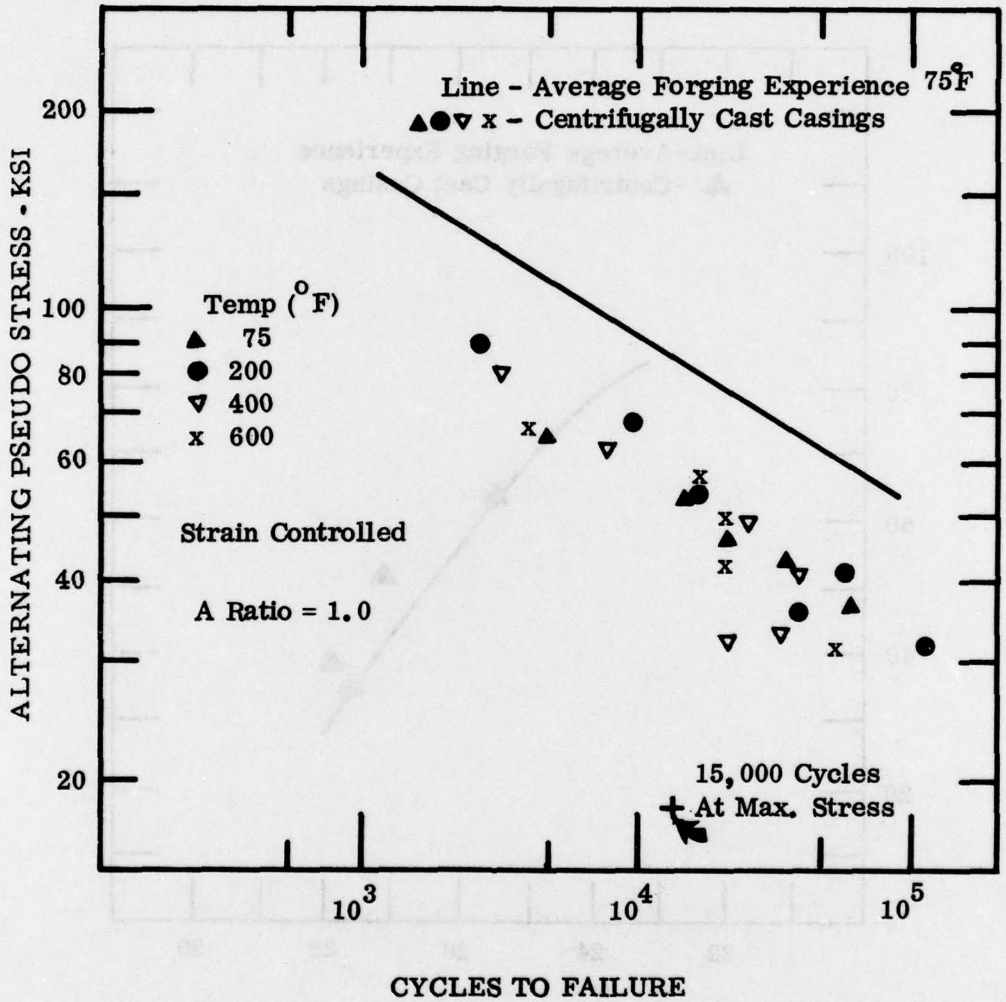

Figure A-9. Low Cycle Fatigue Strength - Casting vs. Forging

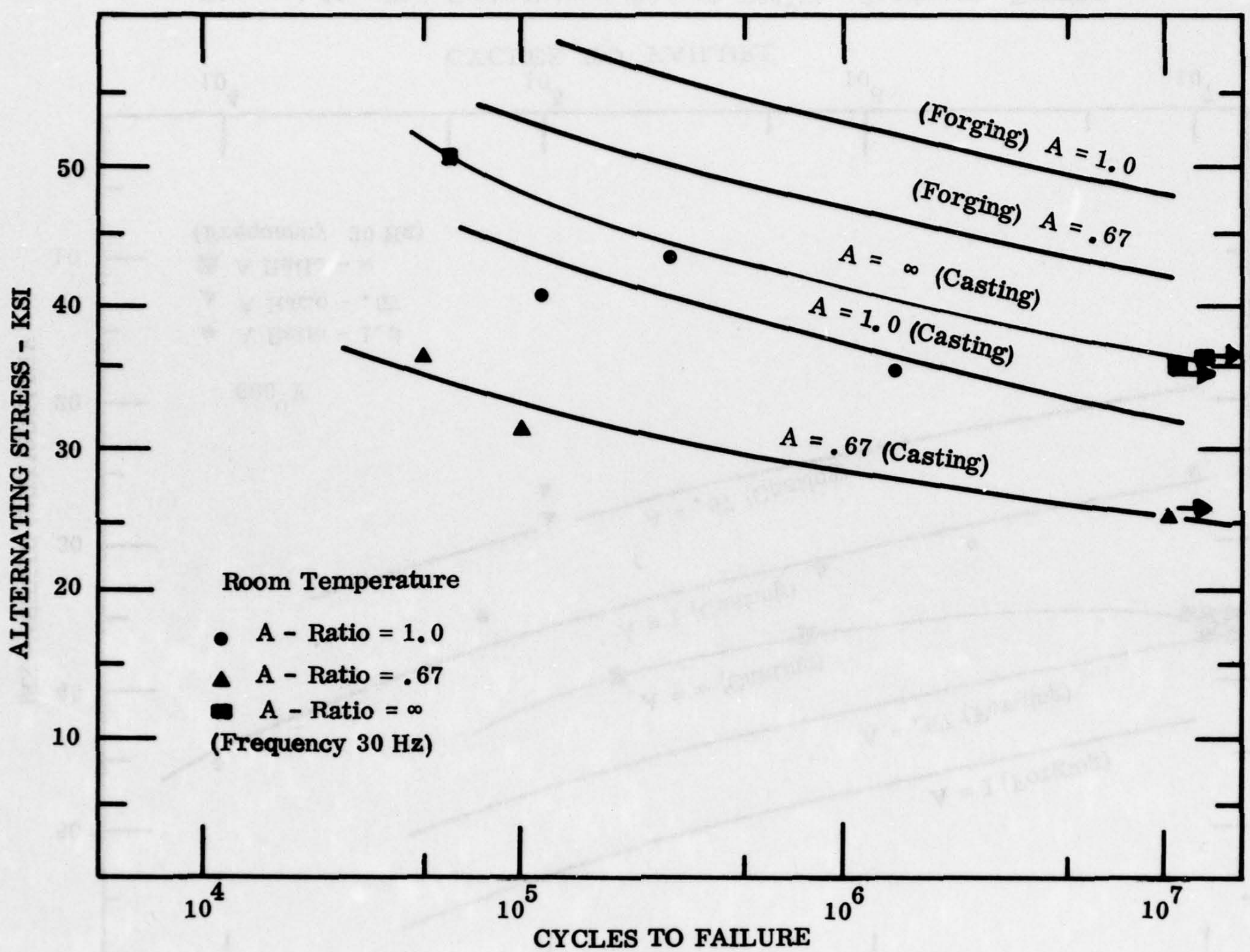

Figure A-10. High Cycle Fatigue Strength (Room Temperature) - Casting vs. Forging

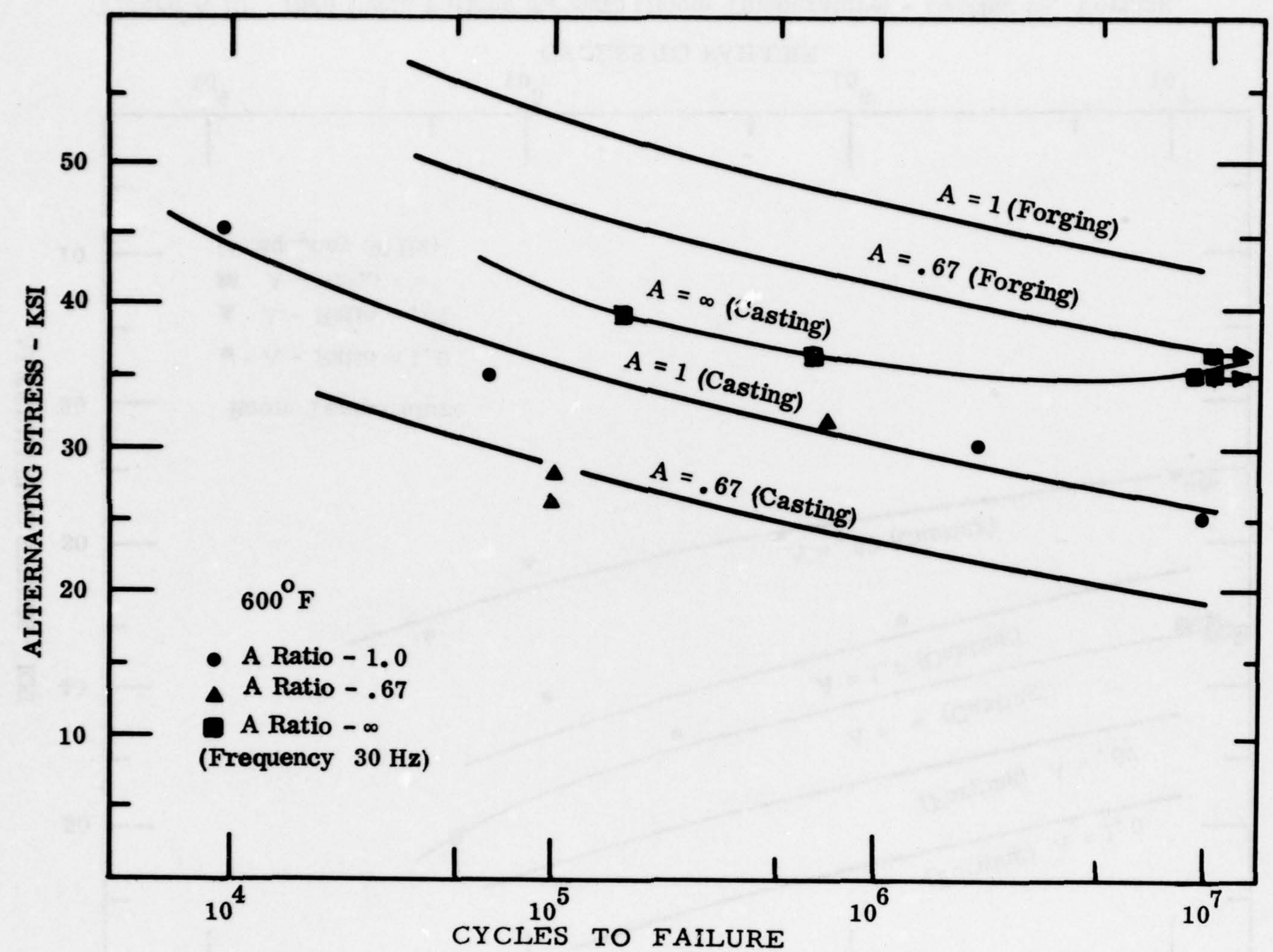

Figure A-11. High Cycle Fatigue Strength (600°F) - Casting vs. Forging

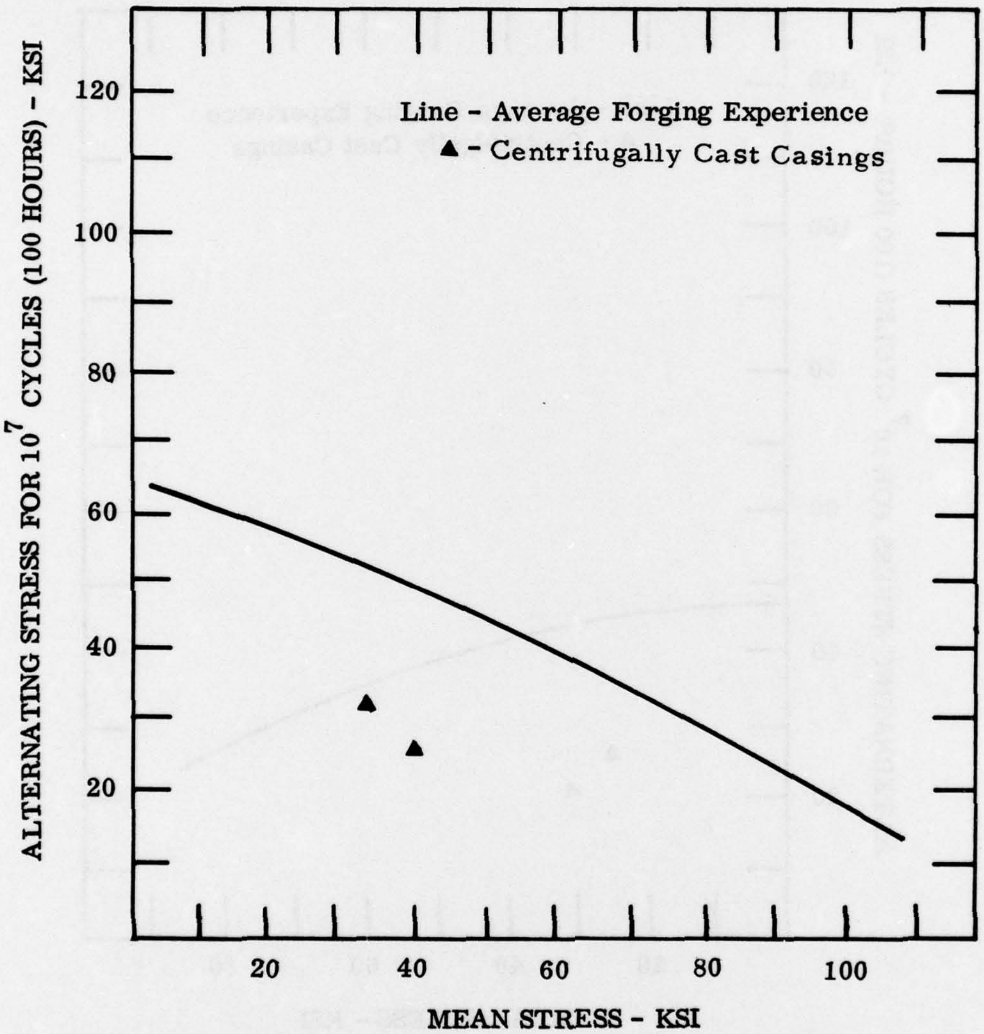

Figure A-12. Modified Goodman Diagram (Room Temperature) - Casting vs. Forging

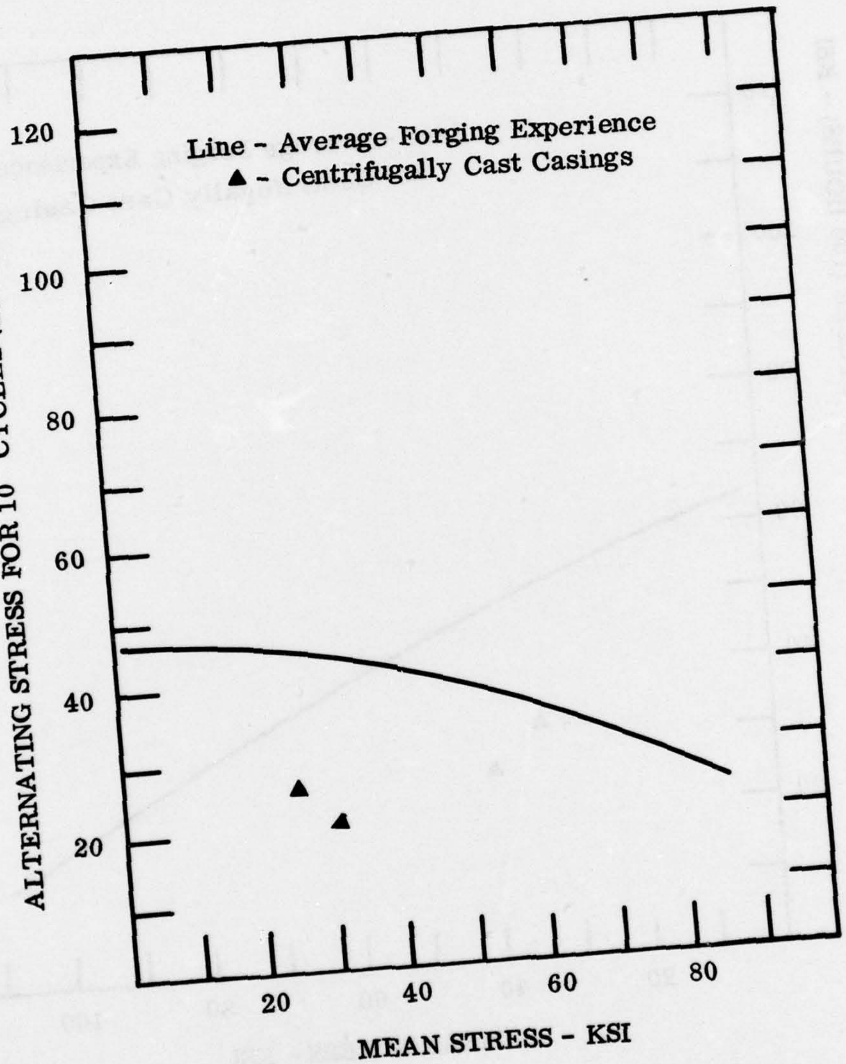

Figure A-13. Modified Goodman Diagram (600°F) - Casting vs. Forging

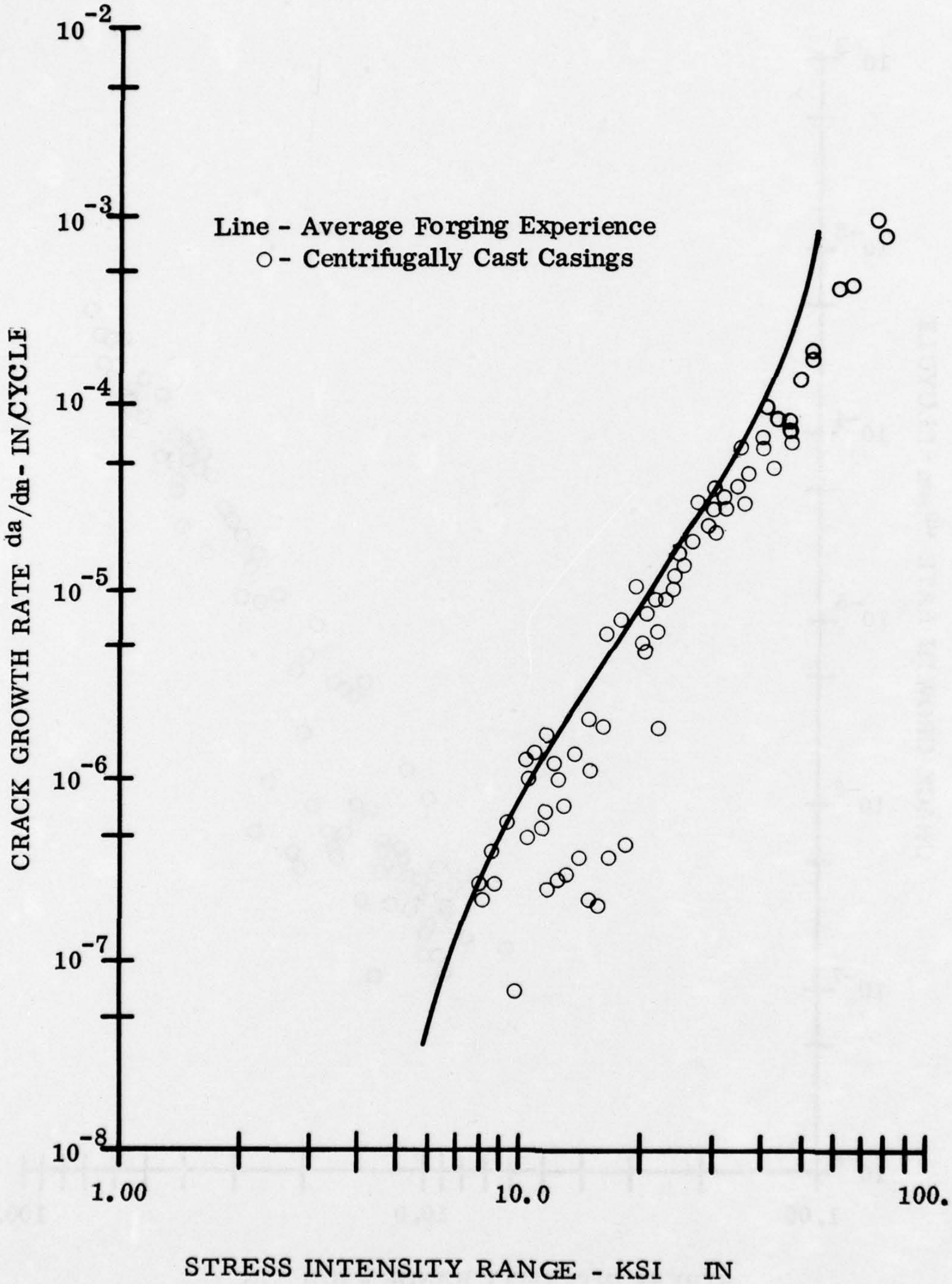

Figure A-14. Crack Growth Rate as a Function of Stress Intensity at Room Temperature - Casting vs. Forging

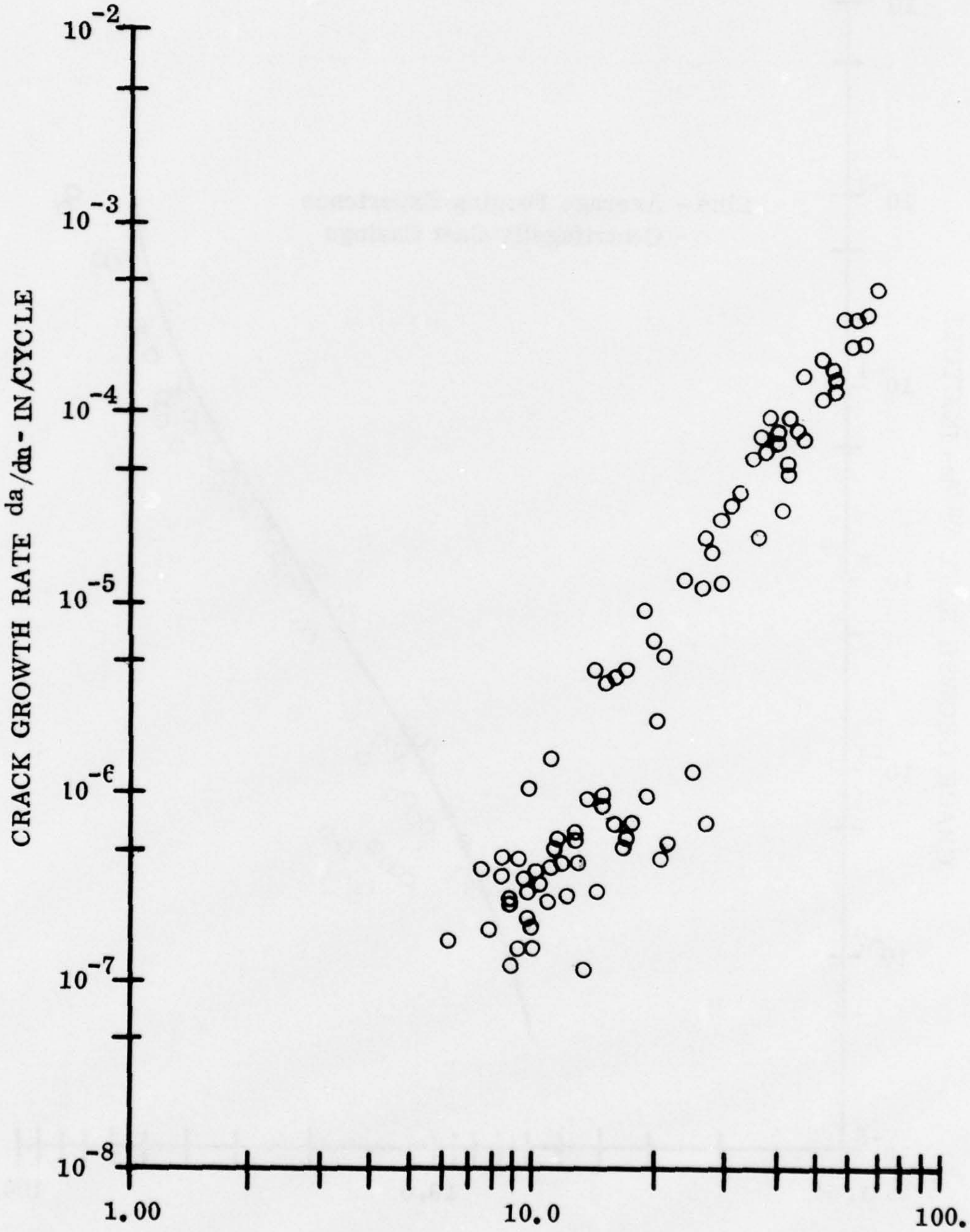

Figure A-15. Crack Growth Rate as a Function of Stress Intensity at 600°F - Casting vs. Forging

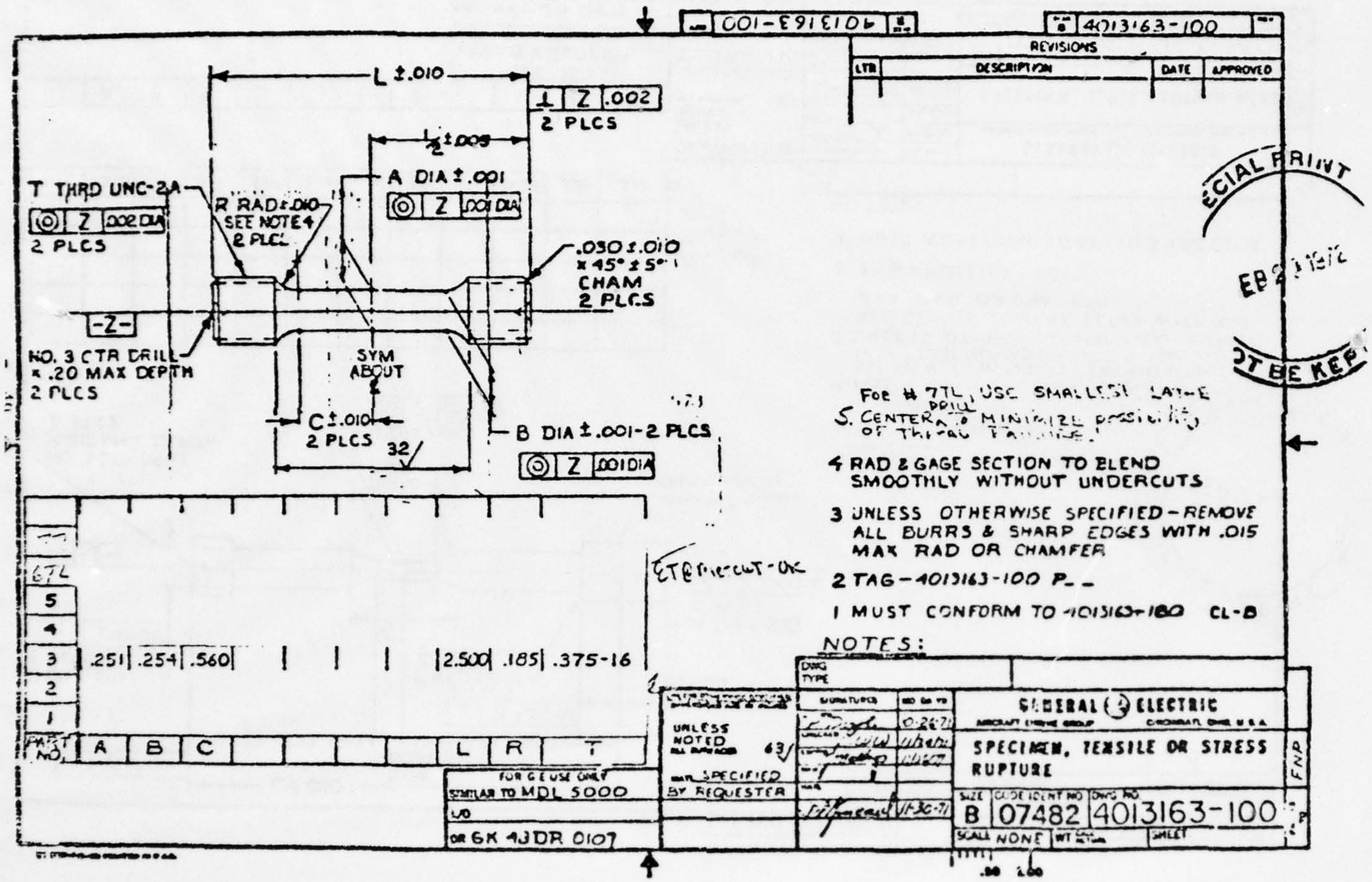

Figure A-16. Specimen, Tensile or Stress Rupture

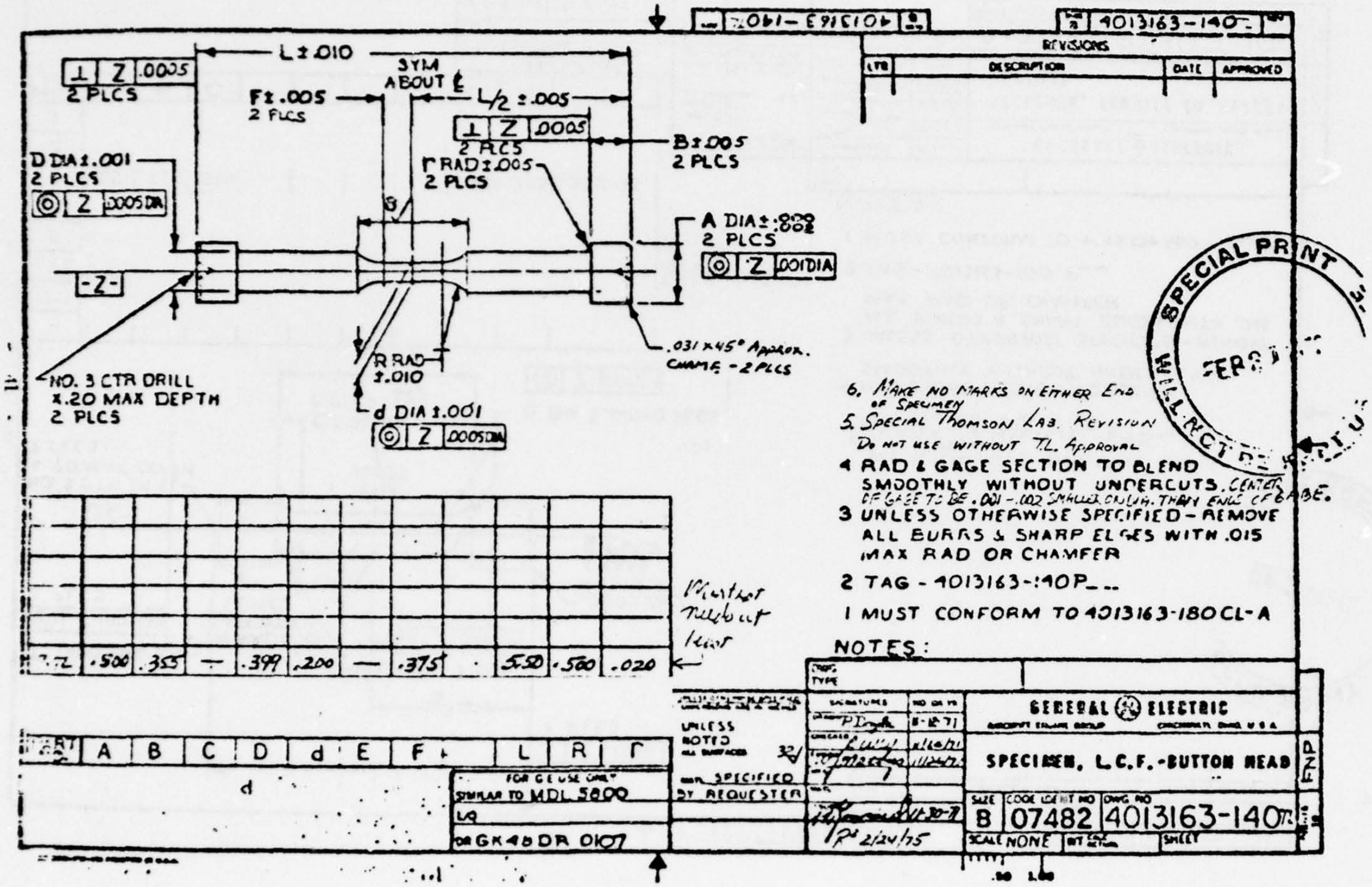

Figure A-17. Specimen, L. C. F. - Button Head

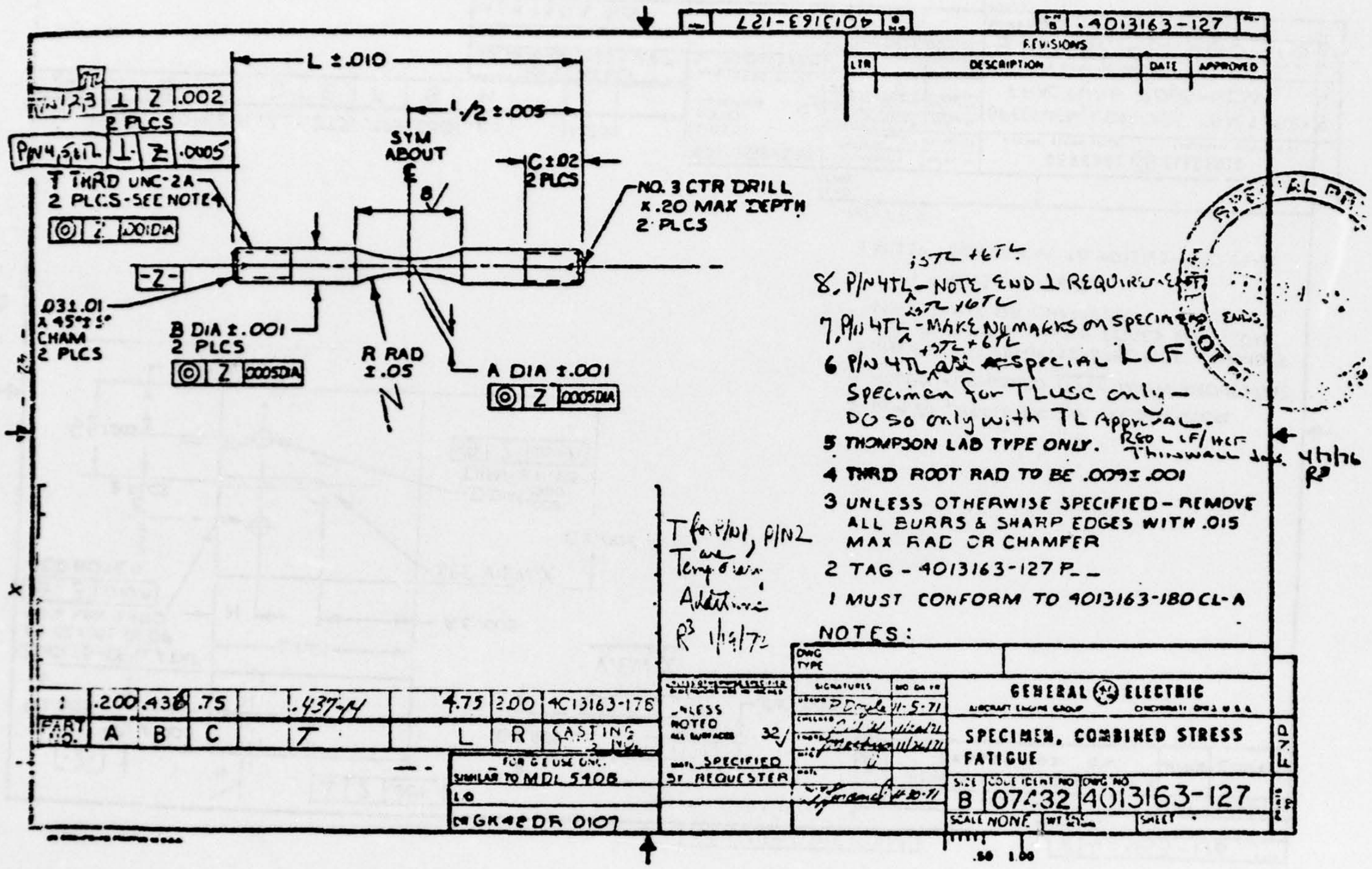

Figure A-18. Specimen, Combined Stress Fatigue

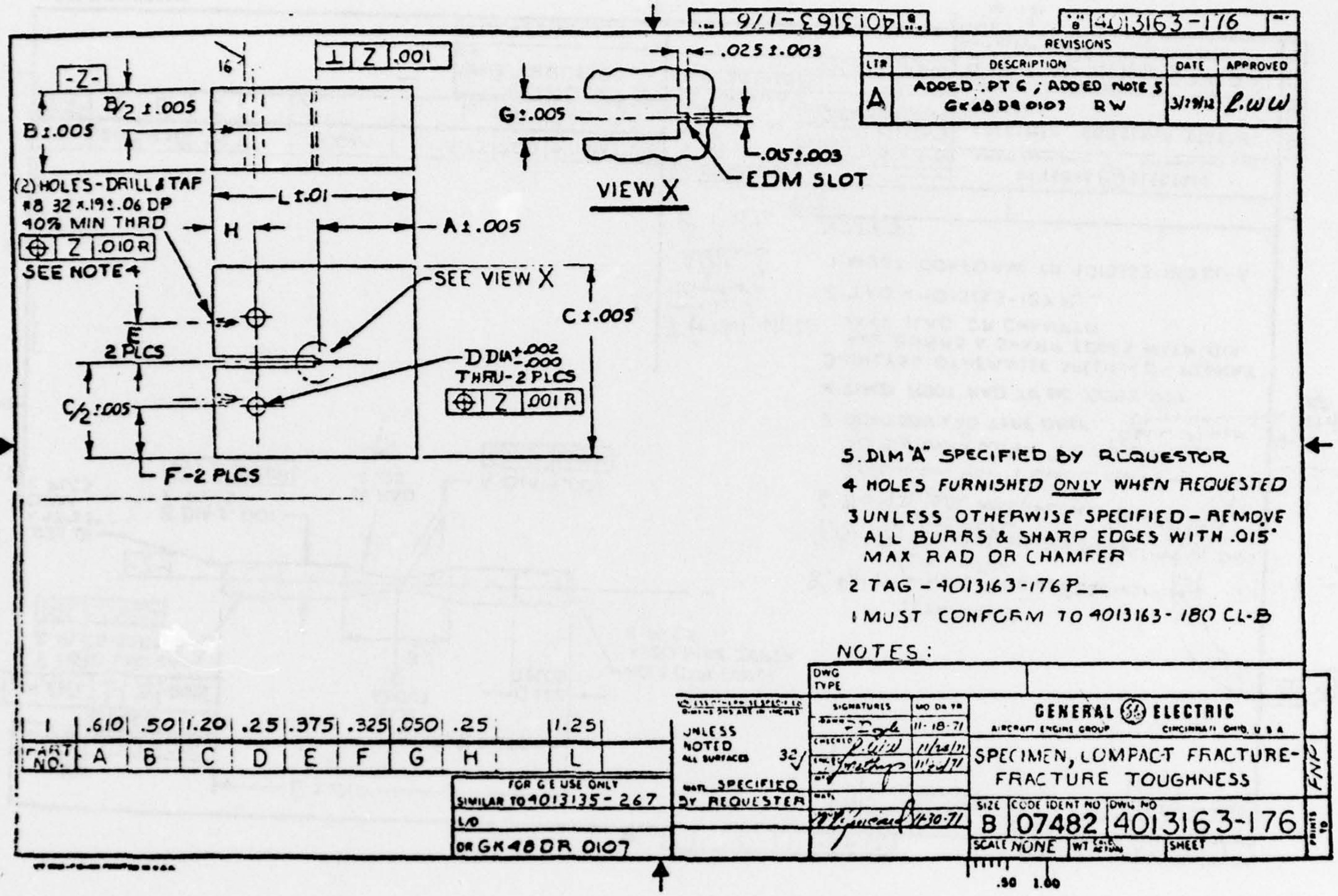

Figure A-19. Specimen, Compact Fracture - Fracture Toughness

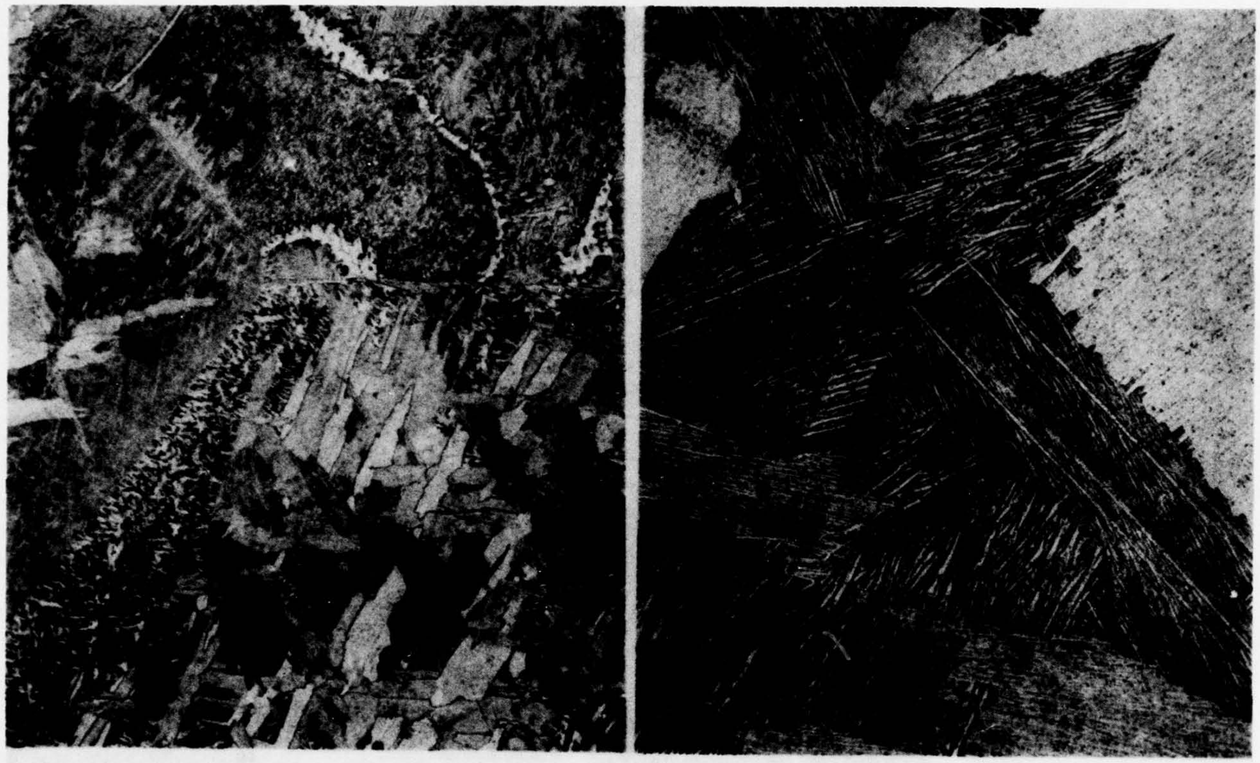

(a) 50X (b) 200X

Figure A-20. Typical Microstructure of Cast Ti 6 Al-4V at Low Magnification

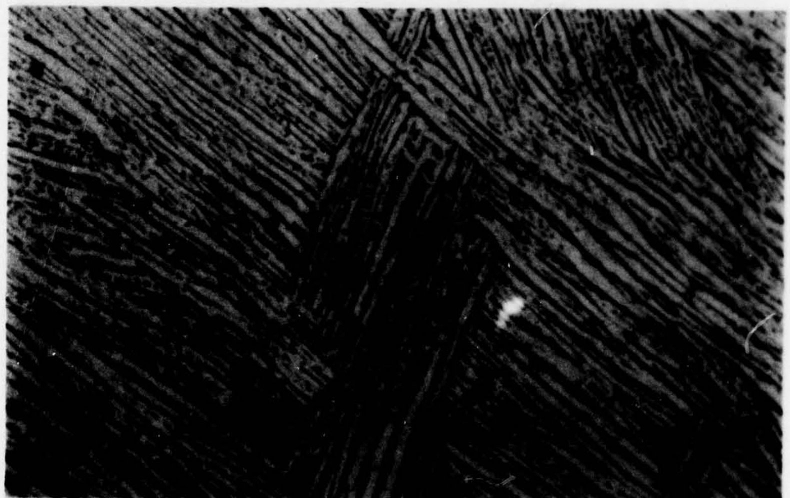

800X

Figure A-21. Typical Microstructure Showing Alpha Platelets (light) and Intergranular Beta (dark)

(a) 100X

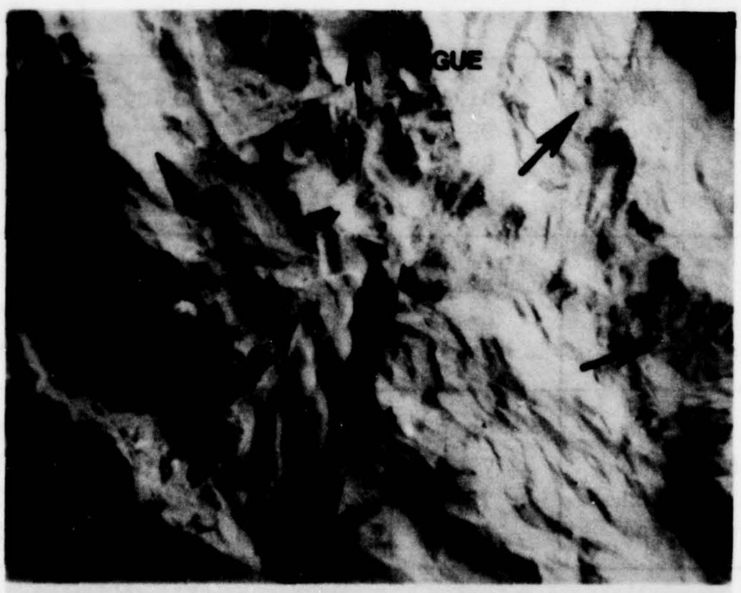

(b) 165X

Figure A-22. Typical Fracture Surfaces of Failed Test Bars in HCF (a) and LCF (b) Showing Fatigue Origins, O and P and the Direction of Propagation (large arrows)

TABLE A-2
TENSILE DATA

Nominal Gage Section: 0.25 in. dia. x 1.0 in. long
Strain Rate through 0.2% Yield: 0.005 in./in./min.
Head Rate thence to Failure: 0.05 in./min.

Specimen No.	Temp (^{O}F)	UTS (ksi)	.2% Y. S. (ksi)	Elong. (%)	R. A. (%)
3-1	75	136.0	127.3	7.2	13.1
9-1	75	131.9	123.0	7.6	23.2
10-13	75	132.7	122.1	7.3	15.3
3-2	200	116.8	102.9	6.9	19.3
3-53	200	112.0	93.2	5.6	16.8
9-2	200	117.8	104.7	6.5	17.8
10-14	200	117.3	82.8	9.8	23.6
3-3	400	101.1	87.0	8.8	24.2
3-54	400	98.2	86.6	8.5	24.9
9-3	400	98.6	85.2	10.9	25.3
10-15	400	103.1	81.2	10.3	22.5
3-4	600	87.9	72.8	12.4	27.0
9-4	600	84.7	63.9	11.3	27.2
10-16	600	88.1	69.0	11.8	26.3
3-5	800	78.9	63.9	11.5	28.4
3-55	800	77.9	63.0	10.7	27.6
9-5	800	78.1	63.5	11.4	31.7
10-17	800	80.4	64.9	10.0	32.0

TABLE A-3
STRESS-RUPTURE DATA

Specimen No.	Temp (^oF)	Stress (ksi)	Rupt. Life (hr)	Elong. (%)	R. A. (%)
9-9	700	65.0	793.3(a)	0.5	--
10-21	700	70.0	600.4(a)	0.9	--
9-10	750	77.0	737.0	9.2	16.3
3-9	750	78.0	1,378.0	9.8	20.0
10-20	800	60.0	2,395.1	8.0	12.8
3-7	800	65.0	1,312.0	7.1	18.4
9-12	800	72.0	142.7	7.7	15.8
3-56	800	73.0	608.3	9.2	14.5
3-10	800	73.0	96.5(b)	11.0	27.1
10-23	800	74.0	130.8	8.3	17.3
3-58	800	75.0	98.9	10.0	23.5
10-22	800	77.0	(c)	13.2	38.1
9-8	800	87.0	(c)	7.9	28.7
10-24	850	58.0	287.3(d)	7.9	17.0
3-12	850	62.0	172.3	6.3	18.9
10-21	850	65.0	113.2(e)	7.4	13.5
9-9	850	68.0	38.7(f)	8.2	15.0
3-57	850	73.0	4.3	8.6	23.6
3-60	850	75.0	(c)	7.9	28.7
9-11	900	40.0	667.7	8.0	11.8
3-11	900	42.0	405.4	7.1	15.8
3-59	900	50.0	141.2	8.1	16.0
3-60	900	55.0	62.1	7.1	13.0
10-19	900	60.0	32.1	7.5	13.4
9-7	900	66.0	5.1	10.3	20.7
10-18	1000	40.0	15.3	6.6	8.2
9-6	1000	46.0	3.0	4.5	7.5

Notes:

(a) Specimen unloaded without failure at time shown.

(b) Beam was accidentally bumped, causing failure at this time.

(c) Specimen failed on loading.

(d) Specimen lost temperature (power loss) at 97.6 hours - was reloaded and run to failure.

(e) Specimen previously tested at $700^oF/65.0$ ksi without failing (results above).

(f) Specimen previously tested at $700^oF/70.0$ ksi without failing (results above).

TABLE A-4
HIGH-CYCLE FATIGUE DATA

Specimen No.	Temp (^oF)	A Ratio	Stress, ksi Max.	Stress, ksi Alt.	Cycles ($x\ 10^3$)	Results
9-53	75	.95	88.3	43.0	289	Failure
9-54	75	.95	82.1	40.0	115	Failure
10-61	75	.95	71.8	35.0	1,424	Failure
18843-1	75	.95	67.7	33.0	97	Failure
18843-8	75	.95	61.6	30.0	50	Failure
9-55	75	.67	89.7	36.0	50	Failure
10-62	75	.67	77.3	31.0	102	Failure
18843-2	75	.67	67.3	27.0	267	Failure
18843-9	75	.67	67.3	27.0	153	Failure
9-56	75	.67	62.3	25.0	10,455	Runout
18843-3	75	∞	50.0	50.0	60	Failure
18843-10	75	∞	40.0	40.0	92	Failure
18843-15	75	∞	38.0	38.0	66	Failure
9-57	75	∞	36.0	36.0	10,753	Runout
18843-13	75	∞	35.0	35.0	10,000	Runout
9-58	600	.95	92.4	45.0	9	Failure
10-65	600	.95	71.8	35.0	63	Failure
9-60	600	.95	61.5	30.0	1,982	Failure
18843-4	600	.95	57.5	28.0	98	Failure
3-37	600	.95	53.4	26.0	829	Failure
10-64	600	.95	51.3	25.0	9,684	Thread Failure
9-59	600	.67	79.8	32.0	595	Thread Failure
9-36	600	.67	79.8	32.0	34	Failure
10-66	600	.67	69.8	28.0	96	Failure
10-63	600	.67	64.8	26.0	99	Failure
3-38	600	.67	54.8	22.0	1,257	Failure
18843-6	600	.67	54.8	22.0	336	Failure
18843-11	600	.67	20.0	8.0	864	Failure in defect
10-52	600	∞	39.0	39.0	114	Failure
18843-12	600	∞	37.0	37.0	110	Failure
18843-7	600	∞	37.0	37.0	680	Failure in defect
10-51	600	∞	37.0	37.0	10,000	Runout
10-67	600	∞	35.0	35.0	8,638	Failure
18843-14	600	∞	35.0	35.0	10,000	Runout

A Ratio: 1.0

Frequency: 20 cpm

TABLE A-5
LOW-CYCLE FATIGUE DATA

Spec. No.	Temp (^oF)	Dia. (in.)	Longitudinal Strain ($x 10^{-2}$) ϵ_e	ϵ_p	ϵ_t	Cycles	E ($x 10^6$)	Engrg P/A Stress (ksi) Max.	Min.	Pseudo Alt Stress (ksi)	N_i Cycles	N_f Cycles
9-34	75	.1990	.796	0	.796	2,050	17.0	109.0	2.4	67.7	2,735	4,289
9-35	75	.1990	.680	0	.680	1,374	17.10	105.4	12.2	58.4	10,283	14,855
10-47	75	.1985	.573	0	.573	14,455	17.10	94.0	3.2	49.0	17,460	20,269
10-50	75	.1985	.530	0	.530	1,830	17.26	87.8	2.3	45.7	26,832	33,442
3-22(a)	75	.1985	.450	0	.450	22,740	17.47	74.3	2.3	39.3	58,327	58,965
9-28	200	.1995	1.066	.033	1.099	1,365	16.48	99.2	71.0	90.6	1,633	2,617
9-29	200	.1990	.830	0	.830	2,032	16.73	96.5	40.5	69.4	6,166	9,495
10-40	200	.1990	.617	0	.617	1,200	17.43	93.2	12.9	53.8	11,251	12,467
10-49	200	.1990	.500	0	.500	30,580	16.85	80.5	2.4	42.1	34,925	59,110
3-27	200	.1992	.447	0	.447	21,788	16.46	71.2	1.3	36.8	36,206	39,160
3-28	200	.1985	.400	0	.400	115,760	16.81	67.5	0	33.6	not reached	116,000
9-31	400	.1993	.940	.073	1.013	1,335	16.03	83.3	64.1	81.2	1,522	3,071
10-41	400	.1990	.787	.013	.800	1,720	15.81	81.3	44.4	63.2	6,854	7,501
9-30	400	.1995	.617	0	.617	4,490	15.95	76.5	20.5	49.2	28,266	31,742
10-48	400	.1995	.527	0	.527	12,010	15.78	71.7	11.2	41.6	32,093	39,300
3-31	400	.1977	.427	0	.427	7,190	15.80	67.4	0	33.7	26,533	35,491
3-29	400	.1985	.417	0	.417	5,075	15.80	66.2	0	32.9	18,220	22,073
10-43	600	.2000	.840	.060	.900	740	15.10	78.3	56.0	67.9	2,964	3,822
9-33	600	.1990	.770	.013	.783	5,600	15.00	76.8	42.7	58.7	13,491	16,983
10-45	600	.1995	.657	.003	.660	2,725	15.50	71.6	31.0	51.1	18,260	20,513
10-46	600	.1990	.580	0	.580	2,320	15.20	66.5	21.5	44.0	15,342	20,198
3-30	600	.1995	.447	0	.447	25,960	14.70	60.1	6.4	32.9	43,498	52,942

(a) S/N 3-22 developed a large visible crack at 58,965 cycles and the tensile load dropped off 65%. The test continued to run to 85,755 cycles and was then returned to the original A = 1.0, but the specimen did not hold the tensile load and decayed to total N_f at 86,585.

A Ratio: Infinity
Frequency: 20 cpm

TABLE A-5 (CONTINUED)
LOW-CYCLE FATIGUE DATA

Spec. No.	Temp (^oF)	Dia. (in.)	Longitudinal Strain ($x 10^{-2}$) ϵ e	ϵ p	ϵ t	Cycles	E ($x 10^6$)	Engrg. Stress P/A (ksi) Max.	Min.	Pseudo Alt Stress (ksi)	N_i Cycles	N_f Cycles
10-39	75	.200	1.153	.047	1.200	1,000	16.97	100.0	101.9	101.8	1,270	2,557
9-27	75	.200	.900	0	.900	3,415	16.76	78.3	74.5	75.4	8,359	11,066
10-44	75	.200	.760	0	.760	7,010	17.10	64.3	65.6	65.0	12,559	19,939
10-42	600	.1995	.780	.020	.800	5,030	15.70	63.3	61.7	62.8	9,675	12,275
9-32	600	.1995	.580	.013	.593	59,337	15.40	46.4	46.1	45.7	not reached	111,300

TABLE A-6
ROOM-TEMPERATURE CRACK GROWTH RATE DATA
(Frequency = 30 HZ/A - Ratio = 0.9)

Specimen No.	Total Cycles (x 10^3)	Crack Length A (in.)	Load Range (lb)	Stress Intensity Range (ksi) ΔK ($\sqrt{in.}$)	Crack Growth Rate dA/dn (in./cycle x 10^{-7})
3-68	0	.390	435	7.57	-
	80	.408	↓	7.92	2.25
	120	.419		8.14	2.62
	150	.431		8.40	4.00
	179	.439		8.58	2.76
	224	.466		9.25	6.00
	424	.480		9.64	7.25
	474	.506		10.41	5.10
	514	.528		11.19	5.62
	564	.542		11.71	2.70
	614	.557		12.34	3.00
	664	.573		13.09	3.20
	714	.592		14.12	3.90
	759	.603		14.74	2.33
	804	.613		15.37	2.22
	849	.630		16.59	3.89
	894	.650		18.20	4.44
	914	.689		22.04	19.30

TABLE A-6 (CONTINUED)

Specimen No.	Total Cycles (x 10^3)	Crack Length A (in.)	Load Range (lb)	Stress Intensity Range (ksi) ΔK ($\sqrt{in.}$)	Crack Growth Rate dA/dn (in./cycle x 10^{-7})
3-69		.475	620	13.64	-
	10	.535		16.41	6.00
	13	.556		17.68	7.17
	15	.577		19.09	10.15
	17	.593		20.28	7.75
	19	.605		21.34	6.25
	21	.629		23.60	11.70
	22	.644		25.32	15.50
	23	.675		29.32	30.50
	23.5	.690		31.65	30.00
	24	.713		35.73	46.00
3-70	0	.412	1074	19.43	-
	4	.432		20.48	5.12
	6	.451		21.55	9.50
	8	.471		22.74	9.75
	10	.505		25.14	17.30
	11	.536		27.67	30.50
	11.5	.548		28.81	24.00
	12	.565		30.57	34.00
	12.5	.597		34.48	64.00
	13	.629		39.38	64.00

TABLE A-6 (CONTINUED)

Specimen No.	Total Cycles (x 10^3)	Crack Length A (in.)	Load Range (lb)	Stress Intensity Range ΔK (ksi) ($\sqrt{in.}$)	Crack Growth Rate dA/dn (in./cycle x 10^{-7})
10T86	0	.401	516	10.19	-
	15	.419	↓	10.67	12.0
	25	.433		11.05	13.5
	35	.450		11.56	17.0
	45	.457		11.79	7.0
	55	.469		12.20	12.5
	65	.479		12.55	10.0
	75	.487		12.83	7.5
	90	.507		13.64	13.7
	100	.529		14.59	21.5
	110	.540		15.15	11.5
	120	.560		16.20	19.5
	130	.613		19.92	53.5
	133	.644		22.81	103.0
	134	.656		24.21	120.0
	135	.676		26.50	195.0
	136	.699		29.78	230.0

TABLE A-6 (CONTINUED)

Specimen No.	Total Cycles (x 10^3)	Crack Length A (in.)	Load Range (lb)	Stress Intensity Range (ksi) ΔK ($\sqrt{in.}$)	Crack Growth Rate dA/dn (in./cycle x 10^{-7})
10T87	0	.404	1384	27.45	-
	.400	.416		28.33	3.12
	.800	.432		29.49	3.88
	1.200	.443		30.36	2.75
	1.600	.456		31.49	3.37
	2.000	.468		32.54	3.00
	2.400	.484		34.00	3.87
	2.800	.496		35.26	3.12
	3.200	.538		40.13	10.40
	3.400	.556		42.66	9.00
	3.600	.572		45.16	8.00
	3.800	.610		52.42	19.30
	3.900	.657		64.32	46.50
	3.930	.687		74.60	102.00
	3.940	.696		77.89	85.00

TABLE A-6 (CONTINUED)

Specimen No.	Total Cycles ($\times 10^3$)	Crack Length A (in.)	Load Range (lb)	Stress Intensity Range ΔK (ksi) ($\sqrt{in.}$)	Crack Growth Rate dA/dn (in./cycle $\times 10^{-7}$)
10B95	0	.394	2210	37.90	-
	.300	.415	↓	39.96	7.00
	.600	.430	↓	41.54	5.00
	.900	.457	↓	44.60	8.83
	1.050	.467	↓	45.97	7.33
	1.200	.489	↓	48.95	14.70
	1.300	.510	↓	51.97	20.00
	1.400	.554	↓	60.18	45.00

TABLE A-7 - 600F CRACK GROWTH RATE DATA
(FREQUENCY = 30 HZ/A-RATIO = 0.9)

Specimen No.	Total Cycles (x 10^3)	Crack Length A (in.)	Load Range (lb)	Stress Intensity Range ΔK (ksi) ($\sqrt{in.}$)	Crack Growth Rate dA/dn (in./cycle x 10^{-7})
3-73	0	.438	414	8.01	-
	40	.457		8.43	4.75
	80	.468		8.69	2.75
	120	.473		8.81	1.25
	160	.484		9.09	2.75
	200	.498		9.47	3.50
	240	.507		9.73	2.25
	280	.515		9.98	2.00
	320	.529		10.43	3.50
	360	.540		10.81	2.75
	400	.563		11.70	5.75
	440	.588		12.83	6.25
	480	.624		14.85	9.00
	520	.647		16.45	5.75
	540	.661		17.56	7.00
	560	.681		19.35	10.00
	580	.691		20.35	5.00
	600	.702		21.53	5.50
	620	.729		24.87	13.50
	640	.743		26.86	7.00

TABLE A-7 (CONTINUED)

Specimen No.	Total Cycles (x 10^3)	Crack Length A (in.)	Load Range (lb)	Stress Intensity Range ΔK (ksi) ($\sqrt{in.}$)	Crack Growth Rate dA/dn (in./cycle x 10^{-6})
3-74	0	.393	736	12.72	-
	10	.439		14.31	4.60
	15	.459		15.11	4.00
	20	.480		16.02	4.20
	25	.503		17.41	4.60
	28	.531		18.70	9.33
	30	.544		19.52	6.50
	32	.549		19.85	2.50
	34	.554		20.20	2.50
	36	.565		21.00	5.50
	38	.593		23.32	14.00
	40	.618		25.81	12.50
	42	.720		42.21	51.00

TABLE A-7 (CONTINUED)

Specimen No.	Total Cycles (x 103)	Crack Length A (in.)	Load Range (lb)	Stress Intensity Range ΔK (ksi) ($\sqrt{in.}$)	Crack Growth Rate dA/dn (in./cycle x 10^{-7})
3-75	0	.428	270	5.09	-
	400	.497		6.17	1.72
	550	.558		7.52	4.07
	600	.568		7.79	2.00
	650	.587		8.36	3.80
	700	.601		8.84	2.80
	750	.609		9.13	1.60
	800	.624		9.73	3.00
	850	.632		10.07	1.60
	900	.653		11.08	4.20
	950	.683		12.82	6.00
	1000	.689		13.21	1.20
	1050	.705		14.35	3.20
	1100	.733		16.69	5.60

TABLE A-7 (CONTINUED)

Specimen No.	Total Cycles (x 10^3)	Crack Length A (in.)	Load Range (lb)	Stress Intensity Range ΔK (ksi) ($\sqrt{\text{in.}}$)	Crack Growth Rate dA/dn (in./cycle x 10^{-7})
10T88	0	.440	414	9.09	-
	20	.449		9.31	4.50
	40	.471		9.89	11.00
	60	.479		10.12	4.00
	80	.503		11.06	15.00
	100	.520		11.44	5.50
	120	.529		11.77	4.50
	140	.535		12.01	3.00
	160	.547		12.50	6.00
	180	.556		12.89	4.50
	200	.575		13.80	9.50
	220	.594		14.84	9.50
	240	.608		15.70	7.00

TABLE A-7 (CONTINUED)

Specimen No.	Total Cycles (x 10^3)	Crack Length A (in.)	Load Range (lb)	Stress Intensity Range ΔK (ksi) ($\sqrt{in.}$)	Crack Growth Rate dA/dn (in./cycle x 10^{-5})
10T89	0	.389	1296	24.94	-
	1.00	.412		26.42	2.30
	1.75	.427		27.47	2.00
	2.25	.441		28.50	2.80
	2.70	.447		28.96	1.33
	3.20	.464		30.34	3.40
	3.70	.484		32.11	4.00
	4.10	.508		34.48	6.00
	4.30	.523		36.14	7.50
	4.50	.536		37.69	6.50
	4.70	.550		39.51	7.00
	4.95	.558		40.63	3.20
	5.15	.590		45.74	16.00
	5.35	.615		50.61	12.50
	5.45	.630		53.98	15.00
	5.55	.654		60.19	24.00
	5.60	.666		63.72	24.00

TABLE A-7 (CONTINUED)

Specimen No.	Total Cycles ($x 10^3$)	Crack Length A (in.)	Load Range (lb)	Stress Intensity Range ΔK (ksi) ($\sqrt{in.}$)	Crack Growth Rate dA/dn (in./cycle x 10^{-5})
10B94	0	.369	2490	34.03	-
	.900	.390		35.81	2.33
	1.150	.412		37.84	8.80
	1.350	.428		39.44	8.00
	1.575	.441		40.82	5.78
	1.775	.460		42.98	9.50
	1.900	.470		44.19	8.00
	2.075	.483		45.86	7.43
	2.250	.516		50.63	18.90
	2.350	.533		53.46	17.00
	2.400	.540		54.71	14.00
	2.450	.556		57.79	32.00
	2.500	.572		61.20	32.00
	2.550	.589		65.27	34.00
	2.575	.601		68.43	48.00

TABLE A-8
FRACTURE TOUGHNESS DATA

Specimen No.	Spec. Thickness B (in.)	Temperature (^{o}F)	K_Q ksi $\sqrt{(in.)}$
3-72	.418	75	78.2
3-78	.418		69.5
3-79	.415		74.5
3-80	.417		70.5
3-81	.418		68.8
10T91	.378		72.8
10B96	.499		70.7
10B97	.499		69.5
10B98	.499		72.9
3-71	.411	600	61.4
3-76	.419		58.5
3-77	.418		57.2
3-84	.418		65.0
3-85	.414		56.0
10T93	.369		50.5
10B99	.498		59.7
10B101	.498		56.5
10B102	.499		60.0

TABLE A-9
CONTAINMENT CAPABILITY OF WROUGHT AND CAST Ti 6Al-4V
(BALLISTIC IMPACT TESTS)

Wrought			Cast		
V (ft /sec)	E (ft -lbs)	Result	V (ft /sec)	E (ft -lbs)	Result
356	67.5	A	390	81.0	A
441	103.6	B	473	119.2	B
539	154.8	C	536	153.1	C
725	280.1	D	686	250.1	D
			760	307.8	D

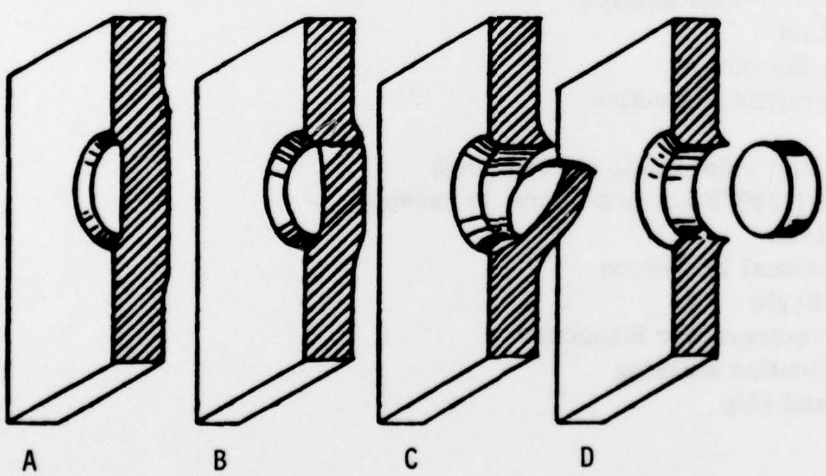

Figure A-23. Impacted Plate Appearance

APPENDIX B - MANUFACTURING METHODS REPORT

A. SCOPE

This report details the entire process with quality controls as developed for producing precision cast titanium alloy compressor casings. Special tooling required and quality controls are identified and quality standards are defined.

B. SEQUENCE OF CASTING OPERATIONS

Description
Inject wax patterns
Assemble wax patterns and gates/size as required
Inspect patterns (visual)
Build ceramic shell molds
Dry shell molds
Remove wax (Autoclave)
Preheat molds (gas-fired oven)
Cast (skull-melting furnace)
Remove shell material
Cut and trim gates
Rough machine inner contour
Mask any surface defects (to be repaired later)
Chemically-mill surface
Grit blast
Visual inspection
Radiographic inspection
Zyglo
Bench and weld repair (as required)
Anneal (1300^{o}F - 1 to 2 hours) in vacuum
Grit blast
Dimensional inspection
Final Zyglo
Final radiographic inspection
Identification marking
Pack and ship

C. SEQUENCE OF MACHINING OPERATIONS

Operation	Description	Special Tooling
010	Inspect casting	Fixture 4096481-133
020	Mill forward and aft flange faces and drill target holes in forward and aft flanges	Milling fixture
030	Mark and split casing	
040	Mill horizontal flanges, drill, back spotface and countersink horizontal flanges	Milling and drilling fixtures
060	Bench and assemble with (12) pins and (10) bolts	
070	Process line ream and assemble without torquing	Drilling fixture
075	Complete assembly including torquing	
080	Semi-finish forward end	Turning fixture
090	Semi-finish aft end	Turning fixture
100	Mill (3) pads, (3) ducts and (1) connector openings; drill and tap bosses	Milling and drilling fixtures
110	Deburr (vibratory)	
120	Bench and fit ducts and connector	
130	Turco Vitro Clean	
140	Weld (3) ducts and (1) connector	Welding fixture
150	Bench duct and connector inside diameters	
160	Zyglo	
170	Turco Vitro Clean	
180	Assemble for heat treatment	
190	Stress relief anneal	
200	Disassemble	
210	Finish machine horizontal flange face	Turning fixture
220	Machine lap horizontal flange face; bench and assemble	
230	Finish machine aft end	Turning fixture
240	Prepare flowpath	
245	Drill bracket holes	Drilling fixture

C. SEQUENCE OF MACHINING OPERATIONS (CONTINUED)

Operation	Description	Special Tooling
250	Steam clean	
260	Disassemble and bench	
270	Zyglo	
280	Turco Vitro Clean	
290	A1-Si coat inner flowpath	Special masking
300	Inspect coating	
310	Machine lap horizontal flange faces and assemble	
320	Finish line ream horizontal holes	Drilling fixture
330	Assemble remaining nuts and bolts	
340	Finish machine forward end	Turning fixture
350	Mill back side of aft flange	Milling fixture
360	Drill holes in forward and aft flanges	Drilling fixture
370	Drill variable vane holes and slots in pads	Drilling fixture
380	Back counterbore and countersink variable vane holes	
385	Disassemble and reassemble with .008 thick shim per Dwg. 6039T04, Note 20	
390	Finish turn flowpath	Turning fixture
395	Disassemble and remove shim	
400	Mill lock slot and seal groove	Milling fixture
410	Bench and assemble hardware	
420	Zyglo	
430	Final inspection	

D. Quality Control Plan

A quality control plan was established by General Electric Quality Control. Major items included in the plan are:

a) 100% radiographic inspection
b) 100% fluorescent penetrant inspection
c) 100% dimensional inspection of initial part from permanent tooling
d) 100% inspection of outer contour radii on all castings
e) Tensile and stress rupture test to qualify each master heat.

E. Master Heat

The master heat chemistry, tensile and stress rupture properties are tested by the casting source. Certification of testing results along with additional test bars are supplied with each casting lot. Tensile testing is done in accordance with ASTM E8 and E21 and stress rupture testing to ASTM E139. The material specification is General Electric B50TF102.

F. Non-Destructive Testing

Non-destructive testing of castings is performed at the casting source and reviewed by a General Electric Company quality control representative. 100% inspection is performed. Final radiographs are supplied with each casting shipment. Details of inspection performed are included in Section G.

G. Dimensional Inspection

Initial parts from a pattern die are subjected to 100% dimensional layout. Any tooling modifications require a layout of the affected areas. One part from each casting lot is checked for external radial dimensions on a three-axis measuring machine using set-up fixture 4096481-133.

H. Quality Inspection Operations

1. Operations at Casting Source:

a. First Inspection - Visual inspection for non-fill and other gross defects.

b. Zyglo (preliminary) - Fluorescent penetrant inspect per G. E. Specification P3TF2. Limits per drawing 6038T86.

c. Alpha Case Removal Verification - Metallographic and microhardness examination of test specimen which was processed through the Chemical Mill cycle with parts.

d. Zyglo (preliminary) - Fluorescent penetrant inspect per G. E. Specification P3TF2. Limits per drawing 6038T86.

e. Visual (preliminary) - Examination for surface pits, shrinkage, gas holes, positive metal and other indications requiring repair/rework.

f. X-ray (preliminary) - Process per G. E. Specification P3TF5, Class A. Interpret to ASTM E192 - limits per drawing.

g. Zyglo (final) - Fluorescent penetrant inspect per G. E. Specification P3TF2. Limits per drawing.

h. Visual (final) - Examination for surface pits, shrinkage, gas holes, positive metal and other indications requiring repair/rework.

i. X-ray (final) - Process per G. E. Specification P3TF5, Class A. Interpret to ASTM E192 - limits per drawing.

2. Operations at General Electric:

a. Review and file material certifications.

b. Review and file radiographs.

c. Dimensionally inspect for outer contour radial dimensions. Frequency one piece per casting lot.

d. Visually inspect 100%.